Formation de Hg°dans des milieux anoxiques tropicaux (lac, sol)

Tania Peretyazhko

Observatoire de Grenoble
et
Laboratoire de Géophysique Interne et Tectonophysique

Thèse

pour obtenir le titre de
Docteur de l'Université Joseph Fourier - Grenoble I
Spécialité : Géophysique - Géochimie - Géomécanique

Présentée
par
Tanya PERETYAZHKO

Formation de Hg° dans des milieux anoxiques tropicaux (lac, sol)

Date de soutenance : 8 janvier 2002
Composition de jury :

Michel VAUCLIN	Président	Directeur de recherche CNRS, Grenoble
Jean-Marc CHOVELON	Rapporteur	Professeur, Université Lyon 1, Lyon
François MOREL	Rapporteur	Professeur, Université Princeton, Princeton
Laurent CHARLET	Examinateur	Professeur, Université Grenoble 1, Grenoble
Vladimir KAZIMIROV	Examinateur	Professeur, Université Kiev, Kiev
Daniel COSSA	Invité	Directeur de recherche, IFREMER, Nantes
Dmitri KULIK	Invité	Professeur, Paul Sherer Institute, Villigen
Philippe GAUCHER	Invité	Responsable des actions scientifiques, DIREN, Cayenne

Observatoire de Grenoble
et
Laboratoire de Géophysique Interne et Tectonophysique

Thèse

pour obtenir le titre de
Docteur de l'Université Joseph Fourier - Grenoble I
Spécialité : Géophysique– Géochimie - Géomécanique

Présentée
par
Tanya PERETYAZHKO

Formation de Hg° dans des milieux anoxiques tropicaux (lac, sol)

Date de soutenance : 8 janvier 2002

Composition de jury :

Michel VAUCLIN	Président	Directeur de recherche CNRS, Grenoble
Jean-Marc CHOVELON	Rapporteur	Professeur, Université Lyon 1, Lyon
François MOREL	Rapporteur	Professeur, Université Princeton, Princeton
Laurent CHARLET	Examinateur	Professeur, Université Grenoble 1, Grenoble
Vladimir KAZIMIROV	Examinateur	Professeur, Université Kiev, Kiev
Daniel Cossa	Invité	Directeur de recherche, IFREMER, Nantes
Dimitri KULIK	Invité	Professeur, Paul Sherer Institute, Zürich
Philippe GAUCHER	Invité	Responsable des actions scientifiques, DIREN, Guyane

Formation de Hg° dans des milieux anoxiques tropicaux (lac, sol)

RESUME

Les mécanismes de production de Hg° dans des milieux anoxiques ont été étudiés en laboratoire. Les résultats sont utilisés pour interpréter les données de terrain mesurées dans la retenue de Petit Saut et dans des sols hydromorphes avoisinants, en Guyane Française (Amérique du Sud).

Dans la retenue, la décomposition des matières organiques, enoyées lors de la mise en eau, crée des conditions anoxiques, et donc une production d'espèces réduites, en accord avec les séquences thermodynamiques. Les sources de mercure dans la retenue sont les zones d'orpaillage situées en amont, ainsi que les sols, qui furent inondés lors de la mise en eaux. La disparition de l'oxygène favorise la libération du mercure par les sols inondés vers la colonne d'eau, où il se transforme chimiquement. Nos expériences de laboratoire démontrent que la production de Hg° au fond du lac est essentiellement d'origine biologique, et que la vitesse de production de Hg° est fonction de la concentration en mercure réactif. Un autre mécanisme responsable de la production de Hg° est la réduction abiotique de Hg(II) par le Fe(II) adsorbé sur des particules, ce que nous avons démontré avec des particules d'hématite et de mica.

Dans les sols, la comparaison de profils du mercure total montre de plus faibles concentrations dans les sols hydromorphes, que dans les oxisols, appartenant à la même toposéquence. Nos expériences de laboratoire démontrent que la réduction de Hg(II) en Hg° a lieu dans les sols hydromorphes en conditions anoxiques. La réduction est plus importante quand ces sols ont été amendés par du citrate de Fe(III). Tant la réduction biologique, que la réduction abiotique par le Fe(II) adsorbé sur les particules peuvent être responsables de la réduction du Hg(II) et de son départ vers l'atmosphère. La disparition du Hg(II) en conditions hydromorphes peut alors être due tant à la lixiviation des complexes organiques de l'ion Hg(II) qu'à sa volatilisation après réduction.

Mots clés: mercure, mercure élémentaire, mercure gazeux, Hg°, réduction, réservoir, sol hydromorphe.

ABSTRACT

Laboratory studies were carried out to investigate mechanisms of elemental mercury (Hg°) production in anoxic environments. The results were applied to interpret field data, obtained in tropical Petit Saut reservoir and hydromorphic soils (French Guiana, South America).

The decay of flooded vegetation in the artificial lake created anoxic conditions and lead to the production of a number of reduced chemical species according to thermodynamic sequence. Principal sources of mercury in Petit Saut reservoir include the upstream gold-mining area and the soils flooded during reservoir impounding. Oxygen disappearance favors mercury release from the floor to the water column, where it undergoes chemical transformations. As shown by laboratory studies, the production of Hg° at the lake bottom layer is due to biotic reduction of mercury and the rate of Hg° production depends on the available reactive mercury. Another Hg° production process in anoxic environment is the abiotic reduction of Hg(II) by Fe(II) adsorbed on particulate matter, as shown in our laboratory experiments with hematite and phlogopite particles.

In soils, a comparison of oxisol and hydromorphic soils located on a same toposequence demonstrates that total mercury content decreases in hydromorphic conditions. Laboratory experiments with these hydromorphic tropical soils showed that a reduction of Hg(II) to Hg° takes place in anoxic conditions, particularly when the soil was amended by Fe(III) citrate. Biotic reduction, together with abiotic reduction by Fe(II) adsorbed on the particles, are suggested to be responsible for mercury redox transformation and release to the atmosphere. Thus removal of Hg from hydromorphic soils may be due both to leaving of Hg(II)-organic complexes but also to a reductive volatilization process.

REMERCIEMENTS

Voici le travail de 3 années passées au LGIT. Ces quelques mots pour remercier toutes les personnes qui, par leurs contributions, travaux, aides et plus généralement leur amitié ont contribués à la rédaction de ce document.

Je voudrai d'abord exprimer ma gratitude envers mes directeurs de thèse : Laurent Charlet, Vladimir P. Kasimirov et Dmirtii Kulik. Merci à Vladimir P. Kasimirov et Dmirtii Kulik, qui par leurs nombreux efforts auprès de l'administration, m'ont aidé à démarrer cette thèse en France. Merci, bien évidemment à Laurent Charlet sans qui je n'aurai pas eu l'opportunité de ce sujet. Je le remercie de m'avoir guidé avec enthousiasme dans mes travaux et de m'avoir permis de découvrir, grâce aux missions de terrain, cette région fabuleuse qu'est la Guyane Française.

Je tiens à remercier particulièrement Gilles Secula, de l'ambassade de France en Ukraine, qui m'a grandement facilité les procédures d'obtention de la bourse du ministère des affaires étrangères et l'obtention du visa.

Un remerciement à Philippe Van Cappellen, Pierre Regnier et Christof Meile, qui m'ont offert leurs précieuses compétences dans l'étude du processus biogéochimiques du lac tropical.

Je voudrai remercier tout particulièrement Daniel Cossa qui m'a transmis son savoir des méthodes d'analyse du mercure et qui est toujours resté disponible pour répondre à mes questions.

Merci à Lorenzo pour son humeur joyeuse, sa patience et sa disponibilité. Merci également à Bruno pour ses conseils qui ont été fort utile.

A Martine et Christophe (qui n'est plus au laboratoire), une pensée spéciale pour les moments magnifiques que nous avons passé en Guyane. Un grand merci à Martine et Delphine pour leur aide dans l'analyse de mes milles échantillons de Guyane ; à Nicolas pour son aide dans les parties techniques et les analyses XRD qu'il a réalisé pour moi ; à Géraldine avec qui il était un plaisir de travailler.

Merci aux étudiants qui m'ont accueillis au laboratoire : Alix, Anne-Claire, Francis, Marie-Pierre, Christophe ; Merci à Gabriela, pour ces conseils judicieux et opportuns. Une sympathie à la nouvelle équipe : Ana, Tatiana, Eric et Sudipto.

Un remerciement énorme à Christine grâce à qui les missions en Guyane ont été très bien organisée et qui a passé son temps à me « sauver la vie » (Surtout lorsque j'ai raté l'avion pour aller à Cayenne).

Je voudrai passer mes salutations à l'association « Chasse et Pêche sportive » : Jacques, Charles et Isman qui nous ont servi de guide et qui nous ont beaucoup aidé pendant les missions en Guyane.

SOMMAIRE

CHAPITRE 1

Synopsis

1. 1 INTRODUCTION

Le mercure métallique est connu de l'homme depuis au moins 3500 av. J.-C. L'utilisation du mercure par l'industrie minière pour amalgamer et concentrer les métaux précieux remonte probablement aux Phéniciens et aux Carthaginois. Les problèmes d'environnement causés par l'utilisation de Hg dans les mines d'or et d'argent ont été rapportés dès l'époque Romaine *(1)*. Pendant plusieurs siècles, du XVI ème jusqu'au début du XXème siècle, le mercure a été sauvagement utilisé partout dans le monde, particulièrement en Amérique du Sud et du Nord, dans les mines d'or et d'argent. Après une utilisation à l'échelle mondiale au début de notre siècle, celle-ci déclina jusqu'à l'arrêt d'exploitation dû à l'épuisement des filons riches en or et en argent en Amérique, et plus tard suite à l'invention des méthodes d'exploitation au cyanure *(1)*. La nouvelle "conquête vers l'or" par des entrepreneurs individuels qui a commencé au début des années 1970 est la source de problèmes sociaux et environnementaux dans les pays situés sous les tropiques *(2)*. En Amérique Latine, tous les pays ont virtuellement une activité artisanale tournant autour des mines d'or. On estime actuellement que plus d'un million de mineurs cherchent de l'or en Amérique Latine et que leur production peut être estimée à environ 200 tonnes d'or par an *(3)*. Bien que le mercure soit illégal dans la plupart des pays, son utilisation pour l'amalgamation de l'or reste la méthode préférée des chercheurs. Le manque de savoir élémentaire concernant la toxicité du mercure *(4)* a amené les travailleurs des mines à évacuer d'énormes quantités de mercure vers l'atmosphère, les rivières et les sols.

Parallèlement à cette source anthropique directe de mercure, des apports peuvent provenir de processus d'érosion des sols, liés aux activités minières, de la déforestation, des aménagements routiers et urbains ou des activités agricoles. En effet, les sols amazoniens, et particulièrement ceux du bouclier guyanais sont naturellement riches en Hg, les concentrations pouvant être dix fois supérieures à celles mesurées dans les sols des régions tempérées et boréales de l'hémisphère Nord. Ces sols tropicaux sont très anciens (plusieurs millions d'années) et ont accumulé des quantités importantes de métal, principalement complexé par les oxyhydroxydes d'aluminiun et de fer *(5, 6)*. Ainsi, l'erosion des particules au niveau des bassins - versants peut être à l'origine d'apports conséquents de Hg dans les hydrosystèmes, ces apports ayant une origine «naturelle ».

Une fois libéré dans le milieu naturel, le mercure va être transformé chimiquement en diverses formes. Parmi ses formes, le methylmercure joue un rôle prépondérant d'un point de vue écotoxicologique, en égard à ses capacités de transfert au travers des barrières biologiques et aux atteintes structurales et fonctionnelles, du différents organes, notamment du système nerveux *(7)*. De grandes concentrations de mercure, due à la propriété de bioaccumulation du mercure *(8, 9)*, avec des pourcentages significatifs de methylmercure, sont trouvés dans les poissons Amazoniens. Ainsi, l'alimentation des populations par des poissons contaminés a causé de sévères maladies affectant le système nerveux et causant des troubles moteurs. En Guyane Française, des risques d'empoisonnement au mercure sont particulièrement rencontrés parmis les amérindiens dont l'alimentation est essentiellement constituée de poissons.

Les effets du mercure dans les sytèmes naturels des climats tempérés sont déjà bien documentés, par exemple au Canada *(10)* , et en Suède *(11)*. Toutefois, relativement peu de données sont disponibles sur les eco-systèmes tropicaux.

Nous avons étudié le cycle du mercure dans le réservoir tropical situé en Guyane Française, et plus particulièrement la formation du mercure élémentaire (Hg°), et sa distribution. Des expériences de laboratoire ont été faites dans le but d'étudier les mécanismes de production de Hg° qui pourrait être considéré comme un procédé naturel d'atténuation qui limiterait la production de methylmercure et son accumulation dans les poissons *(12)*. Les actions principales de ce travail ont été de:

- Réaliser des mesures de terrain au réservoir Petit Saut (Guyane Française), pendant les saisons sèches et humides (1999).
- Etudier la biogeochimie du réservoir artificiel Petit Saut (Guyane Française) en respectant le cycle du mercure.
- Etudier in-situ la distribution de mercure gazeux (Hg°), dans la colonne d'eau par spectrophotométrie de fluorescence atomique à vapeur froide.
- Rechercher en laboratoire les mécanismes de production de Hg° dans les sédiments de surface collectés au réservoir Petit Saut.
- Etudier la production de Hg° par Fe(II) adsorbé sur des particules d'hématite.
- Rechercher la production de Hg° dans les sols tropicaux hydromorphes comme étant un mécanisme possible de la diminution de la concentration totale de mercure des oxisols vers les sols hydromorphes.

1.2 PRINCIPAUX RESULTATS

1.2.1 La site d'étude (la retenue de Petit Saut)

La "zone atelier" choisie pour l'étude du cycle du mercure dans l'eau est la branche Coursibo de la retenue de Petit Saut (Figure 1). La crique Leblond constitue le principal apport en eau à cette branche du lac où une importante partie de la zone d'orpaillage de Saint Elie fait partie de son bassin versant. Les eaux très turbides de la crique Leblond représentent un apport important de mercure à la retenue principalement sous forme particulaire. Une autre source de mercure introduit dans cette branche du lac provient des sols de l'ancien site d'orpaillage "Adieu Vat", situé dans la partie centrale du lac, et qui fut inondé lors de la mise en eaux.

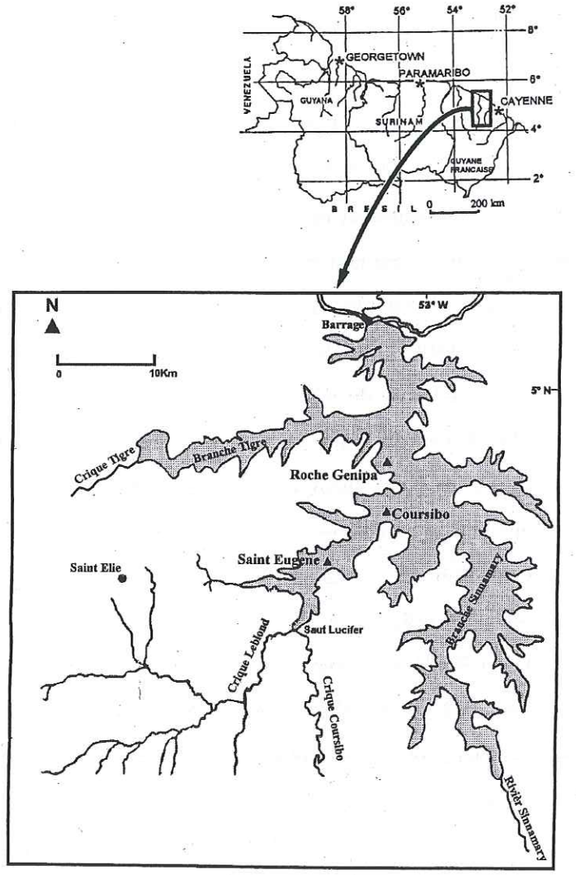

Figure 1. Lieux d'échantillonnage de lac de Petit Saut, Guyane Française.

Deux missions ont été consacrées à ce site en 1999, l'une pendant la période de hautes eaux en juin (« saison humide »), et l'autre pendant la période de basses eaux, en décembre (« saison sèche ») . Dans ce travail, nous présentons essentiellement les résultats des études menées à la station Roche Genipa située dans la partie centrale du réservoir. Les paramètres physico-chimiques (pH, Eh, température, conductivité) ont été mesurés *in situ*. On a analysé la teneur en Fe(II) et l'alcalinité dans un laboratoire installé à coté du barrage. Des mesures de mercure élémentaire, Hg°, et de mercure réactif, Hg_R, par spectrophotométrie de fluorescence atomique à vapeur froide, ont été effectuées sur le terrain. Des échantillons d'eau ont également été prélevés et analysé par un autre laboratoire (M. Coquery, IAEA) pour leurs teneurs en mercure total dissous, Hgd et en mercure particulaire, Hgp. Certaines donnés portant sur le CH_4(aq), CO_2(aq), NH_4^+ et S(-II) ont été obtenues par le laboratoire HYDRECO et son discutés dans le cadre de notre modèle général de la physico-chimies de la retenue.

1.2.2 La biogeochimie de la retenue

Le centre du lac (station Roche Genipa) est stratifié de façon permanente. La température en surface est de 30 à 31^{0}C et celle prise dans la colonne d'eau à partir d'une profondeur de 15 m est constante et égale à 25 – 25.4°C. L'oxygène disparaît brutalement au delà de 4 m de profondeur. Pendant les deux saisons, le pH dans les eaux de surface reste proche de 6.8, et devient plus acide dans les eaux anoxiques avec une valeur moyenne de 5.8 pour l'hypolimnion. Les profils de conductivité dépendent fortement de la saison. A la saison sèche la conductivité augment de 0.024 ± 0.003 mS/cm dans les eaux de surface à 0.057 mS/cm au fond du lac. En saison humide, les variations de conductivité sont moins marquées, avec des valeurs passant de 0.022 mS/cm en surface à 0.027 mS/cm au fond. Le potentiel Eh, varie de 350mV dans la couche oxique à 70 mV dans la couche anoxique.

Avec la disparition de l'oxygène, les espèces réduites, comme NH_4^+, Fe(II), S(-II), CH_4 apparaissent dans l'hypolimnion (Figure 2). Le flux total d'électrons des espèces réduites ((Fe(II), NH_4^+ , CH_4 et S(-II)) de l'hypolimnion vers l'oxycline en saison sèche et humide est égal à respectivement $104 \cdot 10^{-8}$ et $70 \cdot 10^{-8}$ mol d'électrons m^{-2} s^{-1}. Ces valeurs sont plus faibles que les flux en O_2 (accepteur d'électron) vers l'hypolimnion mesurés aux deux saisons: $1080 \cdot 10^{-8}$ et $208 \cdot 10^{-8}$ mol d'électrons m^{-2} s^{-1}, en saison humide et sèche, respectivement. Cette différence suggère que la principale consommation d'oxygène dissout correspond à la décomposition biologique des matières organiques. La présence de matières organiques en

concentration importantes s'explique par l'inondation de 360 km^2 de forêt lors de la mise en eaux du réservoir et par des processus de photosynthèse.

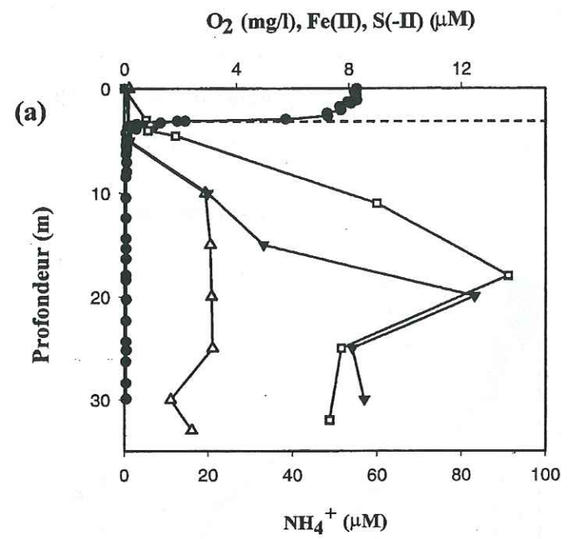

Figure 2 Distribution verticale de Fe(II) (□), de S(-II) (Δ), de NH_4^+ (▼) et de O_2 (●) (a) à la saison humide et (b) à la saison sèche.

Pendant la saison sèche, l'accroissement de l'alcalinité dans la zone anoxique correspond bien en l'accroissement de la conductivité (Figure 3). Une corrélation similaire peut également être trouvée avec la concentration en Fe^{2+}. Etant donné que Fe^{2+} et HCO_3^- (une composante majeur de l'alcalinité) sont les ions les plus présents dans la couche anoxique du lac à la saison sèche et vu que leur distribution verticale correspond bien aux changements de conductivité avec la profondeur, Fe^{2+} et HCO_3^- peuvent être considérés comme les ions principaux déterminant la conductivité.

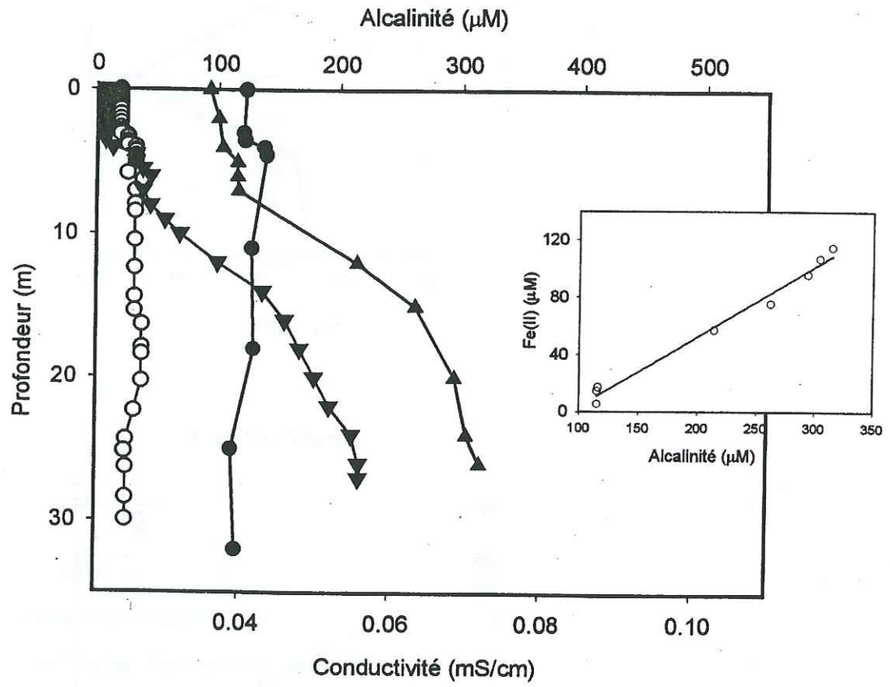

Figure 3 Profils verticaux d'alcalinité en saisons sèche (▲) et humide (●) et de conductivité en saison sèche (▼) et humide (○); Insert: Corrélation entre les teneurs en Fe(II) et en alcalinité, en saison sèche.

Une corrélation positive a été observée entre teneurs en Fe(II) et en alcalinité ([Fe(II)]= 0.5[Alc] – 45) avec un coefficient de régression de $R^2 = 0.986$. Il s'en suit que chaque mole de Fe(II) produite est accompagnée de 2 moles d'alcalinité produites celui correspond à l'équation de la réduction de $Fe(OH)_3(s)$ par la matière organique (« CH_2O »):

$$CH_2O + 4Fe(OH)_3(s) + 7CO_2(aq) = 4Fe^{2+} + 8HCO_3^- + 3H_2O \quad (1)$$

Ainsi, la dissolution réductive d'oxy(hydroxy)de de fer par oxydation de matières organiques est un facteur majeur dans l'accroissement d'alcalinité observé dans les zones anoxiques du réservoir de Petit Saut.

Pendant la saison humide, une dilution de certaines espèces (Fe(II), CH_4, CO_2, HCO_3^-) dans la colonne d'eau est observée. Aussi, un changement de structure du profil vertical a lieu dans l'hypolimnion. On note un accroissement dans la colonne d'eau des concentrations en Fe(II), NH_4^+ quand la profondeur augmente de 10 à 20 m, puis une diminution de ces concentrations au fond du lac (Figure 2a).

Les profils verticaux du coefficient de diffusion de turbulence, K_z, dans l'hypolimnion (Figure 4) suggèrent une différence de régimes de mélange entre saison sèche et saison humide. La différence observée entre les deux saisons se situe principalement au niveaux de la couche situé entre 4 et 11 m (Figure 4), où le mélange est essentiellement due à des précipitations et au flux de ces eaux entre les eaux chaudes de l'épilimnion et les eaux froides de l'hypolimnion. Les turbulences observées dans la couche profonde (22- 35 m) sont attribuées à un accroissement du flux d'eau apporté par les rivières pendant la saison humide.

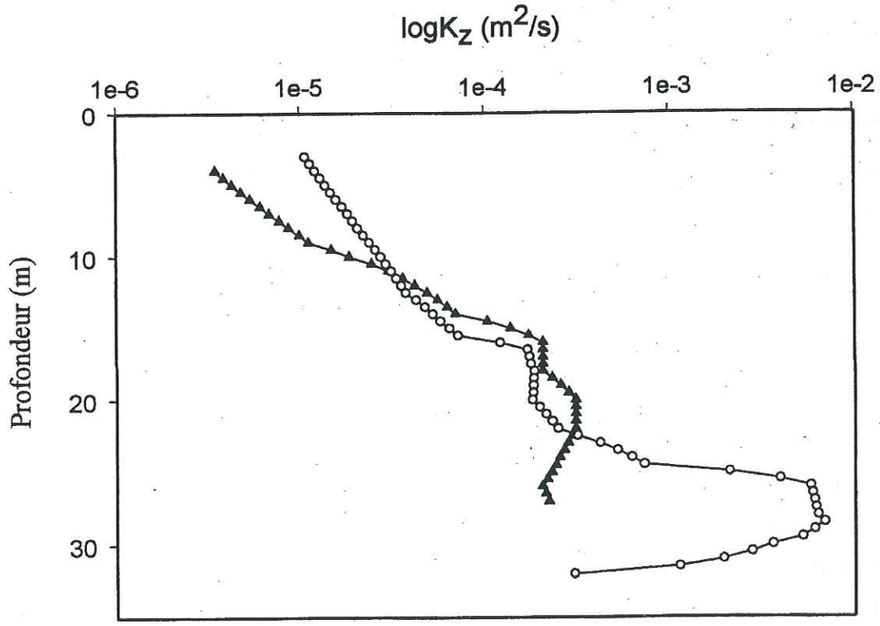

Figure 4 Distribution verticale du coefficient de diffusion turbulent, calculé en saison humide (○) et sèche (▲).

La turbulence forte des eaux profondes peut mener à la remise en suspension de particules de sédiments dans les eaux profondes du lac. Nous supposons que le pic de production de Fe(II) et NH_4^+ trouvé respectivement à 18 et à 20 m à la saison humide, dépend des procédés de remise en suspensions des particules de matière organique et d'oxyde de fer du « sol » inondé. Une dissolution réductive des particules a lieu. A la saison sèche, quand le mélange des eaux diminue en profondeur, le flux de particules dans la colonne d'eau ralentit jusqu'à être nul en fin de saison sèche. Ceci mène à une décomposition graduelle de la matière organique et à une constante augmentation des concentrations d'espèces dissoutes (Fe(II), HCO_3^-, NH_4^+, HS^-).

1.2.3 Mercure dans le retenue de Petit Saut

Pour étudier la distribution de mercure dissout dans l'hypolimnion et pour déterminer la source principale de cette espèce, nous avons estimé les profils théoriques, dus aux phénomènes de mélange de mercure dissout, que cette espèce devrait présenter si seul le mélange physique des eaux affectait sa concentration. La comparaison des profils de distribution calculés pour le mercure dissout (Hgd) avec les valeurs mesurées (Figure 5a,b) suggère que à eux seuls les procédés de mélange dictent la formation du profil et qu'aucune transformation chimique n'a lieu dans la colonne d'eau. La différence notée pour les concentrations de Hgd entre couches oxiques et anoxiques du lac nous laisse supposer que la principale source de mercure dans la colonne d'eau provient des sols inondés. A la saison sèche, le mercure, libéré par les sédiments, pourrait s'accumuler dans la couche au niveau du fond du lac à cause de la faible turbulence de l'eau. A la saison humide le pic de Hgd coïncide bien avec le pic de concentrations en Fe(II) et NH_4^+. En plus de la libération directe de mercure par les sédiments, la remise en suspension de particules de sol joue un rôle important dans le profil de mercure dissout. Le mercure adsorbé sur l'oxy(hydroxy)de de fer et complexé avec les particules de matières organiques va être libéré dans les profondeurs situées entre 10 et 20 m d'eau où la dégradation des particules de matière organiques et d'oxy(hydroxy)de de fer a lieu comme montré ci-dessous. Aussitôt que le mercure est desorbé, il réagit avec les matières organiques dissoutes pour former des complexes stables.

La distribution vertical du mercure dissout et du mercure particulaire permet de calculer le coefficient de distribution ($K_{d(ml/g)}$= Hgp/Hgd) pendant les deux saisons. Les valeurs de $\log K_d$ sont respectivement égal à 5.27 ± 0.17 à 5.23± 0.27 durant la saison humide et la saison sèche. Elles sont remarquablement similaires. Le coefficient de distribution a été utilisé dans

un modèle de complexation de mercure pour un système eau/sédiment et les résultats sont présentés dans le paragraphe suivant.

La diminution de la concentration en mercure « réactif » Hg_R a lieu dans la zone d'accroissement de la concentration en S(-II). Les eaux anoxiques sont sursaturées par rapport au cinnabre, avec un indice de saturation de 19.

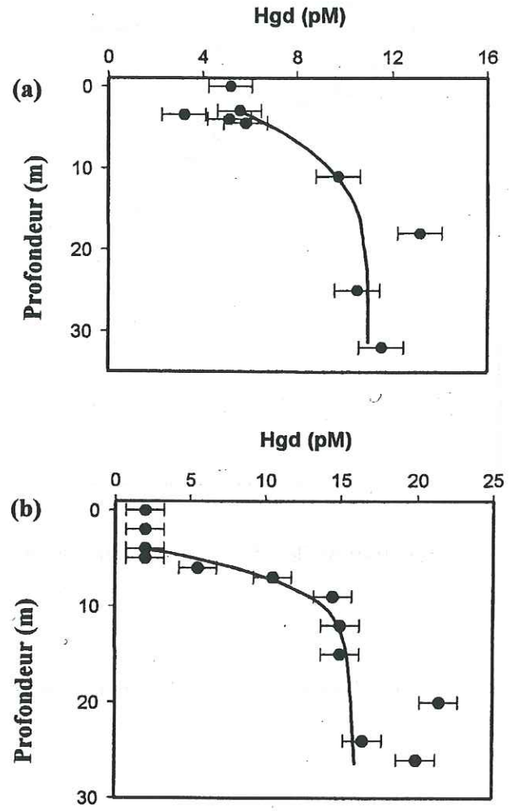

Figure 5. Profil des concentrations calculées (trait plein) et mesurées *(13)* du mercure dissout en saison humide (a) et sèche (b).

Les profils verticaux de Hg° ont été mesurés à la station de Roche Genipa et à celle de Saint Eugène (Figure 6). Ils présentent trois maxima: un en surface, résultat de l'activité photochimique (Roche Genipa et Saint Eugène), un situé sous l'oxycline (Roche Genipa) et un près de l'interface eau/sédiment (Roche Genipa et Saint Eugène). Les deux derniers

maxima résultent, comme nous observons dans nos expériences de laboratoire, d'une réduction par des bactéries et/ou par le fer ferreux, de Hg(II) en Hg°.

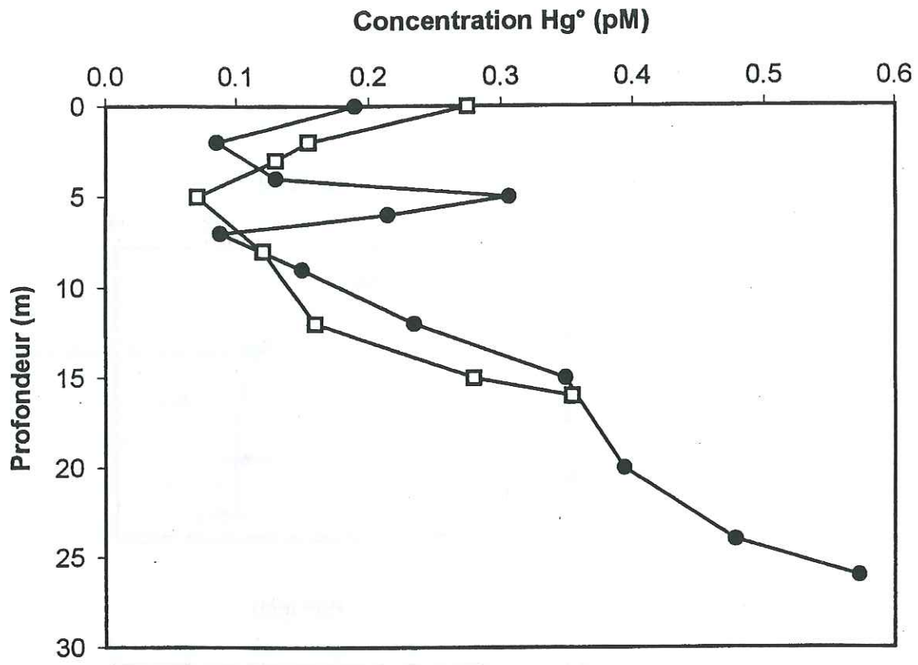

Figure 6. Profile de concentration de Hg° aux stations de Roche Genipa (●) et de Saint Eugène (□) en saison sèche.

1.2.4 Production de mercure élémentaire dans les suspensions anoxiques des sédiments de surface.

Pour étudier les mécanismes de production de Hg° au fond du lac de Petit Saut, nous avons effectué des expériences de laboratoire avec des sédiments et des eaux prélevées au lac de Petit Saut. Les suspensions anoxiques des sédiments, ayant des concentrations en particules de 18g l^{-1}(ps), ont été préparées avec 150 ml d'eau du réservoir à pH 6. La réduction de Hg(II) a été étudiée avec 1.5 nM, 2.5 nM, 4.4 nM, 250 nM de concentration initiale en Hg(II) total. Dans le but de distinguer les mécanismes biotiques des mécanismes abiotiques, une partie des sédiments et de l'eau prélevée a été exposée à des irradiations de rayons gamma pour arrêter l'activité bactérienne. D'autres suspensions de sédiments ont été

soumises au même protocole puis dopée avec NaN_3 pour arrêter toute activité bactérienne rémanente.

Dans les suspensions anoxiques de sédiments de surface non traités, une production de Hg° a lieu aux quatre concentrations initiales en mercure (Figure 7). Avec les sédiments traités par rayons gamma et NaN_3 on a observé une production de Hg° uniquement dans les suspensions ayant une concentration initiale de 250 nM Hg(II). Cela démontre que la production de Hg° au fond du réservoir de Petit Saut est due aux microorganismes. Nos données ont été ajustées de manière satisfaisante à une cinétique de premier ordre. Les constantes cinétiques sont rassemblées dans le Tableau 1a. En regard des faibles valeurs de la constante de vitesse de réduction, la production de Hg° est faible, comparé à la teneur initiale en Hg(II). Seulement 3 % du mercure initial est au mieux réduit en 4 heures de réaction. Les calculs d'équilibre de spéciation de mercure entre la phase solide et la phase aqueuse montrent que 99.96 % du mercure ajouté est adsorbé sur les particules, ce qui est cohérent avec les concentrations en mercure réactif mesurées dans les suspensions étudiées : les concentrations en mercure réactif mesurées dans les suspension avec 4.5 nM, 2.5 nM, 1.5 nM de concentration initiale de Hg(II) total étaient en effet de 1.25 ± 0.2 pM, 1.06 ± 0.2 pM et 0.92 ± 0.2 pM, respectivement. Les concentrations calculées sont respectivement 1.83 pM, 0.95 pM et 0.62 pM. Ainsi, la vitesse totale de la réaction est fonction de la concentration en mercure réactif. Les facteurs limitant la réduction de Hg(II) en Hg° sont les cinétiques de désorption de mercure des oxydes minéraux et de libération de mercure par décomposition de la matière organique.

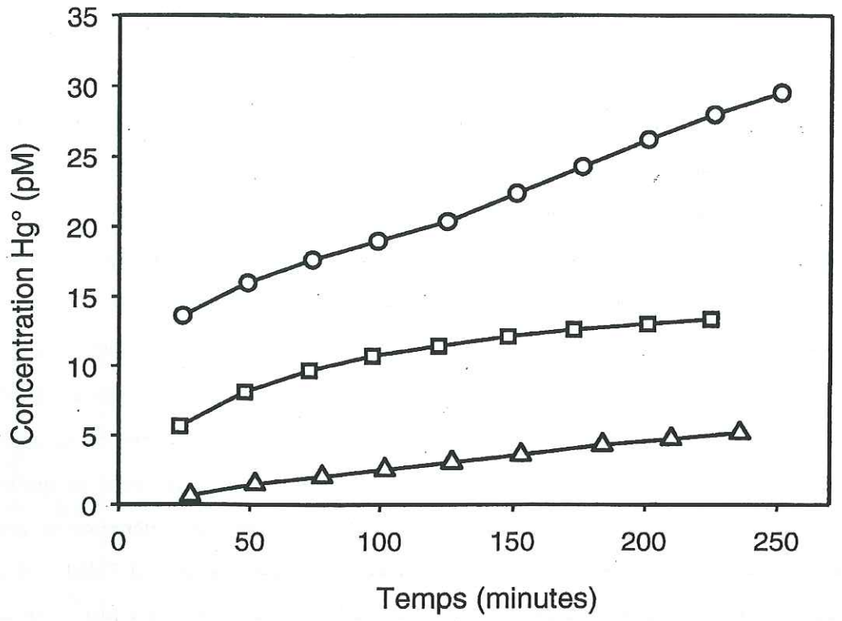

Figure 7. Production cumulative de Hg° dans des suspensions de 18g l^{-1} (ps) sédiment et d'eau du réservoir non traités à pH 6 réalisées avec une concentration initiale en Hg(II) total de 1.5nM (Δ), 2.5nM (□) et 4.4nM (○) .

Tableau 1. Constantes cinétiques de premier ordre obtenues pour des suspension des sédiments, d'hématite, de mica et des fraction argileuses de sols hydromorphes.

(a) Suspension des sédiments de 18 g l^{-1} à pH 6	
Hg(II) total initial, nM	k (R^2), min^{-1}
250	$7*10^{-5}$ (0.89)
250*	$3*10^{-7}$ (0.96)
4.4	$2*10^{-5}$ (0.99)
2.5	$1*10^{-5}$ (0.89)
1.5	$1*10^{-5}$ (0.99)
(b) Suspension d'hématite 5 mg l^{-1}, 1.5 µM de Fe(II), 20pM de Hg(II)	
pH	k (R^2), min^{-1}
6	$2*10^{-3}$ (0.99)
7.4	$3*10^{-3}$ (0.99)
7.8	$6*10^{-3}$ (0.99)
(c) Suspension de mica 3 mg l^{-1}, 10 µM de Fe(II), 50 pM de Hg(II)	
pH	k (R^2), min^{-1}
7.5	$1.16*10^{-2}$ (0.99)
(d) Suspensions de fractions argileuses 0.4 g l^{-1} à pH 7, 2.5 nM de Hg(II), 1 mM de FeCit	
Echantillon	k (R^2), min^{-1}
30-40 cm	$3.0*10^{-4}$ (0.99)
60-70 cm	$3.0*10^{-4}$ (0.99)
90-100 cm	$5.1*10^{-3}$ (0.94)
90-100 cm **	$2.9*10^{-3}$ (0.86)

* Suspension avec NaN_3 ;

** Suspension sans FeCit.

1.2.5 Production de Hg° par Fe(II) dans les suspensions anoxiques d'hématite et de mica.

A la station Roche Genipa, nous observons la production de Hg° sous l'oxycline où divers transformations redox ont lieu, dont celle du fer. Nous avons fait l'hypothèse que Hg(II) pourrait être réduit par le fer ferreux selon la réaction :

$$Fe^{2+} + Hg(OH)_2° + H_2O \rightarrow Hg°(aq) + Fe(OH)_3(s) + H^+ \qquad (2)$$

Les expériences de laboratoire ont été menées avec des suspensions d'hématite de concentration en 5mg l^{-1} à pH 6, 7.4, 7.8. La réduction de Hg(II) a été étudiée avec 20 pM de concentration initiale en Hg(II) total et avec 1.5 µM de concentration initial en Fe(II). En l'absence de particule, la réaction n'a pas lieu (Figure 8). En revanche, en présence de particules d'hématite au bout de deux heures , on observe une production de 4 pM, 8 pM et 12 pM à pH 6, 7.4 et 7.8, respectivement (Figure 8). Ces données montrent que la quantité de Hg° produit, $C_{Hg°}$, dépend du pH initial et augmente avec l'accroissement du pH. Cette augmentation de Hg° est bien corrélée à l'adsorption de Fe(II) sur les particules d'hématite *(14)*. De là, nous pouvons suggérer que la réduction de Hg(II) est liée à une oxydation du Fe(II) adsorbé sur les particules.

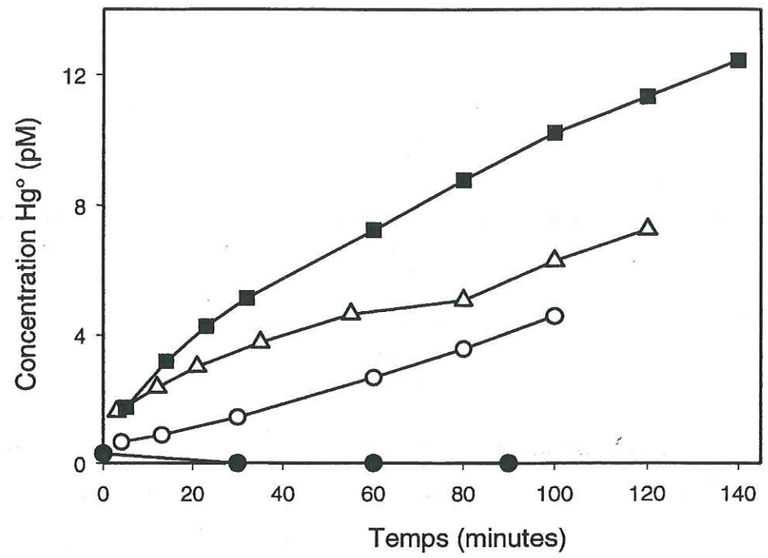

Figure 8. Production de Hg° dans des suspensions de 5 mg l^{-1} d'hématite dopées à 1.5 µM de Fe(II) et 20 pM de Hg(II) à pH 6 (○), 7.4 (Δ) and 7.8 (■),et dans une solution aqueuse contenant Fe(II) et Hg(II) aux mêmes concentrations que si dessus à pH 7.8 mais sans hématite (●).

Un phénomène similaire de production de Hg° a été démontré dans les expériences de réduction de Hg(II) par Fe(II) en présence de particules de mica. Une précipitation de $Fe(OH)_3(s)$, due à la réduction de Hg(II) par le Fe(II) adsorbé à la surface de mica, est observée sur les images obtenu par AFM (Figure 9). Pour les deux minéraux, hématite et mica, nos données ont été ajustées à une cinétique de premier ordre (Table 1b,c).

Nous supposons que la production de Hg° est réalisée par une formation de complexe de « sphère externe » entre des complexe de surface de fer ferreux $>SOFe^{II}(OH)_i^{1-i}$ et l'espèce aqueuse $Hg(OH)_2°$ (l'espèce dominante du mercure réactif) . La formation de ces complexes est assurée par des liaisons hydrogène des groupements OH^- au travers desquelles s'effectue le transfert d'électrons. Un mécanisme de réduction de Hg(II) par le fer ferreux adsorbé sur des particules est ainsi proposé:

(i) $>SOH^{\circ}+Fe^{2+}+iH_2O \xleftrightarrow{K_1} >SOFe^{II}(OH)_i^{1-i}+(i+1)H^+$

(ii) $2>SOFe^{II}(OH)_i^{1-i}+Hg(OH)_2^0 \underset{k_{-2}}{\overset{k_2}{\rightleftharpoons}} \left[>SOFe^{II}(OH)_i \cdots HOHg^{II}OH \cdots (HO)_iFe^{II}OS<\right]$

(iii) $\left[>SOFe^{II}(OH)_i \cdots HOHg^{II}OH \cdots (HO)_iFe^{II}OS<\right] \xrightarrow{k_3} 2>SOFe^{III}(OH)_{1+i}^{1-i}+Hg^{\circ}$

(iv) $>SOFe^{III}(OH)_{1+i}^{1-i}+(2-i)H_2O \xrightarrow{k_4} >SOH^{\circ}+Fe(OH)_{3(s)}^0+(1-i)H^+$

où K_1 est une constante d'équilibre; k_2, k_{-2}, k_3 et k_4 sont les constantes cinétiques, k_2 est une constante de la formation du complexe précurseur, k_{-2} est la constante de dissociation du complexe, k_3 est une constante de la formation de Hg° à partir du complexe précurseur et k_4 est une constante de cinetique de formation de $Fe^{III}(OH)_{3(s)}^0$ à la surface du mica

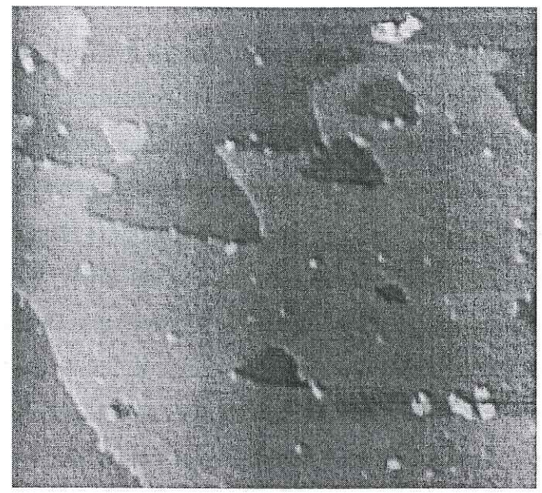

Figure 9. Images AFM d'une surface de phlogopite ayant réagi avec Fe(II) 20 h (a) et 59 h (b) après dopage au Hg(II). (Scan size = 900 µm (a) et 850 µm (b) sur le coté, respectivement).

1.2.6 Production de Hg° dans les sols hydromorphes

La distribution du mercure a été étudié dans une toposéquence située sur la rive gauche de la crique Leblond (Figure 1) *(13)*. La toposéquence est particulièrement intéressante car l'essentiel de la diversité pédologique présenté en Guyane y est observée sur une distance de 300 m. En descendant cette toposéquence nous distinguons un oxisol (S1), un ultisol (S2, S3, S6) et un sol hydromorphe (S4, S5, S7) (Figure 10). La variation de teneur en mercure qui a lieu dans le sol est fonction du type de sol rencontré. Les plus fortes concentrations sont trouvées dans l'oxisol (S1) avec une valeur moyenne de 236 ± 107 ng/g . Dans l'ultisol (S3) les concentrations de mercure diminuent, avec une concentration moyenne de 138 ± 58ng/g . Les concentrations en Hg dans le sol hydromorphe (S5) sont les plus basses, avec une valeur moyenne de 80 ± 40 ng/g.

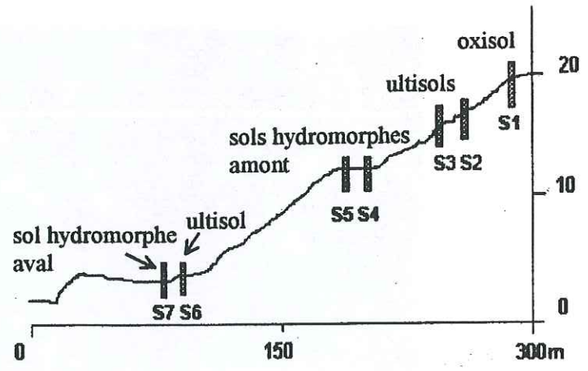

Figure 10. Localisation des profils pédologiques étudiés sur une toposéquence située sur la rive gauche de la crique Leblond, Guyane Française.

Classiquement, les pédologues expliquent l'appauvrissement des sols en métaux à des phénomènes de lixiviation. Dans le cas du mercure, nous supposons qu'un autre mécanisme peut avoir lieu, a savoir la production de Hg° et son évasion dans des conditions anoxiques.

Les expériences de laboratoire sur la réduction de Hg(II) ont été effectuées avec des échantillons de sols hydromorphe (S5) pris à 30-40 cm, 60-70 cm et 90-100cm de profondeur. La réduction de Hg(II) a été étudiée sur la fraction argileuse de sol parce qu'une corrélation positive entre teneur en mercure total et teneur en argile a été observée dans ces sols *(13)*. Les

suspensions anoxiques contenant 0.4 g l^{-1} de fraction argileuse ont été préparées à pH 7. La réduction de Hg(II) a été étudiée avec 2.5 nM de concentration initiale en Hg(II) total. Les suspensions ont été préparées avec ou sans addition de citrate de Fe(III) (FeCit). FeCit a été ajouté à une concentration de 1mM pour étudier l'influence du Fe(II), produit par réduction microbienne du Fe(III), sur la production de Hg°.

Dans les suspensions anoxiques de sol hydromorphe, dans lesquelles FeCit avait été introduit, une production de Hg° a lieu pour les échantillons de sol prélevés à 30-40 cm, 60-70 cm et 90-100cm de profondeur. Après une heure de réaction, la plus forte production de Hg° est observée pour l'échantillon de sol prélevé à 90-100 cm profondeur (Figure 11). Sans FeCit, une production significative de Hg° n'est observée que pour l'échantillon prélevé à 90-100 cm. Nous observons donc que la présence de FeCit augmente la production de mercure gazeux. Les constantes cinétiques sont réunies dans la Table 1d. Les constantes pour l'échantillon de sol hydromorphe collecté entre 90 et 100 cm de profondeur sont du même ordre de grandeur que celles obtenues pour la réduction de Hg(II) par Fe(II) en présence de particules d'hématite et de mica. Dans toutes les suspensions dans lesquelles FeCit avait été introduit la concentration en Fe(II) était d'environ 0.5 mM. La complexité du système ne permet pas de déterminer le mécanisme exact de la production de Hg° dans les sols hydromorphes. Nous supposons cependant qu'une réduction biotique, ainsi qu'une possible réduction abiotique par Fe(II) semblable à celle observée en présence de particules d'hématite et de mica, sont responsables des transformations redox du mercure dans ce sol et de l'appauvrissement des sols hydromorphes en mercure.

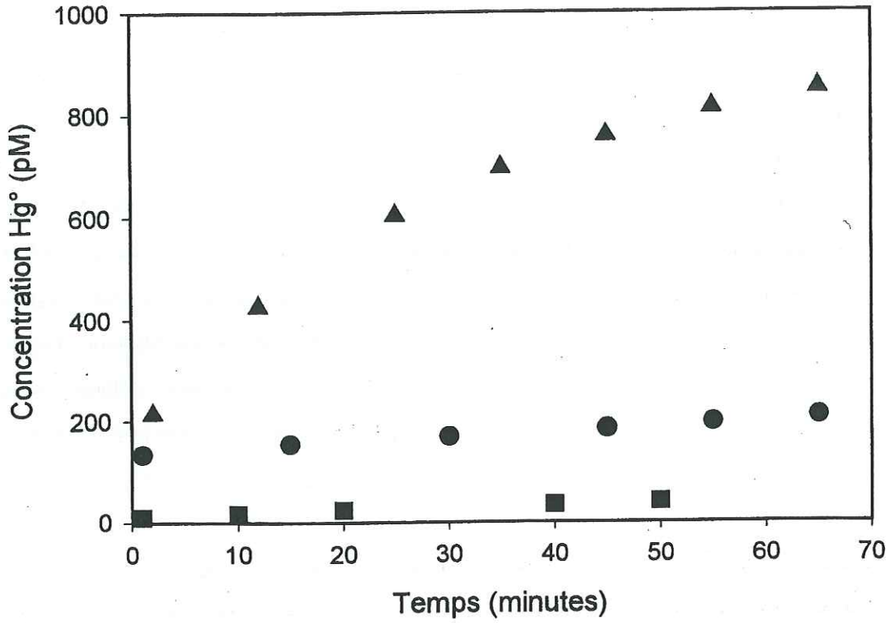

Figure 11. Production de Hg° dans les suspensions de 0.4 g l^{-1} de sols hydromorphes de à pH 7, avec 2.5 nM de concentration initiale en Hg(II) total et 1 mM de FeCit pour des échantillons de sol prélevés 3 trois profondeurs différentes: 30-40cm (●), 60-70cm (■), 90 – 100 cm (▲).

CHAPITRE 2

A short review of biogeochemical cycles of mercury

Mercury is a group 12 transition metal with a closed shell electronic configuration ($5d^{10}6s^2$). Elemental mercury is a silver-white liquid. In nature, mercury mainly occurs as a sulfide (cinnabar), and occasionally as a chloride or as an oxide. Elemental mercury is produced by heating mercury ores (cinnabar) to liberate Hg° vapor followed by condensing the vapor to liquid Hg *(4)*. All mercury compounds are toxic, especially methylmercury. Threshold level of mercury in drinking water is 2 $\mu g\ l^{-1}$, mercury vapor should not exceed 0.1mg m^{-3} in air *(15)*.

2.1 The global mercury cycle

In the atmosphere, mercury occurs primarily as inorganic compounds under two oxidation states : Hg° and Hg(II). Methylated mercury has also been reported at trace levels (< 3% of the total atmospheric mercury) *(16)*. Hg° constitutes the bulk of mercury in the atmosphere (95 to 100 %) and is predominant in the gaseous form *(17)*. Hg(II), on the other hand, tends to be present in atmospheric waters, either dissolved, or adsorbed onto particles in droplets. To date, the identified transformation pathways of atmospheric mercury include the reactions in gaseous and aqueous phase oxidation by ozone, O_3, *(18)*, aqueous phase reduction of Hg(II) by sulfite, SO_3^{2-}, *(19)*, aqueous phase oxidation of Hg° by hydroxyl radicals, $^{\cdot}OH$, *(20)*, aqueous phase oxidation of Hg° by chlorine, $HOCl/OCl^-$ *(21)*, gaseous phase oxidation by nitrate radical, $NO^{\cdot}_3$; peroxide, H_2O_2 *(22)*. Some of the Hg(II) produced in the atmosphere is re-reduced by mechanisms involving photoreduction of Hg(II) inorganic species *(12)*.

The return of mercury from the atmosphere to the Earth's surface occurs chiefly via wet precipitation of dissolved Hg(II). Since Hg° oxidizes relatively slowly to the mercuric state Hg(II), its residence time in the atmosphere is on the order of a year *(8)*. This is a sufficient time for atmospheric mercury to be distributed over the entire planet before returning to the Earth's surface.

Once oxidized, 60% of Hg(II) is deposited into terrestrial environments and 40 % to aqueous systems *(23)*. In oceanic waters, it undergoes a complex set of chemical and biological transformations, most of the Hg(II) is reduced to Hg° and returned to the atmosphere (Figure 1). Particulate scavenging and removal to the deep ocean (i.e., below 1000 m) is much less and does not exceed 1 Mmol yr^{-1} *(23)*. In lakes, the main loss mechanisms for mercury are sedimentation and gas evasion. Similar processes occur on land, resulting apparently in a smaller return of reduced mercury to the atmosphere and a greater permanent burial in soils (Figure 1).

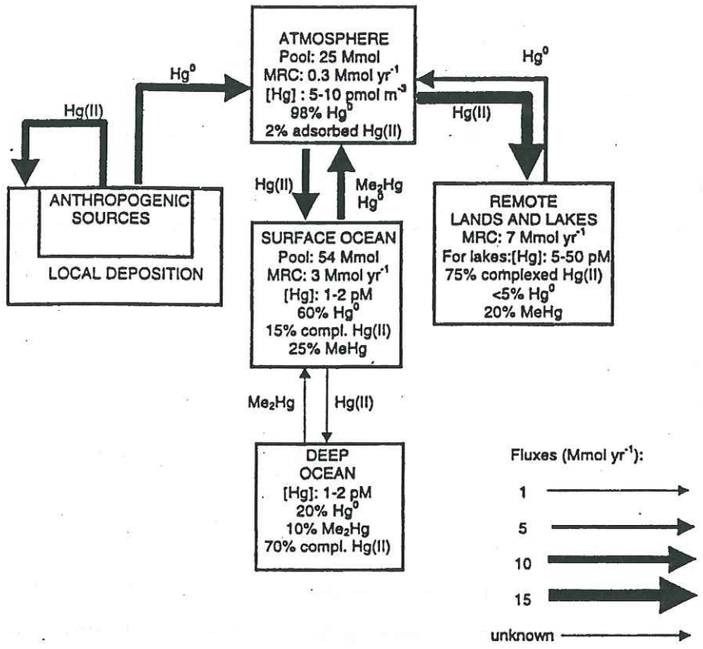

Figure 1. Global mercury cycle (taken from Morel et al, *(8)*).

2.2 Mercury speciation in natural waters

In natural waters, mercury exists in various chemical forms, i.e., elemental mercury (Hg°), inorganic species (Hg^{2+} and complexes with OH^- and Cl^- ligands), organomercurial complexes (monomethylmercury CH_3Hg^+, dimethylmercury $(CH_3)_2Hg°$), thiocomplexes (HgSR), complexes with humic and fulvic acids. In anoxic waters, mercury speciation may be dominated by sulfide and bisulfide complexes. HgS(s), cinnabar, is a particulate mercury species that is buried in sedimens and controls Hg(II) solubility in anoxic waters *(8)*. Principal mercury transformations in natural waters are summarized in Figure 2.

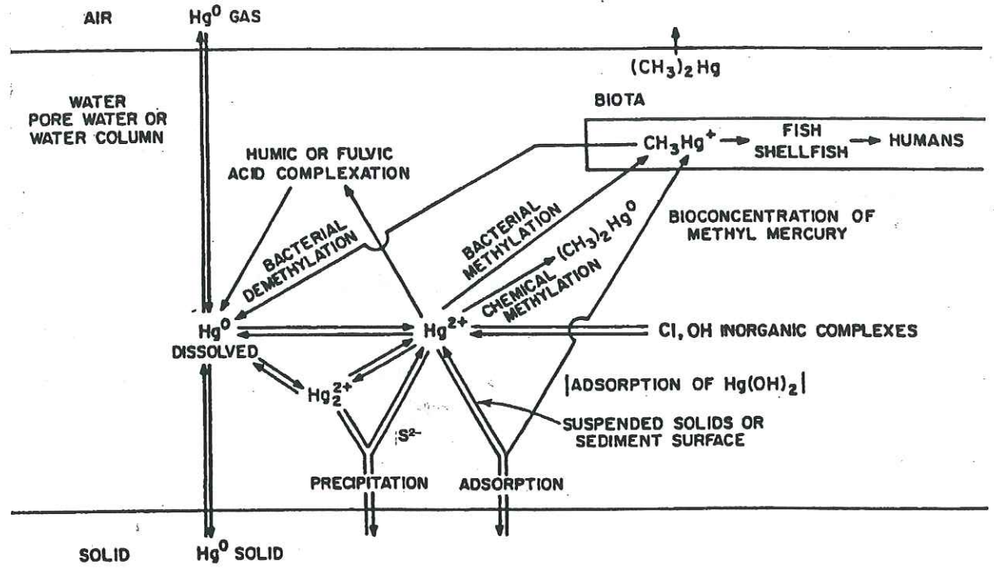

Figure 2. Schematic of mercury reactions in natural waters including bioaccumulation, precipitation, methylation and redox reactions (taken from Schnoor *(24)*).

2.2.1 Hg° production in surface oxic waters

Concentrations of Hg° are typically between 10 fM and 1 pM in natural waters. Usually, concentrations of Hg° are higher near the air-water interface with little elemental mercury found in anoxic sulfidic waters *(23)*. Natural waters are usually supersaturated in Hg°(aq) compared to the air above, and volatilization thus results in a flux of Hg° from the water into the atmosphere. This oversaturation is maximal during summer days, when photoreduction of Hg(II) in surficial waters is at its peak.

Reduction of Hg(II) to Hg° may be affected by biological and chemical (abiotic) processes. Some abiotic mechanisms of photoreduction of mercury species are discussed in details by Nriagu *(12)*. They may include direct photolysis, photoreduction involving inorganic particles and organic matter.

In the direct photolysis, the Hg species absorbs the incident solar energy and is reduced in its excited state. This can occur because many Hg species, such as complexes with OH^-, HS^-, Cl^-, and methylmercury compounds can absorb radiation in the high energy UV range (270-400 nm) of solar spectrum. Kunkely et al, *(25)* suggested that the UV absorption is

of the ligand-to-metal charge transfer (LMCT) type, and that the 6s orbital of Hg(II) is assumed to be the acceptor orbital. Typically, the photons initiate a series of electron transfer reactions that result in the formation of reduced Hg ion and a free ligand radical.

Although homogeneous photochemical reduction of some mercury species, for instance $Hg(OH)_2$ and HgS_2^{2-}, was shown to occur in laboratory *(26)*, its significance in natural waters is still not clear. The efficiency of the photoreduction depends on concentration of reducible Hg(II) complexes. In lakes with high concentrations of dissolved organic matter (DOC), DOC seems to act as a competitive inhibitor of solar radiation, reducing the availability of ultra-violet for photoreduction of Hg radiation *(27)*. The formation of strong Hg chloride complexes presumably reduces the production of Hg° in seawater compared to freshwater. Thus, abiotic direct Hg° production in seawater ($0.5 \cdot 10^{-7}$ s^{-1}) is only about 40 % of the rate in distilled water ($1.2 \cdot 10^{-7}$ s^{-1}) and is also lower than in lakewater $(1.2 \pm 0.7) \cdot 10^{-7} s^{-1}$ *(28)*.

It is likely that the photoreduction of Hg natural waters is indirect, mediated by iron or manganese photoredox reactions as suggested by Nriagu *(12)*. Fe and Mn oxides have semiconducting properties; when a semiconducing particle is exposed to light of a wavelength more energetic than its band gap, an electron is excited from the valence gap into the conduction band leaving a hole in the valence band. In the case of iron oxide, the formation of the electron/hole pair can be schematized as:

$$Fe_2O_3 + h\nu \rightarrow Fe_2O_3 (e^- \ldots h^+) \rightarrow e^-_{cb} + h^+_{vb} \qquad (1)$$

where Fe_2O_3 and $Fe_2O_3 (e^- \ldots h^+)$ are iron oxide in the natural and photoactive states, e^-_{cb} is a conduction band electron and h^+_{vb} is a valence band hole. Photochemical reductive dissolution of iron oxide may occur heterogeneously at the surface of the semiconducting particle,

$$e^-_{cb} + Fe_2O_3 + h\nu \rightarrow \{Fe_2O_3\}^* \rightarrow Fe^{2+} + \text{products} \qquad (2)$$

or homogeneously by the photolysis of dissolved metal species

$$Fe(OH)_2^+ + h\nu \rightarrow \{Fe^{2+}(OH)_2\}^* \rightarrow Fe^{2+} + 2OH^{\cdot} \qquad (3)$$

where $\{Fe_2O_3\}^*$ and $\{Fe^{2+}(OH)_2\}^*$ refer to complexes in the exited state. For the reactions above to proceed, they must be linked to the oxidation of organic compounds (or appropriate charge acceptors) by the holes. The Fe^{2+} so formed can reduce the adsorbed Hg(II) or Hg(II) ions in solution:

$$Fe^{2+} + Hg^{2+} \rightarrow Hg^\circ + Fe^{3+} \qquad (4)$$

Since Fe^{3+} can then be reduced again, Fe essentially plays a catalytic role in the Hg reduction processes.

The ability of dissolved organic matter (DOM), especially humic (HA) and fulvic (FA) acids, to reduce mercury abiotically has been shown by Allard and Arsenie, 1991 *(29)*. These authors demonstrated that abiotic production of Hg° by humic acids is highest in the illuminated system devoid of oxygen and chloride ions. The lowest rates were found in an aerated system kept in the dark. The reduction was inhibited by the competing ions, Cl^- and Eu^{+3} (which forms complexes with HA). The inhibition of Hg° production by reducing the member of available complexation sites on HA by complexation with Eu would implicate an intra- molecular electron transfer process.

Solar radiation can be absorbed effectively by many dissolved organic compounds found in natural waters, including humic acids, fulvic acids, proteins, flavins, porphirin derivatives and organic pollutants. These organics can form complexes with Hg in solution. Once irradiated, {DOM}*, the molecule is excited to a new species which can release an electron $\{DOM^{\cdot} + e^-\}^*$. According to Nriagu *(12)*, the photoinduced reduction of mercury by DOM can be depicted as:

$$DOM + h\nu \rightarrow \{DOM\}^* \rightarrow \{DOM^{\cdot} + e^-\}^* + Hg^{2+}_{complexed}$$
$$\rightarrow DOM^{\cdot} + Hg^\circ \qquad (5)$$

The results of laboratory investigations presented by Zhang and Lindberg, *(30)* demonstrated that exposure of freshwater spiked with fresh Fe(III) (~ 5 or 10 μM) to sunlight led to significantly larger increases in dissolved gaseous mercury production than exposure without the spike. The authors propose that first, the sunlight-induced photochemical production of highly reducing organic free radicals through photolysis of Fe(III)-organic acid coordination compounds (Fe(III)-OACC), and then subsequent reduction of Hg(II) by the organic free radicals could take place:

$$Fe(III) + \text{natural organic acid} \rightarrow Fe(III)\text{-OACC} \qquad (6)$$

$$Fe(III)\text{-OACC} + h\nu \rightarrow Fe(II) + \text{organic free radicals} \qquad (7)$$

$$\text{organic free radicals} + Hg(II) \rightarrow Hg^\circ + \text{products} \qquad (8)$$

Comparison of the mechanisms of Hg(II) reduction by dissolved organic matter, proposed by Nriagu *(12)* and Zhang and Lindberg, *(30)*, demonstrates several pathways of the transformation. Complexed mercury can be reduced directly by the electrons photoproduced by the DOM or/and aqueous mercury can be reduced by organic radicals formed through Fe(III)-organic acid coordination compounds. The latter mechanisms suggest that Fe species in freshwaters may be influential in Hg aquatic chemistry.

Part of the light dependence of the reduction may result from the activity of photosynthetic phytoplankton and cyanobacteria. As shown in laboratory experiments with

seawater and freshwater by Mason et al, *(28)*, phytoplankton is capable of reducing Hg(II) to Hg°, but the rate of reduction (0.16 – 2.05 pmol μg^{-1} chl a day^{-1}, where chl a is chlorophyll a) is insufficient to account for the observed reduction rates in the incubated field samples of freshwater (5.2 – 120 pmol μg^{-1} chl a day^{-1}). Bacteria are thus presumably the more important Hg(II) reducers. In seawater, the evidence suggests that cyanobacteria could be important reducers.

Production of elemental mercury in bacteria can be important in the environments with high mercury concentrations. The principal mechanism include the *mer* - operon in bacteria *(7, 31)*. As discussed by Morel et al, *(8)*, natural mercury in surface waters occurs in the low picomolar concentration range, and its reduction seems to be effected chiefly by photochemical processes, whereas in polluted waters, where the mercury concentration exceeds 50 pM (the threshold value), microbial reduction by the mer-operon mechanism likely becomes the predominant mechanism of Hg(II) reduction.

The mer-operon consists of a series of enzyme-encoding genes whose transcription is activated by Hg(II). These enzymes include a MerT membrane protein that transports Hg(II) into the cell and a MerA reductase that reduces Hg(II) to Hg° *(8)*. The mercuric reductase enzyme has a flavine adenine nucleotide moiety (FAD) and a thiol reagent for enzyme activity. In a reductive mechanism, the coenzyme nicotinamide adenine dinucleotide phosphate (NADPH), an electron-storing compound, is participating . The schematic diagram of Hg(II) enzymatic reduction mechanism is shown in Figure 3.

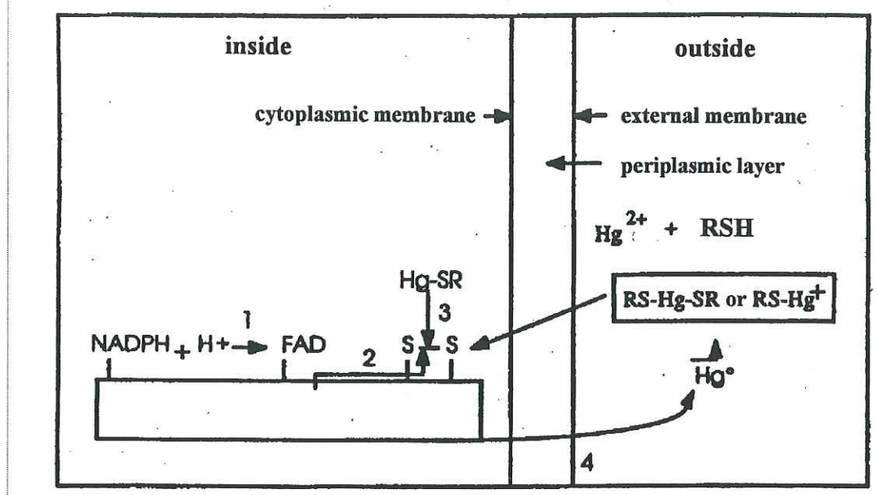

Figure 3. Schematic diagram of Hg(II) enzymatic reduction mechanism (taken from Robinson and Tuovinen,*(32)*) .

Some mer operons carry a gen, MerB, that supports bacterial resistance to organomercury compounds. The MerB enzyme catalyzes the hydrolysis reactions (Figure 4), leading to the formation of Hg(II), which is reduced by mercuric reductase *(7)*.

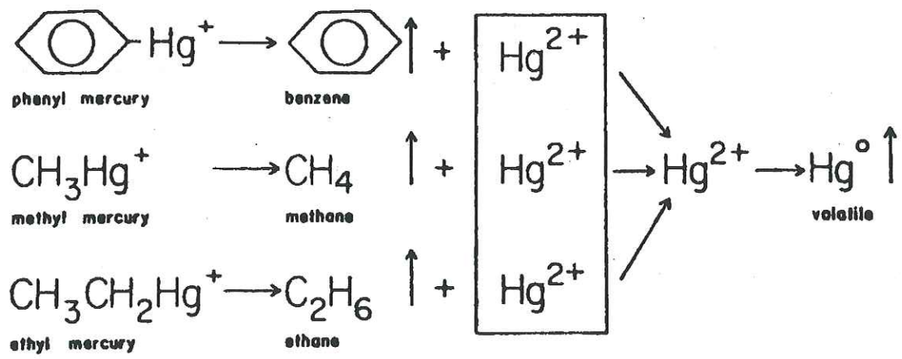

Figure 4. The detoxification of Hg(II) and organomercurials (from Summers and Silver, *(31)*).

2.2.2 Hg° production in anoxic waters

In anoxic waters, mercury also can be reduced by bacterial activity *(7)*. To date, not a lot of information is available on Hg(II) abiotic reduction in anoxic waters. The results of Allard and Arsenie, *(29)* show that reduction of Hg(II) may take place by humic acids in the system devoid of oxygen, suggesting the influence of organic matter in anoxic redox processes.

2.2.3 Hg° back oxidation

Elemental mercury was considered to be relatively unreactive *(8, 33)* and Hg° chemical transformations have not been much studied. Recently, Amyot et al, *(34)* observed that dissolved Hg° can undergo dark oxidation at a significant rate in the presence of high Cl^- concentrations. Zhang and Lindberg, *(30)*, observed a decrease in Hg° concentration during the storage of the water samples in the dark after sunlight exposure, suggesting the oxidation of Hg° by photochemically originated oxidants (e.g., $^{\cdot}OH$). Lalond et al, *(33)* carried out investigations in order to identify the parameters that control the photooxidation of Hg° and to assess the possible importance of this process in aquatic systems. Significant oxidation was observed in UV-B irradiated artificial solutions and natural samples containing both chloride ions and benzoquinone. These results indicate that processes of Hg° oxidation in natural waters should not be ignored and observed production of Hg° represent a net balance between Hg(II) reduction and Hg° oxidation.

CHAPITRE 3

Anthropogenic sources of mercury

3.1 ANTHROPOGENIC INFLUENCE ON GLOBAL MERCURY CYCLING

Human activities now have major impact on the global and regional cycles of most of the trace elements *(35)*. The estimations of Mason et al, *(23)* of the current and premodern global mercury cycles (Figure 1) demonstrate that the annual direct anthropogenic Hg release to the atmosphere is equal to 4000 tons (20 Mmol) and total Hg emission is 7000 tons yr^{-1} (35 Mmol). The premodern global mercury cycle (Figure 2b) corresponds to the 1890 period. A comparison of these simulations provides a revealing and insightful assessment of the extent to which anthropogenic Hg emissions may have perturbed the mercury cycle over the past century. It is evident that terrestrial systems, ocean waters and the atmosphere should be significantly contaminated with Hg released by human activities over the 100 year period considered of these mass balances.

The principal anthropogenic sources of mercury are from electricity generation through coal and oil burning, solid and urban wastes, agriculture and forestry practices, metal production, chlor-alkali, and pulp industries *(35-37)*. Natural inputs to the atmosphere include degassing and wind entrainment of dust particles from land, volcanic eruptions, forest, fires, biogenic emissions of volatile and particulate compounds, and degassing from water surfaces *(8, 38)*.

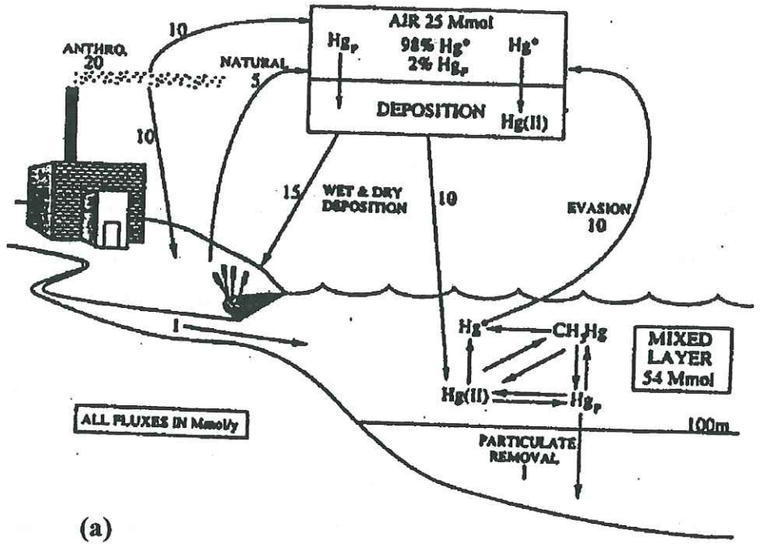

(a)

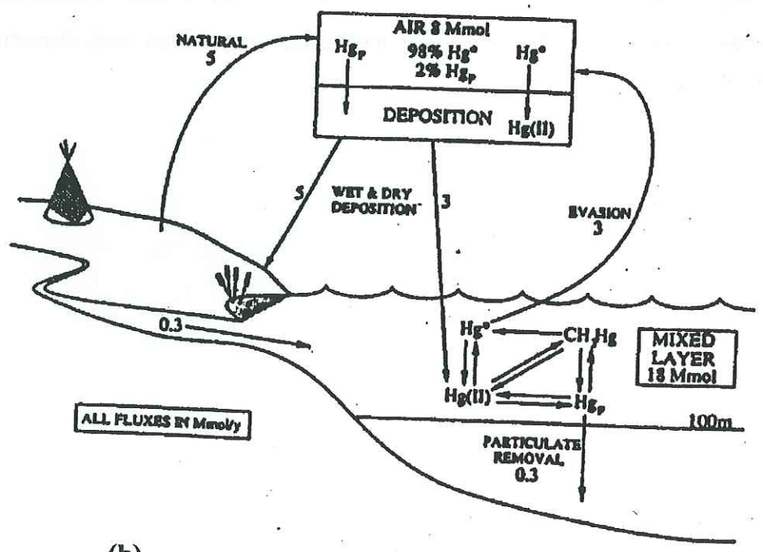

(b)

Figure 1. (a) The current global Hg cycle; (b) a premodern view of the global Hg cycle (taken from Mason et al, *(23)*)

3.2 MERCURY UTILIZATION IN TROPICAL COUNTRIES

In Latin America, the main anthropogenic source of mercury is the gold mining activity, where mercury is used in amalgamation step. Amalgamation is the preferred method used by artisanal gold miners in Latin America because mercury is an effective (extract more than 90 % of gold from gravity concentrates), simple and very inexpensive reagent to extract gold (1 kg of Hg costs 1 g of Au) *(2)*.

The various procedures presently in use can be grouped into two large categories *(1)*.

The first one involves the recuperation of gold from soils and rocks, whereby the content of gold ranges from 4 to 20 g ton^{-1}. This procedure consists of digging up large amounts of metal-rich material, passing it through grounding mills, and centrifuging to produce a metal-rich concentrate (Figure 2). This procedure may result in pronounced deforestation along rivers. The concentrate is moved to small amalgamation ponds (a few square meters) or to the amalgamation drums, where it is mixed with liquid mercury and separated later in round pans. The Hg-Au amalgam is then squeezed to remove excess Hg and taken to a retort for roasting. Unfortunately, the use of retort, although cheap and simple, is far from being a common practice in most mining regions. Instead, amalgam is more frequently roasted in pans in open air, thus releasing the entire Hg content of the amalgam directly to the atmosphere. After an area is exhausted, tailings are left with spots of high Hg concentrations located in previous amalgamation ponds. This method is widely used in central Brazil and northeastern Amazon, and southwest Colombia.

The second typical process is carried out in most Amazonian rivers (Figure 3). Gold is extracted from bottom sediments by dredging. The gold-bearing material passes through iron nets of different mesh sizes to remove large stones. The material is then passed through carpeted riffles which retain heavier particles. This operation lasts for 20 to 30h, then the dredging stops and the heavy fraction is collected in barrels for amalgamation, which can be done by hand or by using mechanical stirres. However, residues of the procedure are released into rivers, vaporization of mercury and losses due to poor handling also occur.

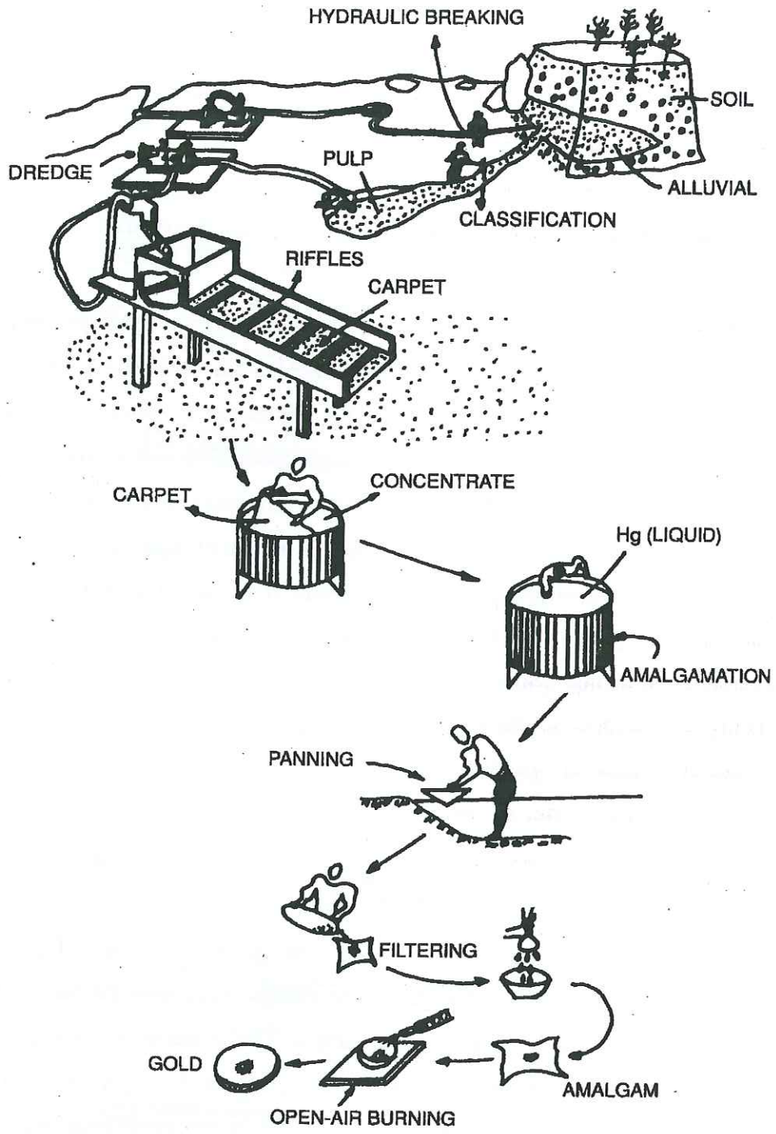

Figure 2. Steps in gold production and Hg utilization in soil and rock mining (taken from Lacerda and Salomons *(1)*).

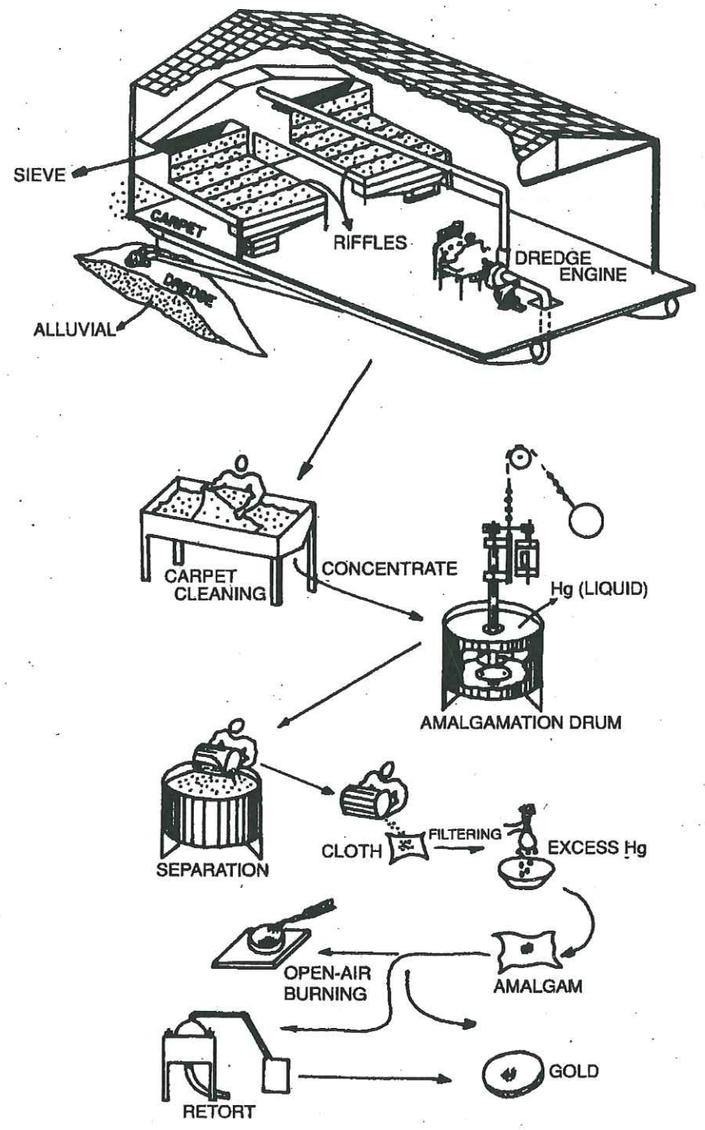

Figure 3. Steps in gold production in river mining typical of Amazon rivers (taken from Lacerda and Salomons, *(1)*).

The emission of mercury to different environmental compartments during the whole extraction processes has been studied by some authors. Pfeiffer and Lacerda, *(39)* estimated that the major proportion of Hg loss is during the burning of the amalgam (50 to 60 % of the

total Hg loss). 40 to 50 % of Hg is lost to rivers during the amalgamation process as metallic mercury. The emission factor is estimated to be circa 1.32 kg.

It is estimated that as many as 1 million artisanal miners are currently mining for gold in Latin America, producing about 200 tonnes of gold emitting over 200 tonnes of mercury annually to the environment *(2)*.

REFERENCES BIBLIOGRAPHIQUES

Pour les chapitres 1 à 3

(1) Lacerda L.D.,Salomons W., (1998). *Mercury from gold and silver mining: a chemical time bomb?* Springer. 146 p.

(2) Veiga M.M. *Mercury in artisanal gold mining in Latin America: facts, fantasies and solutions*. in *UNIDO- Expert group meeting- Introducing new technologies for abatemeny of global mercury pollution deriving from artisanal gold minig*. 1997. Vienna.

(3) Veiga M.M., Hinton J., Lilly C. *mercury in the Amazon: a comprehensive review with special emphasis on bioaccumulation and bioindicator.* in *Proc. NIMD(National Institute for Minamate disease)*. 1999. Minamata, Japon.

(4) Emsley J., (1998). *The elements*. Clarendon press. 292 p.

(5) Roulet M., Lucotte M., Canuel R., Rheault I., Tran S., De Freitos Gog Y.G., Farella N., Souza do Vale R., Sousa Passos C.J., De Jesus de Silva E., Mergler D., Amorim M., (1998). *Distribution and partition of total mercury in waters of the Tapajos River basin, Brazilian Amazon.* The sciecnce of the Total Environment, 213: p. 203-211.

(6) Roulet M., Lucotte M., Saint-Aubin A., Tran S., Rheault I., Farella N., De Jesus Da Silva E., Dezencourt J., Sousa Passos C.-J., Santos Soares G., Guimaraes J.-R., Mergler D., Amorim M., (1998). *The geochemistry of mercury in central Amazonian soils developed on the Alter- do- Chao formation of the lower Tapajos River Valley, Para state, Brazil.* The sience of the total environment, 223: p. 1-24.

(7) Baldi F., *Microbial transformation of mercury species and their importance in the biogeochemical cycle of mercury*, in *Metal ions in biological systems*, S.H. Sigel A., Editor. 1997. p. 213-257.

(8) Morel F.M.M., Kraepiel A.M.L., Amyot M., (1998). *The chemical cycle and bioaccumulation of mercury.* Annual Reviews Ecol.Syst., 29: p. 543-566.

(9) Mason R.P., Reinfelder J.R., Morel F.M.M., (1995). *Bioaccumulation of mercury and methylmercury.* water, air and soil pollution, 80: p. 915-921.

(10) Lucotte M, Schetangne R., Therien N., langlois C., Tremblay A., (editors), (1999). *Mercury in the biochemical cycle:natural environments and hydroelectric reservoirs of Nothern Quebec(Canada).* Springer. 334 p.

(11) (1991). *Mercury in the Swedish environment.* Water, air and soil pollution, 55: p. 261.

(12) Nriagu J.O., (1994). *Mechanistic steps in the photoreduction of mercury in natural waters.* The science of the total environment, 154: p. 1-8.

(13) Programme mercure en Guyane: region de Saint Elie et retenue de Petit Saut.. 2001.

(14) Liger E., Charlet L., Van Cappellen P., (1999). *Surface catalysis of uranium(VI) reduction by iron(II).* Geochimica et cosmochimica Acta., 63(19/20): p. 2939-2955.

(15) Office of water regulation and standards q.c.f.w., (1986). EPA-440/5-86-001, U.S. Environmental protection agency, Washington, DC p.

(16) Fitzgerald W. F., Mason R. P., Vandal G. M., (1991). *Atmospheric cycling and air-water exchange of mercury over mid-continental lacusterine regions.* Water, air and soil pollution., 56: p. 745-767.

(17) Fitzgerald W.,Mason R., *The global mercury cycle: oceanic and anthropogenic aspects*, in *Global and regional mercury cycles: sources, fluxes and mass balances*, e.a. Baeyens W., Editor. 1994. p. 85-108.

(18) Munthe J., (1992). *Aqueous oxidation of elemental Hg by O3.* Atmospheric environment, 26A: p. 1461-1468.

(19) Munthe J., Xiao Z.F., Lindqvist O., (1991). *The aqueous reduction of divalent mercury by sulfite.* Water, air and soil pollution., 54.

(20) Lin C.-J.,Pehkonen S.O., (1997). *Aqueous free radical chemistry of mercury in the presence of iron oxides and ambient aerosol.* Atmospheric environment, 31: p. 4125-4137.

(21) Kobayashi T., (1987). *Oxidation of metallic mercury in aqueous solution by hydrogen peroxide and chlorine.* Journal of Japan Society for air pollution, 22: p. 230-236.

(22) Lin C.-J.,Pehkonen S.O., (1999). *The chemistry of atmospheric mercury: a review.* Atmospheric environment, 33: p. 2067-2079.

(23) Mason R.P., Fitzgerald W.F., Morel F.M.M., (1994). *The biogeochemical cycling of elemental mercury: Anthropogenic influences.* Geochimica et Cosmochimica Acta, 58(15): p. 3191-3198.

(24) Schnoor J.L., (1996). *Environmental modeling: fate and transport of pollutants in water, air, and soil*. John Wiley&Sons. 682 p.

(25) Kunkely H., Horvath O., Vogler A., (1997). *Photophysics and photochemistry of mercury complexes.* Coordination chemistry reviews, 159: p. 85-93.

(26) Xiao Z.F., Munthe J., Stromberg D., Lindqvist O., *Photochemical behavior of inorganic mercury compounds in aqueous solution*, in *Mercury as a global pollutant- integration and synthesis*, Watras C.J. and Huchabee J.W., Editors. 1994, lewis Publishers. p. 581-592.

(27) Amyot M., Mierle G., Lean D., McQueen D.J., (1997). *Effect of solar radiation on the formation of dissolved gaseus mercury in temperate lakes.* Geochimica et cosmochimica acta., 61(5): p. 975-987.

(28) Mason R. P., Morel F. M. M., Hemond H. F., (1995). *The role of microorganisms in elemental mercury formation in natural waters.*

(29) Allard B.,Arsenie I., (1991). *Abiotic reduction if mercury by humic substances in aquatic system- an important process for the mercury cycle.* Water Air and Soil Pollution, 56: p. 457-463.

(30) Zhang H.,Lindberg S.E., (2001). *Sunlight and iron(III)-induced photochemical production of dissolved gaseous mercury in freshwater.* Environmental science and technology., 35: p. 928-935.

(31) Summers A.O.,Silver S., (1978). *Microbial transformations of metals.* Ann. Rev. Microbiol., 32: p. 637-672.

(32) Robinson J.B.,Tuovinen O.H., (1984). *Mechanisms of microbial resistance and detoxifation of mercury and organomercury compounds: physiological, biochemical, and genetic analysis.* Microbiological reviews, 48(2): p. 95-124.

(33) Lalonde J.D., Amyot M., Kraepiel A.M.L., Morel F.M.M., (2001). *Potooxidation of Hg(0) in artificial and natural waters.* Environmental science and technology., 35: p. 1367-1372.

(34) Amyot M., Gill G.A., Morel F.M.M., (1997). *Production and loss of dissolved geseous mercury in coastal seawater.* Environ. Sci. Technol., 31: p. 3606-3611.

(35) Nriagu J.O.,Pacyna J.M., (1988). *Quantitative assessment of worldwide contamination of air, water and soils by trace metals.* Nature, 333(12): p. 134-139.

(36) Lodenius M., (1991). *Mercury concentrations in an aquatic ecosystem during twenty years following abatement the pollution source.* Water, air and soil pollution, 56: p. 323-332.

(37) Chu P.,Porcella D.B., (1995). *Mercury stack emossions from U.S. electric utility power plants.* Water, Air and Soil Pollution, 80: p. 135-144.

(38) Nriagu J.O., (1989). *A global assessment of natural sources of atmospheric trace metals.* Nature, 338(2): p. 47-49.

(39) Pfeiffèr W.C.,Lacerda L.D., (1988). *Mercury inputs into the Amazon region, Brazil.* Environ.Technol.Lett,(9):p.325-330.

CHAPITRE 4

Biogeochemistry of a tropical reservoir lake (Petit Saut, French Guiana): implications for the mercury cycle.

T. Peretyazhko, P. Van Cappellen, M. Coquery, C.Meile, M. Musso, P. Regnier, L. Charlet

INTRODUCTION

Biogeochemical cycling of mercury has recently received considerable attention in the tropical countries of the South America due to a new gold rush in these countries over the last 20 years *(1)*. Amalgamation processes using mercury cause its discharge into river systems and into atmosphere *(2)*. Once discharged, it can be transported and deposited in terrestrial and aquatic environments, where it may undergo further reactions including methylation and assimilation by the biota *(3)*. This may be particularly significant in hydroelectric reservoirs, where concentrations of mercury in fish may be up to five times higher than in natural lakes *(4-8)*. The high levels of Hg in the biota in these reservoirs are believed to be due to the remobilization of Hg from inundated soils to the water column following microbial degradation of the terrestrial organic matter *(9)*. The building of tropical reservoirs is generally achieved by flooding of large areas of primary forests *(10, 11)*. It creates several serious environmental problems due to the high amounts of flooded organic matter released from soils and vegetation and geographic considerations, i.e. the elevated temperatures. Decay of vegetation left in tropical artificial reservoirs creates anoxic conditions, i.e. favorable conditions for greenhouse gases production and methylation of mercury *(10, 12)*. As it was shown by Roulet and Lucotte, *(13)* the forest soils of French Guiana contain relatively high Hg concentrations comparing to other Amazonian soils. Flooding of such soils lead to a release of mercury due to the microbial reduction of the Fe (hydr)oxides and to the migration of the organo-metallic complexes to the water of reservoir.

Mercury biogeochemical cycling in aqueous environment should be considered within the assemblage of various physical and chemical processes governing the temporal and spatial variability of reservoirs and natural lakes. The important variables include seasonal effects, such as mixing characteristics, biological productivity, sedimentation of algal blooms, the supply of elements from external sources, or redox conditions *(14-16)*.

The predominant mechanism driving to the development of anoxic conditions in lakes are plankton synthesis in surface waters and the bacterial degradation of organic matter in subsurface waters and sediments *(17)*. Organic matter degradation proceeds through a series of redox reactions in which oxidants (O_2, NO_3^-, MnO_2, $Fe(OH)_3$, SO_4^{2-}) are consumed theoretically in order of decreasing free energy yield *(18)*. In practice, the reaction sequence is subject to oxidant availability and kinetic constraints *(17)*. Elements may be affected by redox transformations in a variety of different ways. They may be adsorbed or assimilated by plankton in surface waters and released back into solution at depth, possibly in different redox

state. Alternatively, the elements may act directly as terminal electron acceptors in the microbial degradation of organic matter or the redox state may be altered by purely chemical redox reactions.

The occurrence of anoxic conditions causes a significant cycling especially of iron and manganese at the oxic/anoxic interface, due to changes in solubility related to the changes in oxidation state *(19)*. Under oxic conditions, Fe and Mn oxides, together with organic matter, are generally regarded as the most important scavenging or carrier phases for the labile trace element fraction in aquatic environments *(20, 21)*, while in anoxic conditions, sulfide precipitation can also play an important role in these processes. Thus, variations in redox conditions influence the chemical speciation and the cycling of the trace elements in the suboxic and anoxic environments through iron and manganese cycling, organic matter turnover or production of sulfide *(22)*.

The present work was carried out on equatorial hydroelectric reservoir Petit Saut, French Guiana during dry and wet seasons. The aim of this work was to study the seasonal changes in the principal physico-chemical parameters (dissolved oxygen, temperature, conductivity, pH), the fate of chemical species, including Fe(II), NH_4^+, S(-II), HCO_3^- and mercury distribution in the tropical reservoir Petit Saut. Together with field measurements the concept of turbulent diffusion was applied to estimate different mixing processes influence on mercury and other chemicals vertical distribution in the water column.

FIELD SITE AND METHODS

Study site: Petit Saut Reservoir.

The Petit Saut reservoir is located 50 km of Kourou on the Sinnamary river. The Sinnamary has its source in the central part of French Guiana, the Coursibo and the Tigre streams run into it before the Sinnamary flows into Atlantic ocean (Figure1). The reservoir covers 80 km of the river course. Its construction took place from 1989 to 1995. Impounding started in January 1994 and was completed in July 1995. The Petit Saut reservoir maximal depth is 35 m and water level varies between 35 and 31.5 m depending on hydroelectric station exploitation. Total water volume stored is $3.5 \cdot 10^9$ m^3, mean annual entrant water flow is 260 $m^3 s^{-1}$ *(23)* and average residence time of water in the reservoir is 5 months *(24)*.

During impounding approximately 350 km^2 of uncleared tropical forest were flooded. The Petit Saut is a huge zone of dead forest with dead trunks still emerging from water, and some areas of open water corresponding either to the deforestation areas or to ancient river-bed. Within the dam water-body the decomposition of submerged vegetation takes place, with slow degradation kinetics. According to observations made in other reservoirs located in Amazonian region, trees disappearance takes place by two processes: (1) rapid decomposition of crown constituents for 2-5 years, (2) slow disappearance of trunks during 20-50 years depending on wood hardness.

Possible localized sources of mercury contamination in Petit Saut reservoir include the upstream Saint Elie gold-mining area and impounded "Adieu Vat" former mining sites, located near Roche Genipa sampling site (Figure 1).

The climate is of humid tropical type. The annual rainfall, measured over 1999 is 3153mm. During dry season, from October to December precipitation was 350mm (Sissakian, personal communication)

The principal field measurements were carried at Roche Genipa (N 4°56'474", W53°02'468"), Coursibo (N 4°53'100", W 53°00'656") and Saint Eugene (N 4°51'250", W53°04'155") sites located along the Coursibo branch of Petit Saut reservoir (Figure 1). In this paper we mainly use data from Roche Genipa sampling site situated in the central part of the reservoir. Measurements were performed in June (wet season) and December (end of dry season) 1999.

Sample collection and analyses.

Physico-chemical characteristics

The major physico-chemical parameters, temperature, pH, dissolved oxygen, conductivity and Eh, along a vertical profile were recorded *in situ* with a YSI Multiparameter probe sonde 600XLM.

Mercury sampling and analysis

Samples were collected using a Teflon pumping system including an all-Teflon diaphragm pump and Teflon tubing. Water was transferred into Teflon bottles. The bottles were sealed using pliers and kept in double polyethylene bags until analyses. Before sampling

all bottles were washed in 5% HNO_3 for ten days and rinsed several times with Milli-Q water. Cleaned bottles were filled with Milli-Q water, acidified with ultrapure HCl (v/v 1%) and stored in double polyethylene bags until use. Sample collection was performed using polyethylene gloves for handling operations.

The reactive mercury (Hg_R) analysis were performed in field laboratory. It was determined by reduction with 20% $SnCl_2$ (w/v). The 50ml sample was purged for 7 min immediately after adding $SnCl_2$ with ultra-pure Ar and mercury concentration was determined after gold amalgamation by CVAFS detection. Detection limit was 35 pg/l.

Analysis of dissolved and particulate mercury (Hgd, Hgp) were carried out in IAEA laboratory (Monaco). Water samples for dissolved mercury analysis were filtered in the field through GF/F glass fibre filters (Whatman) and acidified to 0.5 % (v/v) with concentrated HCl (Merck Suprapur). The suspended particulate matter collected on GF/F filters was digested with concentrated HNO_3 and particulate mercury was determined after $SnCl_2$ reduction step. Dissolved mercury was determined after decomposition of dissolved organic mercury compounds by BrCl oxidation before the reduction step with $SnCl_2$. Filtration and analysis were carried out according to the protocol described by Quémerais and Cossa *(25)*.

Chemical characteristics

Samples were taken for dissolved iron(II), alkalinity, major cations and anions determinations.

Samples for Fe(II) measurements (10 ml) were immediately mixed with O-phenantroline and buffer pH 3.5 solutions and Fe(II) was analyzed calorimetrically *(26)* within 5 hours after sampling.

Alkalinity was measured within 12 hr after sampling. Samples were titrated by HCl $5 \cdot 10^{-3}$ M till pH=4 and alkalinity was determined by the Gran method *(18)*.

Samples for major cation determination were filtered (0.45μm) and acidified with HNO_3 and analyzed by ICP-AES. Major anions were analyzed by capillary electrophoresis with Waters Capillary Ion Analyzer.

Mixing processes

Mixing of solutes in the Petit Saut is described here with the concept of turbulent diffusion, where the flux of a solute is expressed as the product of a vertical turbulent diffusion coefficient, K_z ($m^2\ s^{-1}$), and the concentration gradient.

Eddy diffusivities in the permanently stratified reservoir Petit Saut are estimated based on wind speed data and temperature profiles, measured in both dry and wet season at Roche Genipa site.

In well-mixed surface layer turbulence is assumed to be wind driven and K_z is estimated by *(27)*:

$$K_z = \gamma_{mix}\left(\frac{\rho_{air} C_{10}}{\rho}\right)^{3/2} \frac{w_{10}^3}{N^2 kh} \qquad (1)$$

where γ_{mix} is the non-dimensional mixing efficiency, typically within the range 0.05-0.25 depending on the mixing regime; a value of 0.15 was assumed here. W_{10} is the wind speed ($m\ s^{-1}$) at 10 m altitude, about 5 $m\ s^{-1}$ in both dry and wet seasons *(24)*. The wind-stress coefficient C_{10} is approximately 0.001 for $w_{10} \leq 7\ m\ s^{-1}$ *(27)*. N is the stability frequency (s^{-1}), defined as $N = \left(-\frac{g}{\rho}\frac{d\rho}{dh}\right)^{1/2}$, k = 0.41 is the Karman constant, h is depth (m), and ρ and ρ_{air} are the densities of water and air ($kg\ m^{-3}$), respectively.

Equation (1) is used to estimate the K_z value at the lower boundary (3 to 5m depth) of the well-mixed epilimnion, K_{z0}. Below, temperature, measured in dry and wet seasons, is used as a conservative tracer in order to determine the mixing profile from:

$$K_{z0} * (dT/dx)_0 = K_{zi} * (dT/dx)_i \qquad (2)$$

where T is temperature and (dT/dx) is the temperature gradient.

The effect of changing mixing intensities alone was determined by numerically solving the steady state concentration profiles due to mixing only, defined by $0 = \frac{\partial}{\partial x}\left(K_z \frac{\partial C}{\partial x}\right)$, and applying fixed concentration boundary conditions, obtained from the measured profiles at the lower end of the mixed surface layer (3-5 m) and at the lake bottom. Differences between these "conservative" profiles and measured concentrations thus indicate depth of consumption or production.

The upper boundary condition was equal to the measured concentration at the layer between 3 and 5 m, the lower boundary condition was adjusted to get the best fit. Profiles of

Hgd were fitted with the following boundary conditions: 5 pM at 3 m and 12 pM at 32 m in wet season and 2 pM at 4 m and 16 pM at 27 m in dry season, i.e. the lower boundary conditions for Hgd are close to the measured concentrations at the bottom layer. For Fe(II) vertical profiles we applied the following fixed boundary conditions: 0 μM at 3 m and 7.5 μM at 32m in wet season and 0 μM at 4 m and 40 μM at 27 m in dry season. For alkalinity vertical distribution the boundary conditions were 103 μM at 4m and 120 μM at 27 m in dry season. In the wet season alkalinity changes slightly with depth in the hypolimnion (Table 1) and could not be described by mixing phenomena. For alkalinity and Fe(II) vertical distributions measured in the dry season, the lower boundary condition was much less than the measured concentration at the bottom layer.

Ammonium and sulfide profiles were measured in September 1999 (S(-II)), December 2000 (S(-II) and NH_4^+) and June 2001 (NH_4^+) by HYDRECO laboratory (S. Richard, personal communication). In order to calculate the conservative curves for these to species, we first recalculated the temperature profiles for dates when S(-II) and NH_4^+ concentration profiles were measured. Temperature profiles were reproduced well with the K_z values obtained in June 1999 for wet season temperature vertical distributions and December 1999 for dry season. This allows us to use the K_z series to compute S(-II) and NH_4^+ vertical profiles. For S(-II) we applied the following fixed boundary conditions: 0 μM at 5 m and 3.2 μM at 32 m in wet season and 0.39 μM at 8m and 2.7 μM at 32 m in dry season. For NH_4^+ the boundary conditions were 0 μM at 5 m and 40 μM at 32m in wet season and 0 μM at 5 m and 91 μM at 27 m in dry season.

RESULTS AND DISCUSSION

A. Physical chemistry of the lake

Dissolved O_2 profiles are presented in Figure 2a. Two zones could be observed in the reservoir: a well oxygenated upper part and a lower anoxic part. In wet season, O_2 oversaturation is detected in the surface waters and, in dry season, surface O_2 concentration is closed to saturation. Oxygen concentration starts to drop sharply from 7.2 to 0.1 mg/l and from 6.8 to 0.1 mg/l in the transition zone located from 2.6 to 4 m and from 3 to 5 m depth, in wet and dry seasons, respectively.

The water pH in the oxic part of the water column is circum neutral, close to 6.8, and becomes slightly acidic in anoxic waters with a pH 5.8 average value for the hypolimnion, in both seasons (Figure 2b).

Temperature profiles are fairly constant with season (Fig.2c): at Roche Genipa, surface water temperature varies between 30 and 31^{0}C between June and December, i.e. it is slightly cooler during the wet season, and temperature in the water column below 15 m is constant (25.1 - 25.4°C). Average air temperature is 31°C.

Conductivity profiles (Figure 2d) strongly depend on the season. It jumps from 0.022-0.027 mS/cm at and above the oxycline to 0.057 mS/cm in bottom waters, in dry season. In wet season conductivity varies much less, and is equal to 0.022 mS/cm in surface waters and to 0.027 mS/cm at the bottom.

Measured Eh (data not shown) varies from 350 mV in the oxic layer to 70 mV in the anoxic layer in wet and dry seasons.

B. Physical structure of the lake

Size and shape of Petit Saut reservoir, external forcing (wind stress, precipitation, river inflow, regulation of reservoir output, etc.,) and stratification are factors that determine the physical structure of the artificial lake.

Vertical profiles of turbulent diffusion coefficient, K_z, in the hypolimnion are shown in Figure 3. The obtained K_z profiles suggest a difference of mixing regimes in dry and wet seasons. In dry season, a nearly constant K_z value is observed from 15 m down to the lake bottom and corresponds to the part of water column with constant temperature and density (Figure 2c). In wet season, mixing is likely to be significantly more intense in the bottom layer.

One of the important factors affecting vertical mixing could be the seasonal variation of precipitation. Precipitations measured during the nine months of wet season 1999 was 2800 mm (with 507 mm in June only) while during the dry season 1999 they were 350mm (with 263 mm in December). Possible massive rain water influx in the deeper waters of the reservoir can be caused by the difference in water density of lake water and precipitation. Rain water temperature is about 25-26°C and thus has a higher density than surface water (whose temperature is around 30 to 31°C). On the contrary, rainwater and hypolimnion waters have same temperature. Thus, it appears to penetrate by density below the surface layer and to be the cause a high degree of mixing in the both the epilimnion and the hypolimnion *(27)*.

According to these phenomena we propose that the observed difference, between wet and dry seasons, of water mixing in the layer between 4 and 11 m (Figure 3) is mainly due to strong precipitation and inflow of water between warm epilimnic waters and cold hypolimnic waters, while turbulence observed in the bottom layer (22- 35 m) is due to an increased input of the Coursibo, the Tigre and the Sinnamary inflow river waters during the wet season, as no groundwater inputs in the Petit Saut reservoir is found.

The high turbulence of bottom waters can cause the resuspension of sediment particles in lake deep waters. The distribution of suspended matter is shown in Figure 4. In dry season the highest SPM concentrations, 5 mg/l occurred in the surface waters and it decreases down to ~1 mg/l near 9 m to be homogeneous throughout the water column below 9 m, where the particle concentration is lower than 0.5 mg/l. However, the particle distribution changes dramatically in the wet season. The suspended matter concentration was maximum in the surface waters (8 mg/l), then decreased down to 3 mg/l near 5 m, to finally increase sharply in the bottom layer of the reservoir up to 7 mg/l. The driving force for the SPM concentration increase in the bottom waters is expected to be the high turbulence of bottom waters. According to Figure 4, two fluxes of particles could be determined: one downward (during dry and wet seasons) and one upward (only during the wet season).

Different mixing processes in Petit Saut reservoir define five boxes in the water column. The first box is the epilimnion, a well mixed compartment, which coincide with the oxic layer. In the second "box" or transition zone, the oxycline is located. The three "boxes" of anoxic waters correspond to (i) a linear increase of K_z(III box), (ii) a constant K_z (IV-V boxes in dry season and IV in wet season) and (iii) a maximum K_z (V box in wet season). The chemical composition and physico-chemical parameters of each "box" are summarized in Table 1. A conceptual model of the Coursibo- Sinnamary branch of Petit Saut reservoir is shown in Figure 5. Mixing through river inflow and precipitation can change the physical structure of lake and, consequently, may influence chemical transformations and speciation of solute and contaminants in the lake. The well developed oxycline and the sediment/water interface play an important role in biogeochemical cycling of elements, including bacterially mediated redox transformations, reactions of adsorption/desorption and precipitation *(17)*.

C. Oxic/anoxic transition

The sharp decrease of dissolved oxygen concentration takes place in the transition zone (II, Table 1) and O_2 is depleted completely at depth 4 and 5m in wet and dry seasons,

respectively. Subsequent to the disappearance of oxygen, reduced species, such as NH_4^+, Fe(II), S(-II), CH_4 and traces of Mn(II) appear in the hypolimnion.

Gradients and fluxes of reduced species and dissolved oxygen are presented in Table 2. Calculated gradients of NH_4^+ and S(-II) do not change with season whereas Fe(II) and CH_4 gradients are larger in dry season. We did not include the Mn(II)/MnO_2 couple in the consideration of redox transformations because its concentration in the water column never exceeded 1.3 µM.

Results for O_2 demonstrate that the ratio of gradients of two seasons is 1.8 whereas flux ratio is 5.2, a difference is due to large K_z difference between the two seasons. Fluxes of reduced species, in the contrary, do not change strongly with seasons except for NH_4^+ which is three times higher in the wet season than in the dry season.

Figure 6 shows distribution of some reduced species (Fe(II), NH_4^+ and S(-II)). The total flux of electrons from reduced species is equal to $104 \cdot 10^{-8}$ and $70 \cdot 10^{-8}$ mol m^{-2} s^{-1} in wet and dry seasons, respectively. These values are much lower than O_2 fluxes in both seasons ($1080 \cdot 10^{-8}$ mol m^{-2} s^{-1} and $208 \cdot 10^{-8}$ mol m^{-2} s^{-1} electron fluxes in wet and dry seasons, respectively). The difference suggests that the principal consumption of dissolved oxygen is the biological decomposition of organic matter.

The following chemical transformations occur in the lower oxycline (box II) according to the thermodynamic redox sequence *(18)* and Figure 6:

Aerobic respiration: $\{CH_2O\} + O_2 = CO_2 + H_2O$ (3)

Nitrification: $NH_4^+ + 2O_2 = NO_3^- + H_2O + 2H^+$ (4)

Ferrous oxidation: $8Fe^{2+} + 7O_2 + 4H^+ + 10H_2O = 8Fe(OH)_3(s)$ (5)

Sulfide oxidation: $HS^- + 2O_2 = SO_4^{2-} + H^+$ (6)

$H_2S + 2O_2 = SO_4^{2-} + 2H^+$ (7)

Methane oxidation: $CH_4 + 2O_2 = CO_2 + 2H_2O$ (8)

According to Figure 6a, in wet season, S(-II) disappears at 10 m depth, that is below the oxic zone. We suggest that oxidation of S(-II) occurs by freshly precipitated $Fe(OH)_3(s)$. As demonstrated by dos Santos Afonso and Stumm , *(28)* H_2S can reductively dissolve iron (hydr)oxides, according to

$8Fe(OH)_3(s) + H_2S + 14H^+ = SO_4^{2-} + 20H_2O + 8Fe^{2+}$ (9)

Fe(II), transported by diffusion toward the oxycline, is oxidized by O_2 from 4.5 m to 4 m to amorphous iron (hydr)oxide according to the equation 5. The freshly precipitated $Fe(OH)_3(s)$ precipitates and may be reductively dissolved (equation 9).

D. Anoxic zone

Dry season

Conductivity (Figure 2d) depends on the ion concentration present in the solution and on the specific mobility of each species. In dry season, conductivity (Figure 2d and 7) increases steadily in hypolimnion with depth, up to a maximum value in the bottom waters. It follows from Figure 8, that the increase in alkalinity in anoxic part is well correlated with conductivity increase. Similar correlation may be found with Fe^{2+} concentration. We assumed alkalinity to be entirely due to bicarbonate ions because of the much lower concentration of other proton reactive ligands such as HS^- (total S(-II) does not exceed 2.7 μM with 7% of HS^- at pH 5.8) and the near neutral pH observed in the water column. Since these two ions are dominant species in the anoxic part of the lake in dry season and since their vertical distributions is well correlated with conductivity changes with depth, Fe^{2+} and HCO_3^- may be considered the principal conductivity determining ions.

The alkalinity excess in hypolimnic waters, compared with respect to epilimnic waters suggests that alkalinity production takes place *in situ*, i.e. in deeper waters. The balance of alkalinity can be affected on the one hand to the calcium carbonate equilibrium and on the other hand to organic matter mineralization. In the Petit Saut tropical reservoir, as well as in the entire Sinnamary catchment area, no $CaCO_3(s)$ traces can be detected in soils and sediments. Hypolimnic waters are undersaturated with respect to calcium carbonate, with a log(saturation index) of -4. This means that in the anoxic part of Petit Saut reservoir alkalinity is created by organic matter decay, i.e. by biomass and flooded vegetation decomposition. According to the thermodynamics, in a system with high amount of organic matter (denoted CH_2O), oxidation first involves O_2 reduction in the oxycline layer (II), then denitrification. In the water column, no significant nitrate concentration could be detected suggesting a rapid nitrate incorporation by the biota. The following redox transformations linked to organic matter decay are reduction of Mn oxides and reductive dissolution of Fe oxides. As the Mn(II) concentration does not exceed 1.3 μM in the hypolimnion, that is a concentration lower than 1% of the total alkalinity we can conclude that reduction of Mn(IV) oxides does not have a significant influence on the alkalinity increase with depth observed in the dry season.

Reduction of $Fe(OH)_3(s)$ could then be described by the following equation

$$CH_2O + 4Fe(OH)_3(s) + 7CO_2 = 4Fe^{2+} + 8HCO_3^- + 3H_2O \qquad (10)$$

According to eqn.(10), the ratio [Fe(II)]/[Alkalinity] is 0.5. The insert (a) in Figure 8 shows the distribution of Fe(II) concentration vs. alkalinity. A positive correlation $y = 0.5x - 45$ with a regression coefficient of $R^2 = 0.986$ is observed, where y is Fe(II) concentration and x is alkalinity. It follows from the regression equation that [Fe(II)]/[Alkalinity] = 0.5, i.e., the same as from equation (10). Hence, the reductive dissolution of iron (hydro)oxides by dissolved organic matter is the major factor responsible for alkalinity increase in anoxic part of the Petit Saut reservoir.

The insert (b) in Figure 7 shows the distribution of NH_4^+ vs. excess of alkalinity. In this case also a linear correlation is observed. The equation of regression $y = 0.4x - 29.5$ ($R^2 = 0.998$), where y is NH_4^+ concentration and x is alkalinity, gives a $[NH_4^+]/[Alk]$, i.e. N/C, ratio of 0.4. During photosynthesis carbon, nitrogen and phosphate are taken up together in the proportion C/N/P = 106:16:1 (Redfield stoichiometry ratio) by algal biomass. As a consequence of decay of dead organisms, elements are released in approximately the same ration, that is in a carbon to nitrogen C/N ratio of 7, whereas we observe a ratio C/N of 2.5. The observed difference could be due to several reason as decomposition of algal biomasses is not the only source of carbon and nitrogen in the water column. The flooded organic matter, for instance amino acids, can increase the input of nitrogen which lead to the decrease of C/N ratio. Another source of uncertainty in our C/N ratio estimate, is our first level assumption that all C is present as HCO_3^-, although CH_4 and CO_2 are present in the hypolimnion *(12, 24)*. Thus, concentrations of dissolved CO_2 and CH_4 reach 42 mg/l and 10 mg/l, respectively, at the bottom layer in december 2000 (S. Richard, personal communication). Figure 9 shows measured vertical profiles of dissolved CO_2 and profiles computed on the basis of alkalinity and pH profiles, assuming thermodynamic equilibrium. Comparison of computed and experimental results show good agreement of the two sets of data recorded on two different years.

Wet season

In wet season the increased mixing of deep waters due to inflowing rivers and heavy precipitation could influence the distribution of chemical species. Together with a general decrease of some species concentrations (Fe(II), CH_4, CO_2) in the water column, a change of vertical profile structure is observed. An increase in concentrations in water column from 10 to 20 m with following decrease in the bottom layer is found for Fe(II) and NH_4^+ (Figure 7a).

As shown by Galy-Lacaux et al, *(12)*, a seasonal variation in CH_4 concentration with depth is observed in the water column. Methane concentration reaches a maximum value at the end of the dry season, and then steadily decreases toward the end of the wet season. Similar seasonal trend is observed for CO_2 vertical distribution (Figure 9). These variations appear to be related to a dilution effect linked to water flow variations and primarily with the entrant water flow in the reservoir.

Similar seasonal variations are observed for Fe(II) concentrations. In wet season Fe(II) concentrations dramatically decrease in deeper waters. The ratios between Fe(II) and S(-II) are 80/2 = 40 and 9.4/2.7≈ 3.5 in dry and wet seasons, respectively. According to thermodynamics, hypolimnic waters are undersaturated with respect to FeS, with a log(saturation index) of –2 and –3 for the reaction $FeS(am) + H^+ = Fe^{2+} + HS^-$ in dry and wet seasons, respectively. Indeed, sediments and suspended matter collected during field trips were light brown. Thus, no precipitation of FeS occurs in the lake and observed decrease in ferrous iron concentration with depth during wet season may be due to dilution of Fe(II) or oxidation by O_2 entering deeper waters together with rainwater and inflow river waters by reaction (5) of thermodynamic sequence.

E. Production rates of reduced species based on water residence time.

Calculated and measured Fe(II) profiles in dry and wet seasons are plotted in Figure 9. In wet season the vertical distribution of Fe(II) both in the bottom layer (25 to 32 m), and in the zone of O_2 depletion, (3 to 4.5 m) is dominated by mixing. According to our calculations Fe(II) production occurs between 11 and 18 m. In dry season we could describe satisfactory well only the vertical distribution of Fe(II) from 4 to 9 m, while below the mixing curve underestimates strongly the measured data. Similar observations are made for the alkalinity distribution in dry season. We were able to describe the vertical distribution of alkalinity only between 4 and 9 m, while below the "mixing-only" curve underestimated the measured data. This demonstrates that production of Fe(II) and HCO_3^- takes place mostly within the water column, and particularly below 9m.

The estimated profiles of NH_4^+ demonstrate that production occurs mostly in water body (data not shown). In wet season, a maximum NH_4^+ concentration is detected in water column at 20 m depth, i.e. at the same depth where a Fe(II) concentration peak is found (Figure 7a). For S(II) distributions, the production zones are also located mainly in water body.

We propose that the peak of production of Fe(II) and NH_4^+ found respectively at 18 and 20 m, in wet season, depends on the resuspension processes. The strong mixing of bottom waters cause the transport of particulate organic matter and iron (hydro)oxides from the sediment up to 15 m depth. In this zone of lower K_z values, reductive dissolution of particles takes place. In dry season, when mixing decreases in bottom waters, the flux of particles in the water column slows down and almost reaches zero at the end of dry season (Figure 5). This leads to a gradual decomposition of particulate matter and constant increase in concentrations of dissolved species (Fe(II), HCO_3^-, NH_4^+, HS^-).

A mass balance on reduced species in hypolimnion (III-V boxes) can be described by the following equation:

Accumulation = Input – Output + Production (11)

Assuming the system to be at steady state and the input of reduced species by inflowing river waters to be equal to zero, the output equals the production rate, R_p (mol m^{-2} s^{-1}). We estimated R_p for a given species i as the product of water flux, F_{H2O} (m s^{-1}), and the average hypolimnion concentration in this species, C^i :

$$R_p = C^i \times F_{H2O} \quad (12)$$

Water flux is obtained as the turbine water flow (m^3s^{-1}) to reservoir surface area (m^2) ratio. The later is estimated from total volume (m^3) and average depth (m) of the lake. In June and December 1999 the turbine flow was 230 and 144 $m^{-3}s$ and average depth 15 and 10 m, respectively (C. Sissakian, personal communication). Thus, water fluxes are equal to $4.1*10^{-7}$ and $1*10^{-6}$ m s^{-1} in dry and wet season, respectively.

The obtained production rates are shown in Table 2. It follows from Table 2 that among the reduced species, methane has the highest rate of production in dry season and a rate about 5 times higher than in wet season due to changes in hydrological budgets. Comparison of the upward fluxes toward the oxycline and outflow fluxes (Table 2) shows for methane that the outflow flux dominates the overall methane emission from the reservoir. Volatilization therefore occurs just after the turbines, in the artificial cascades where H_2S is also volatilised *(23)*. These estimates are in good agreements with results from Galy-Lacaux and co-workers *(12, 24)* who showed that the principal source of methane to atmosphere is the emission of CH_4 downstream of dam, rather than diffusive or bubbling fluxes. Our calculations for Fe(II) show the decrease of production rate from dry to wet season. In contrast, NH_4^+ and S(-II) production rates remain almost constant independent of season. This is supported by the constant smell of H_2S perceived downstream of the reservoir.

F. Mercury

Vertical distributions of reactive mercury to dissolved mercury ratio are shown in Figure 10. Maximum values, 30-40 %, are observed in the oxic part of the reservoir. Then the ratio decreases sharply with depth below oxycline and remains almost constant in the hypolimnion with values less than 10 % of the ones recorded in anoxic layer. The results show that ~ 60 % and 90 % of dissolved mercury in oxic and anoxic layers, respectively, are complexed by organic matter. The organic dissolved mercury can include organometallic species (like CH_3Hg^+ complexes) and complexes of Hg(II) with humic acids, the assemblage of poorly defined organic compounds that constitute 50-90% of dissolved organic matter in natural waters *(29)*. Recent spectroscopic studies of humic acids explained the high affinity of mercury to organic matter by sorption on reduced sulfur functional groups (thiol(R-SH) and disulfide) *(30, 31)*. The reactions of Hg(II) complexation are relatively fast *(3)* and once equilibrium is reached, mixing is the main process responsible for Hgd cycling in the anoxic part of the reservoir. These considerations are confirmed by our calculations. Calculated profiles of Hgd are compared with measured values in Figure 11a,b. They suggest that only mixing processes dictate the profile shape and no chemical transformations occurs. In wet season a theoretical curve underestimates Hgd concentration only near 18m and below 20m in dry season. Observed difference in Hgd concentrations in oxic and anoxic parts of the lake let us assume that the principal source of mercury in water column are soils flooded by the dam impounding, as also shown for temperate water reservoirs *(4-6)*. Forest soils in French Guiana contain relatively high Hg concentrations *(13, 32)* compared to other Amazonian soils. Thus, the flooding of such soils leads to a release of mercury into aqueous environment due to the microbial activity *(33)*. In dry season mercury released from sediments may accumulate in the bottom layer because of relatively low mixing processes. In wet season, the peak of Hgd coincides well with the peak of Fe(II) and NH_4^+ concentrations. Thus, together with the direct release from sediments to the bottom water, resuspension of soil particles plays an important role in mercury availability. Mercury adsorbed on iron(hydro)oxides and complexed to particulate organic matter will release dissolved mercury in 10 and 20 m deep waters, where the degradation of particulate matter takes place as shown above. As soon as mercury desorbs, it reacts with dissolved organic matter and forms stable complexes.

The partition coefficient (K_d(ml/g) = Hgp/Hgd) remains constant, with logK_d values equal to 5.27 ± 0.17 and 5.23 ± 0.27 in wet and dry seasons, respectively. These values are similar to the average 5.0-6.0 log K_d reported in surface waters for different riverine, estuarine

and coastal systems *(34-36)*. The Hgd to Hgp ratio is plotted as a function of suspended matter concentration in Figure 12. In both seasons, the zone of constant ratio of Hgd to Hgp is observed when SPM varies from 2 to 8 mg/l. Only in dry season we observe sharp increase in Hgd to Hgp ratio with a rapid decrease in SPM concentration below 9 m, i.e. a mercury release from particulate matter takes place. Thus, we can distinguish two zones: a zone with high Hgd to Hgp ratio (Hgd/Hgp 8-12) and low SPM ($\leq$ 0.5mg/l), and a zone with constant Hgd/Hgp ratio (Hgd/Hgp near 2) and relatively high SPM (2 – 8mg/l).

The decrease in Hg_R concentration with respect to dissolved mercury corresponds to the layer on S(-II) increase. According to thermodynamics, anoxic waters are oversaturated with respect to cinnabar, HgS, with log(saturation index) of 19.

CONCLUSIONS

In Petit Saut reservoir, thermal stratification is permanent in the water column. The sharp decrease of dissolved oxygen concentration takes place in the transition zone (box II) and O_2 depletes completely at depth between 4 and 5m in both seasons. Subsequent to the disappearance of oxygen, reduced species, such as NH_4^+, Fe(II), S(-II), CH_4 appear in the hypolimnion. Calculated fluxes of reduced species and O_2 towards the oxycline show that the total flux of reduced species is much lower than O_2 flux in both seasons. Thus the principal consumption of dissolved oxygen is a biological decomposition of organic matter.

During the dry season, conductivity increases constantly with depth and its vertical distribution depends on the vertical distributions of alkalinity and Fe(II). The reductive dissolution of iron (hydro)oxides by dissolved organic matter is a major factor responsible for the alkalinity increase observed in the anoxic part of the Petit Saut reservoir in dry season.

In wet season, dilution of some species (Fe(II), CH_4, CO_2) occurs in the water column. A change of vertical profile structure is also observed: an increase in concentrations in water column from 10 to 20 m with following decrease in the bottom layer is found for Fe(II) and NH_4^+.

The obtained turbulent diffusion coefficient, K_z, profiles suggest a difference of mixing regime in dry and wet seasons. The observed difference, between two seasons, of water mixing in the layer between 4 and 10 m is mainly due to strong precipitation and inflow of water between warm epilimnic waters and cold hypolimnic waters, while turbulence

observed in the bottom layer (22- 35 m) is due to an increased input of inflow river waters during the wet season.

Due to the turbulence of bottom waters, sediments are reintroduced to the water column during the wet season. We propose that the peak of production of Fe(II) and NH_4^+ found between 10 and 20 m in wet season, depends on the resuspension processes. The strong mixing of bottom waters cause the transport of particulate organic matter and iron (hydro)oxides from the sediment up to 15 m depth. In this zone of lower K_z values, reductive dissolution of particles takes place. In dry season, when mixing decreases in bottom waters, the flux of particles in the water column slows down and almost reaches zero at the end of dry season. This leads to a gradual decomposition of SPM and constant increase in concentrations of dissolved species (Fe(II), HCO_3^-, NH_4^+, HS^-) in the water column. These observations could be confirmed by the modelling of the distribution of dissolved species species due to mixing.

60-90 % of the dissolved mercury is complexed with organic matter in the water column. Vertical distribution of dissolved mercury (Hgd) demonstrates that mixing processes dictate the profile shape and chemical transformations are of minor importance in the hypolimnion. The obtained results suggest that the principal source of mercury in water column are sediments. During the wet season, together with the direct release from the sediments to the bottom layer, the resuspension of soil particles plays an important role in dissolved mercury cycling. The decrease of reactive mercury concentration, observed in anoxic waters could be explained by the cinnabar precipitation.

FIGURE CAPTIONS

Figure 1. Map of Petit Saut reservoir, French Guiana, South America with three sampling sites location (Roche Genipa, Saint Eugene, Coursibo).

Figure 2. Vertical profiles of physico-chemical parameters at Roche Genipa sampling site in wet (○) and dry (▲) seasons: (a) dissolved oxygen ,(b) pH,(c) temperature, (d) conductivity. The full line in (c) indicated the temperature computed based on K_z values (see text).

Figure 3. Vertical profiles of computed vertical turbulent diffusion coefficient, K_z, in wet (○) and dry (▲) seasons.

Figure 4. Vertical profiles of suspended matter in wet (○) and dry (▲) seasons.

Figure 5. Conceptual lake model.

Figure 6. Vertical distributions of Fe(II), S(-II), NH_4^+ and O_2 in (a) wet and (b) dry seasons at Roche Genipa sampling site.

Figure 7. Vertical profiles of alkalinity in wet (●) and dry (▲) seasons; Vertical distribution of conductivity in wet (○) and dry (▼) seasons at Roche Genipa sampling site. Insert (a): distribution of Fe(II) as a function of alkalinity; insert(b): distribution of NH_4^+ as a function of alkalinity in dry season.

Figure 8. Calculated profiles of CO_2(aq) (dotted line) based on alkalinity and pH profiles in dry (December 1999) (▲) and wet (June 1999) (○) seasons and measured ones (full line) in dry (December 2000) (◊) and wet (June 2001) (□) seasons at Roche Genipa sampling site.

Figure 9. Calculated vertical distribution (full line) and measured concentrations (●) of Fe(II) at Roche Genipa sampling site in (a) wet and (b) dry seasons.

Figure 10. Ratio of reactive mercury (Hg_R) to dissolved mercury (Hgd) as a function of depth at Roche Genipa sampling site in wet (○) and dry (▲) seasons.

Figure 11. Calculated vertical distribution (full line) and measured concentrations (●) of dissolved mercury *(32)*in (a) wet and (b) dry seasons.

Figure 12. Ratio of total dissolved mercury (Hgd) to particulate mercury (Hgp) as a function of suspended matter concentration in wet (○) and dry (▲) seasons.

Table 1. Chemical composition of water column boxes.

DRY SEASON (DECEMBER 1999)

	I 0-3 m	II 3-5 m	III 5-16 m	IV 16-24 m	V 24-27 m
t°C	31	31-29.6	29.6-25.6	25.5	25.4
pH	6.7	6.7-5.7	~5.7	5.7	5.7
Cond (mS cm^{-1})	0.022	0.022-0.026	0.027-0.046	0.046-0.055	0.056
O_{2dis} (mg l^{-1})	~6.8	6.8-0	0	0	0
Fe(II) (μM)	0	0	~5 to 75	~96 to 107	115
Alkalinity (μM)	95	108	114-262	298	314
Hg_R (pM)	0.76	~0.7	~0.7-1.55	1.82	~1.5
Hgd (pM)		2	5.5-15	21	20
Ca^{2+} (μM)	22	24-27	27-33	34	34.8
Mg^{2+} (μM)	21	21	22-25	27	27.1
Na^{+} (μM)	86	90	90	87	87
K^{+} (μM)	18	18	17	18	18
K_z (m^2 s^{-1})			$3.5\cdot10^{-6}$- $1.7\cdot10^{-4}$	$2.5\cdot10^{-4}$	$2.5\cdot10^{-4}$

WET SEASON (JUNE 1999)

	I 0-2.6 m	II 2.6-4 m	III 4-16 m	IV 16-22.5 m	V 22.5-33 m
t°C	29.7	29.4-28.8	28.7 - 25.4	25.1	25.1
pH	6.7	6.7-5.7	~5.7	5.7	5.7
Cond (mS cm^{-1})	0.024	0.024- 0.026	0.026	0.027	0.025
O_{2dis} (mg l^{-1})	~7.9	7.26 - 0	0	0	0
Fe(II) (µM)	0	0.8	~1 to 10	~14	7.5
Alkalinity (µM)	120	120 - 137	~140	~130	110
Hg_R (pM)	0.37	1.74	~0.2	0.2	0.5 - 1
Hgd (pM)	5	3	10	13	10
Hgp (pM)	3.5	3	8	9.7	14
Mg^{2+} (µM)	23	23	18	17.6	17
Na^{+} (µM)	65	68	74	69	65
K^{+} (µM)	18·	18	15	14	13
K_z (m^2 s^{-1})			$1.1 \cdot 10^{-5}$- $7.1 \cdot 10^{-5}$	$2 \cdot 10^{-4}$	$6.3 \cdot 10^{-3}$

Table 2. Gradients and fluxes towards the oxycline, and output fluxes equal to production rates, R_p, in hypolimnion.

	Wet season $K_z = (1.2 \pm 0.1) \cdot 10^{-5}$ (m^2 s^{-1})		Dry season $K_z = (4.35 \pm 0.8) \cdot 10^{-6}$ (m^2 s^{-1})		$R_p * 10^{-8}$ (mol m^{-2} s^{-1})	
	Gradient$*10^{-3}$ (mol m^{-4})	Flux$*10^{-8}$ (mol m^{-2} s^{-1})	Gradient$*10^{-3}$ (mol m^{-4})	Flux$*10^{-8}$ (mol m^{-2} s^{-1})	Wet season	Dry season
NH_4^+	3.7 ± 0.9	4.5 ± 1.1	3.4 ± 0.9	1.5 ± 0.5	5	3
S(-II)	0.55 ± 0.05	0.66 ± 0.08	1 ± 0.3	0.45± 0.15	0.2	0.1
Fe(II)	2 ± 1	2.3 ± 1.3	8.9 ± 2.5	3.9 ± 1.3	0.9	3.3
CH_4	6.25 ± 3.5	7.5 ± 4.2	20 ± 4	6.3 ± 1	6	21
O_2	-(220 ± 60)	-(270 ± 77)	- (120 ± 30)	- (52 ± 16)		

REFERENCES

(1) Lacerda L.D.,Salomons W., (1998). *Mercury from gold and silver mining: a chemical time bomb?* Springer. 146 p.

(2) Pfeiffer W.C.,Lacerda L.D., (1988). *Mercury inputs into the Amazon region, Brazil.* Environ.Technol. Lett, (9): p. 325-330.

(3) Morel F.M.M., Kraepiel A.M.L., Amyot M., (1998). *The chemical cycle and bioaccumulation of mercury.* Annual Reviews Ecol.Syst., 29: p. 543-566.

(4) Mucci A., Lucotte M., Mantgomery S., Plourde Y., Pichet S., Tra H.V., (1995). *Mercury remobilization from flooded soils in hydroelectric reservoir of northenrn Quebec, La Grande -2 : results of a soil resuspention experiment.* Can. J.Fish.Aquat.Sci., 52: p. 2507-2517.

(5) Louchouarn P., Lucotte M., Mucci A., Pichet P., (1993). *Geochemistry of mercury in two hydroelectric reservoirs in Quebec, Canada.* Can. J. Fish., Aquat. Sci., 50: p. 269-281.

(6) Thérien N.,Morrison K.A., *In vitro release of mercury and methylmercury from flooded organic matter*, in *Mercury in the biogeochemical cycle*, Lucotte M, et al., Editors. 1999, Springer. p. 147-164.

(7) Verdon R.,Tremblay A., *Mercury accumulation in fish from the La Grande complex: influence of feeding habits and concentration of mercury in ingested prey*, in *Mercury in the biogeochemical cycle*, Lucotte M, et al., Editors. 1999, Springer. p. 215-233.

(8) Schetangne R.,Verdon R., *Post-impoundment evolution of fish mercury levels at the la Grand complex, Quebec, Canada (from 1978 to 1996)*, in *mercury in the biogeochemical cycle*, Lucotte M, et al., Editors. 1999, Springer. p. 235-258.

(9) Jackson T.A., (1988). *The mercury problem in recently formed reservoirs of northen Manitoba (Canada): effects of impoundment and other factors on the production of methylmercury by microorganisms in sediments.* Can. J. Fish Aquat. Sci., 45: p. 97-121.

(10) Fearnside P.M., (2001). *Environmental impacts of Brazil's Tucurui Dam: unlearned lessons for hydroelectric development in Amazonia.* Environmental management, 27(3): p. 377-396.

(11) Mol J.H., Ramlal J.S., Lietar C., Verloo M., (2001). *Mercury contamination in freshwater, estuarine, and marine fishes in relation to small-scale gold-minig in Suriname, South America.* Environmental research, 86(2): p. 183-197.

(12) Galy-Lacaux C., Delmas R., Kouadio G., Richard S., Gosse P., (1999). *Long-term greenhouse gas emission from hydroelectric reservoirs in tropical forest regions.* Global biochemical cycles, 13(2): p. 503-517.

(13) Roulet M.,Lucotte M., (1995). *Geochemistry of mercury in pristine and flooded ferralitic soils of a tropical rain forest in French Guiana, South America.* Water, air and soil pollution, 80: p. 1079-1088.

(14) Lerman A., Imboden D., Gat J.,(1995), ed.^eds. *Physics and chemistry of lakes*. 2nd ed. Springer. 334.

(15) Watras C.,Bloom N., *The vertical distribution of mercury species in Wiskonsin Lakes: accumulation in plankton layers.*, in *Mercury pollution: integration and synthesis*, H.J. Watras C., Editor. 1994, Lewis publishers. p. 137-185.

(16) Cossa D, Mason R. P., Fitzgerald W. F., *Chemical speciation of mercury in a Meromictic lake*, in *Mercury pollution: integration and synthesis*, W.C. J. and H.J. W., Editors. 1994, CRC Press, Inc. p. 57-67.

(17) Hamilton-Taylor J.,Davison W., *Redox-driven cycling of trace elements in lakes*, in *Physics and chemistry of lakes*, Lerman A., Imboden D., and Gat J., Editors. 1995, Spronger. p. 334.

(18) Stumm W.,Morgan J.J., (1996). *Aquatic chemistry*. John Wiley&Sons. 1022 p.

(19) Davison W., (1993). *Iron and manganese in lakes.* Earth science review, 34: p. 119-163.

(20) Sigg L., *Metal transfer mechanisms in lakes; the role of settling particles*, in *Chemical processes in lakes*, S. W., Editor. 1985, Wiley: New York. p. 283-310.

(21) Tessier A., *Sorption of trace elementson natural particles in oxic environment*, in *Environmental particles*, Buffle J. and van Leeuwen H.P., Editors. 1992, Lewis, Boca Raton. p. 425-453.

(22) Sigg L., Johnson A.C., Kuhn A., (1991). *Redox conditions and alkalinity generation in a seasonally anoxic lake (Lake Greifen).* Marine Chemistry, 36: p. 9-26.

(23) Sissakian C., (1997). *Présentation général de l'aménagement hydroélectrique de Petit Saut (Gyuane française) et du programme de suivi écologique lié à sa mise en eau.* Hydroecologie appliquée, 9(1-2): p. 1-21.

(24) Galy-Lacaux C., Delmas R., Jambert C. , Dumestre J.-F., Labroue L., Richard S., Gosse P., (1997). *Gaseous emissions and oxygen consumption in hydroelectric dams: A case study in French Guyana.* Global biogeochemical cycles, 11(4): p. 471-483.

(25) Quémerais B.,Cossa D., *Procedures for sampling and analysis of mercury in natural waters.*. 1997, Environmental Canada-Québec Region, Environmental Conservation, St Laurence Centre. Scientific and technical report. p. 36.

(26) Vogel A.I., (1989). *Vogel's textbook of quantitative chemical analysis*. Longman Scientific and technical. 877 p.

(27) Imboden D.,Wuest A., *Mixing mechanisms in lakes*, in *Physics and chemistry of lakes*, Lerman A., Imboden D., and Gat J., Editors. 1995, Springer. p. 83-138.

(28) dos Santos Afonso M.,Stumm W., (1992). *Reductive dissolution of iron(III) (hydr)oxides by hydroge sulfide.* Langmuir, (8): p. 1671-1675.

(29) Morel F.M.M.,Hering J.G., (1993). *Principles and applications of aquatic chemistry.* Wiley Interscience. 588 p.

(30) Xia K., Skyllberg U.L., Bleam W.F., Bloom P.R., Nater E.A., Helmke, (2001). *X-ray adsorption spectroscopic evidence for the complexation of Hg(II) by reduced sulfur in soil humic substances.* Environmental science and technology., 33: p. 257-261.

(31) Skyllberg U., Xia K., Bloom P.R., Nater E.A., Bleam W.F., (2000). *Binding of mercury(II) to reduced sulfur in soil organic matter along upland-peat soil transects.* Journal of environmental quality., 29: p. 855-865.

(32) Programme mercure en Guyane: region de Saint Elie et retenue de Petit Saut.. 2001.

(33) Dumestre J.-F., Vaquer A., Gosse P., Richard S., Labroue L., (1999). *Bacterial ecology of a young equatorial hydroelectric reservoir (Petit Saut, French Guiana).* Hydrobiologia, 400: p. 75-83.

(34) Coquery M., Cossa D., Martin J., (1995). *The distribution of dissolved and particulate mercury in three Siberian estuaries and adjacent arctic coastal waters.* Water, Air, and Soil Pollution, 80: p. 653-664.

(35) Cossa D., Elbaz-Poulichet F., Nieto J.M., (2001). *Mercury in the Tinto-Odiel estuarine system (Gulf of cadiz, Spain): sources and dispertion.* Aquatic geochemistry, (7): p. 1-12.

(36) Coquery M.,Cossa D., (1995). *Mercury speciation in surface waters of the North Sea.* Netherland Journal of Sea Research, 34: p. 245-257.

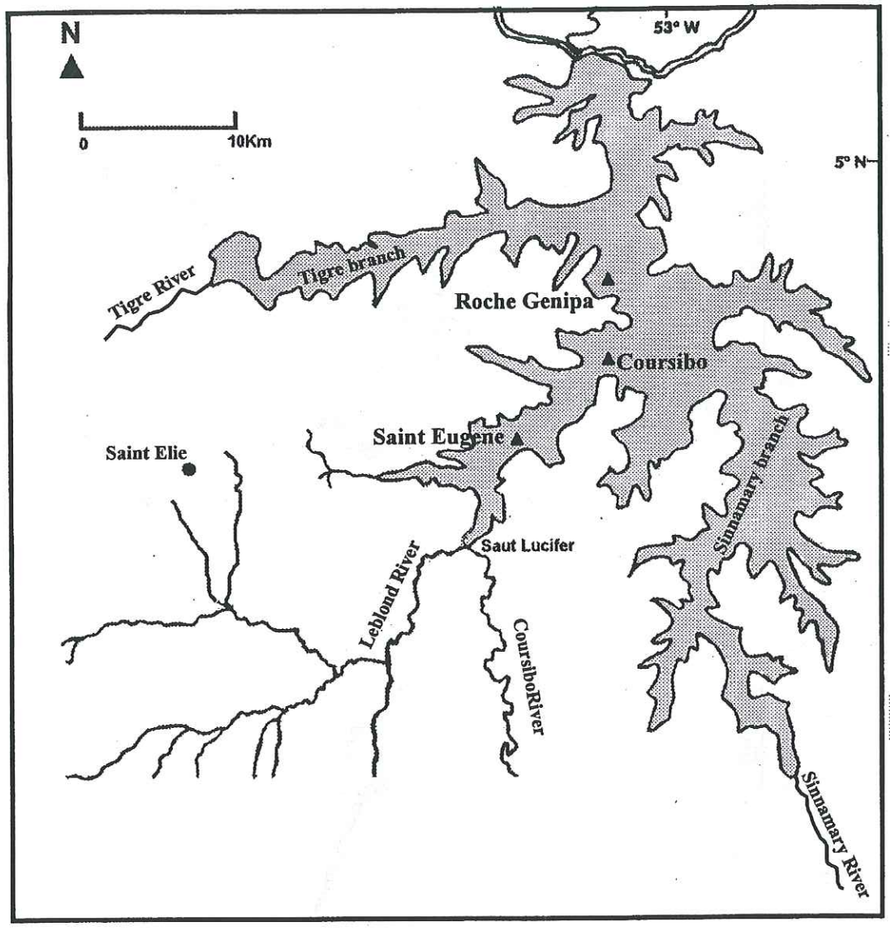
N
0
10Km
53° W
5° N
Tigre River
Tigre branch
Roche Genipa
Coursibo
Saint Eugene
Saint Elie
Saut Lucifer
Leblond River
CoursiboRiver
Sinnamary branch
Sinnamary River

Figure 1

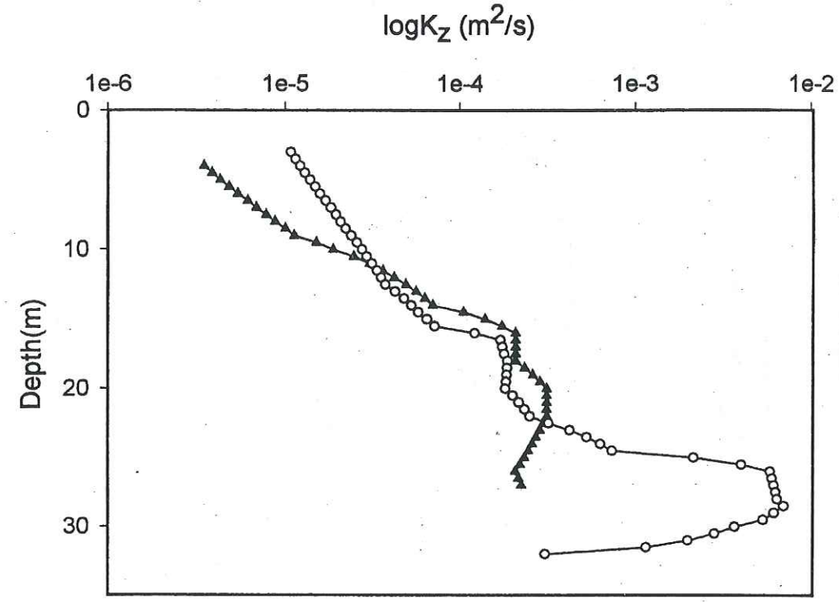

Figure 3

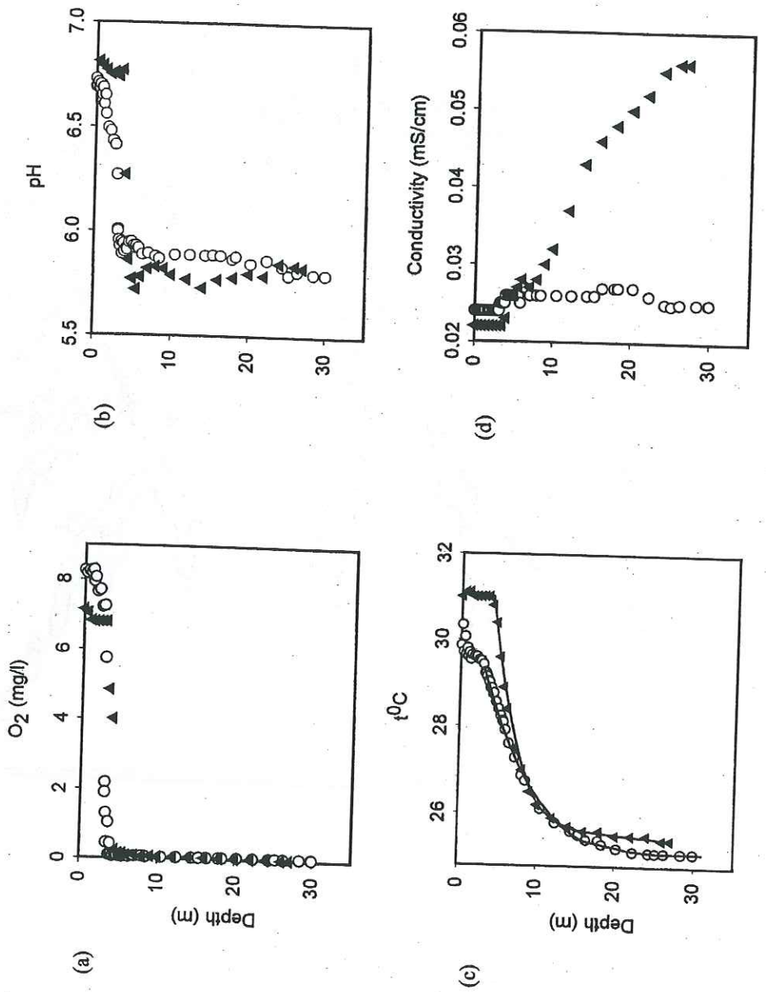

Figure 2

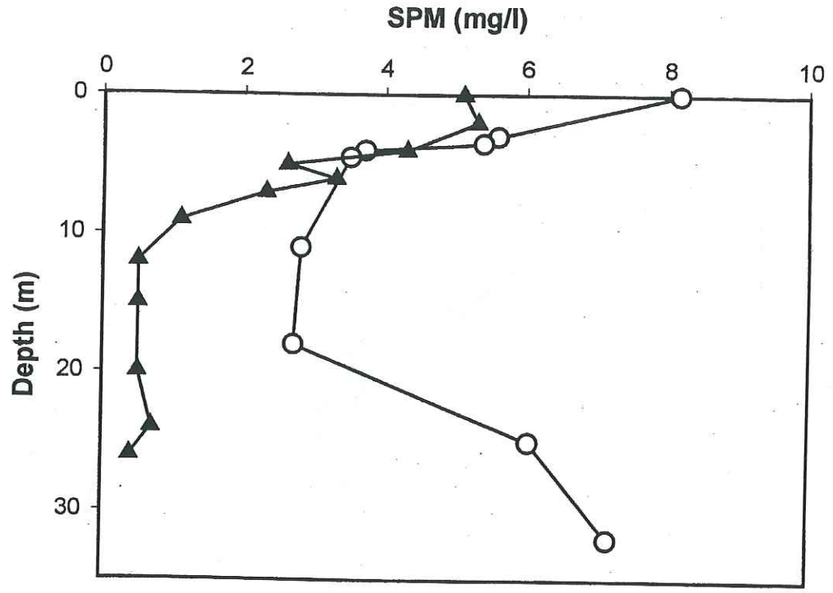

Figure 4

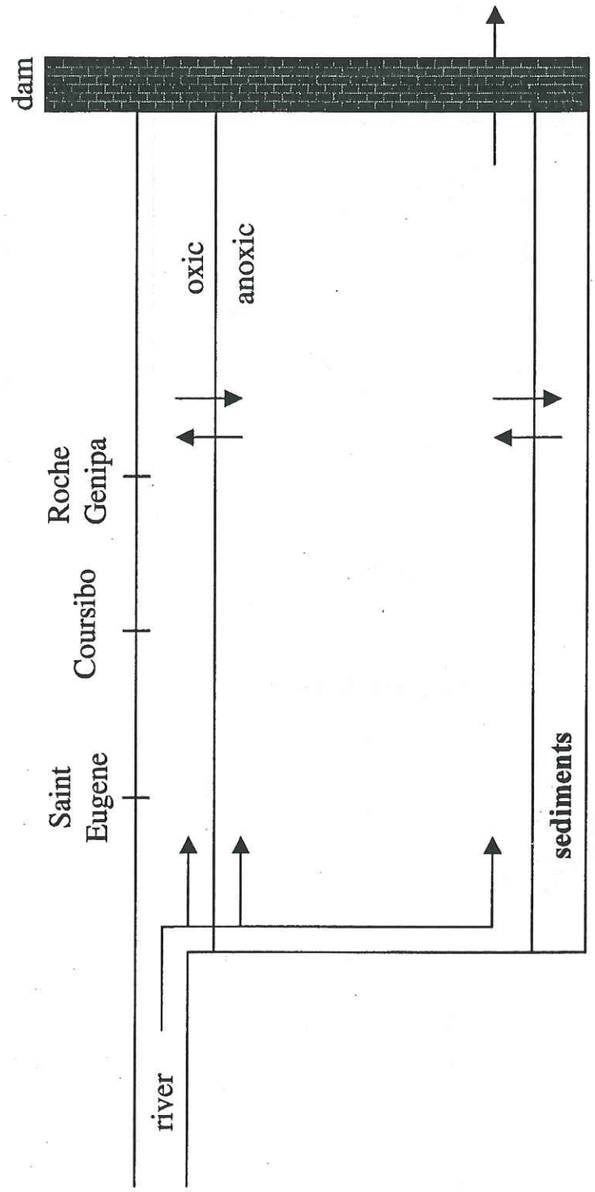

Figure 5

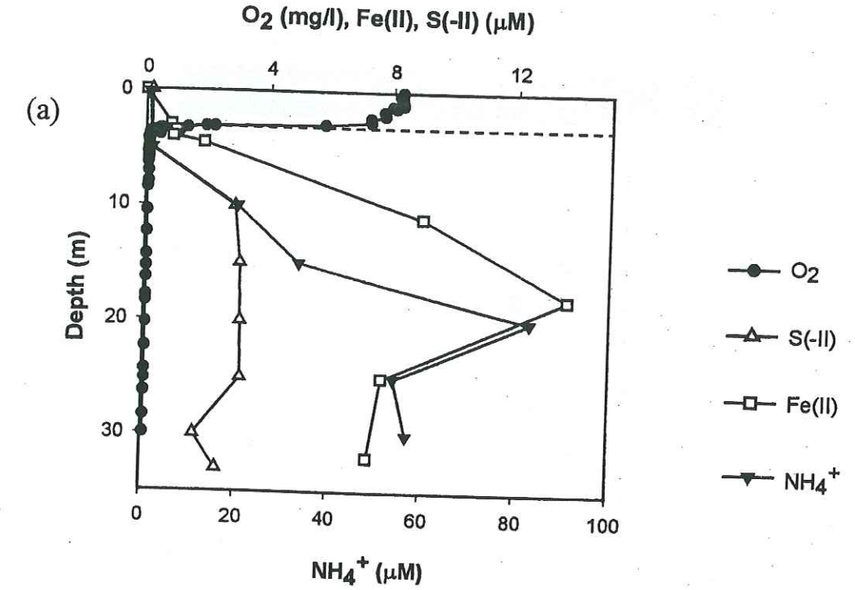

Figure 6

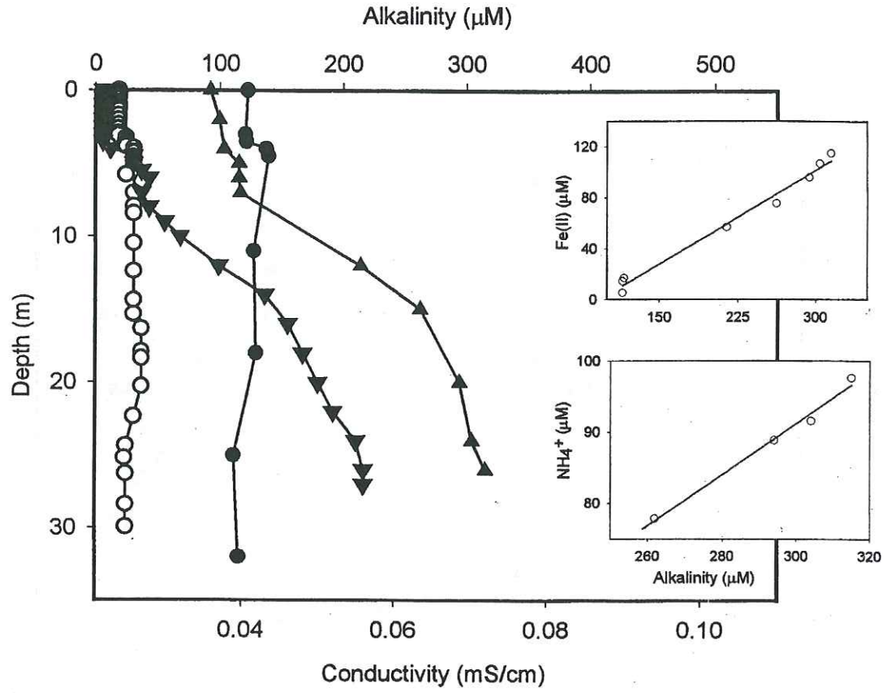

Figure 7

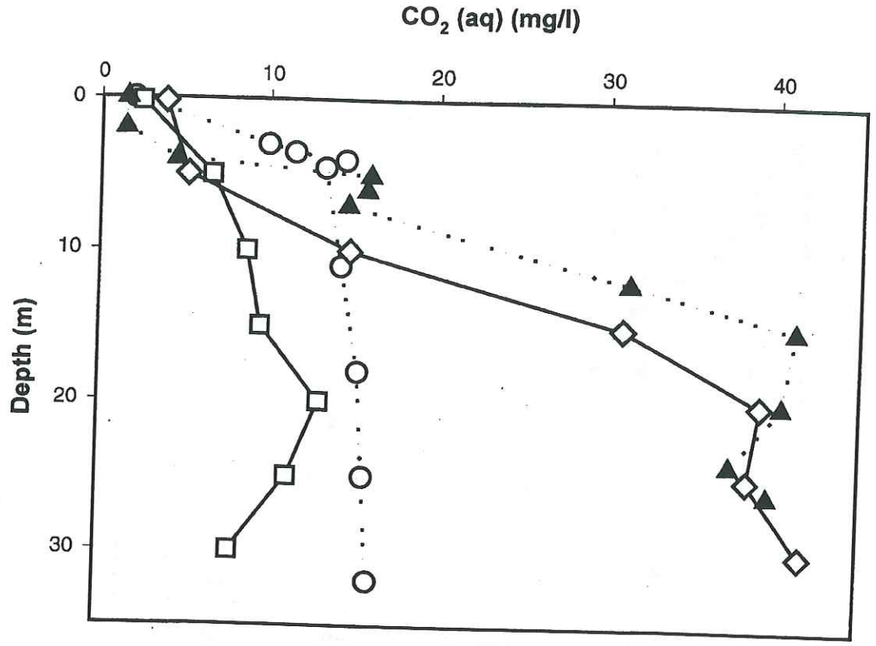

Figure 8

(a)

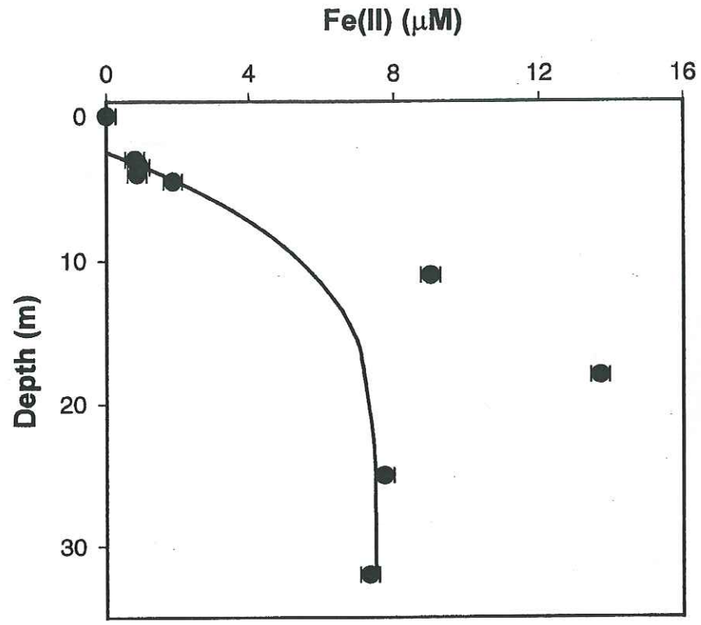

(b)

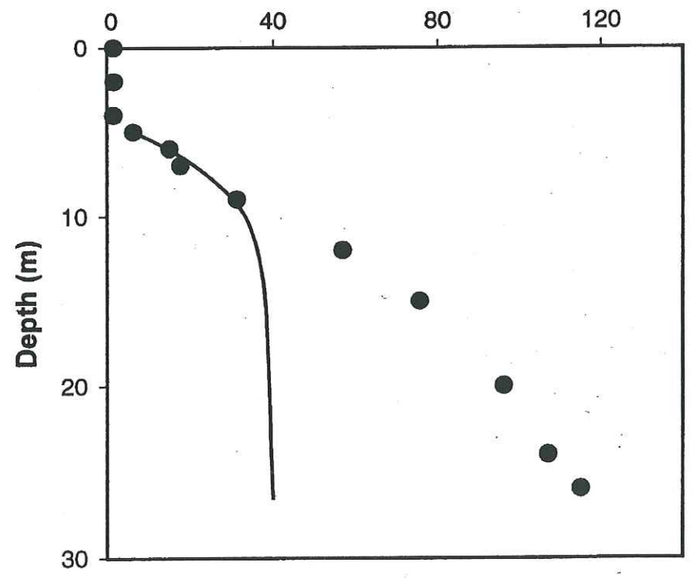

Figure 9

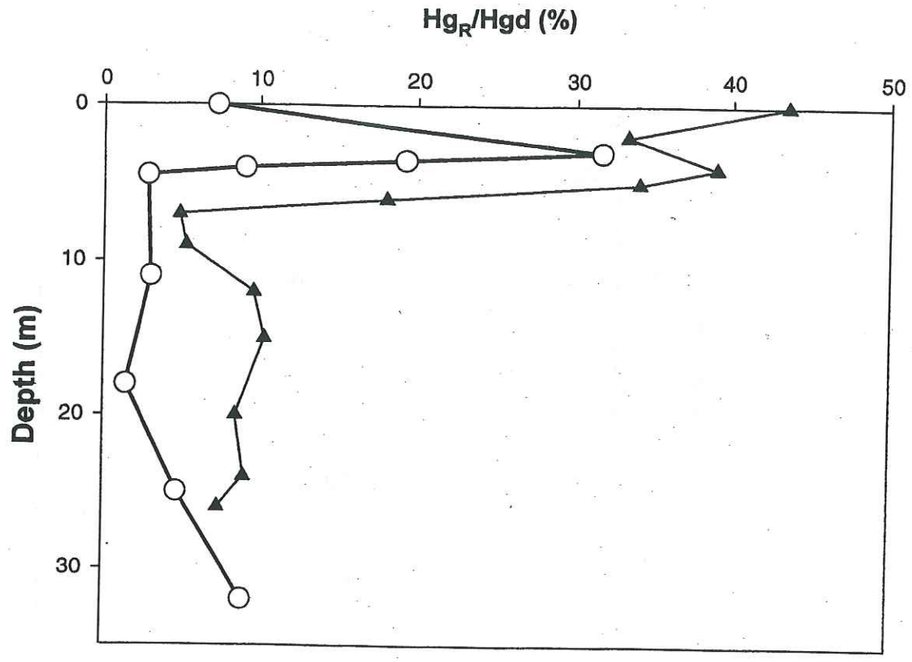

Figure 10

(a)

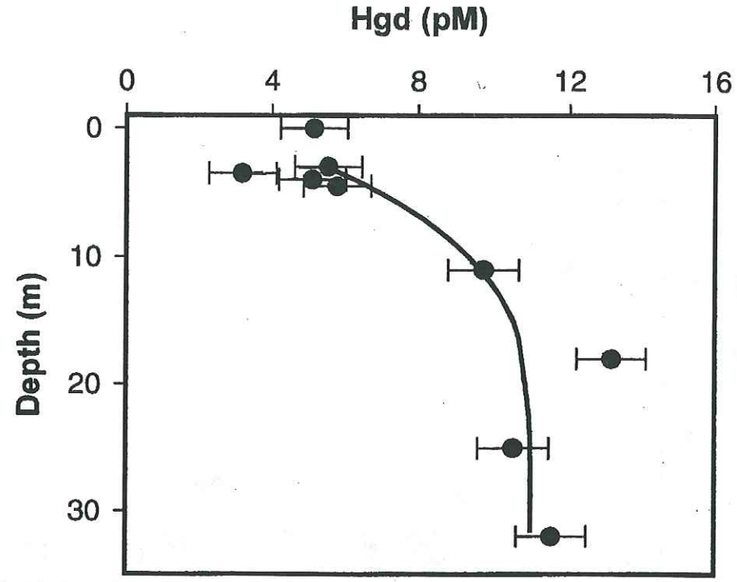

(b)

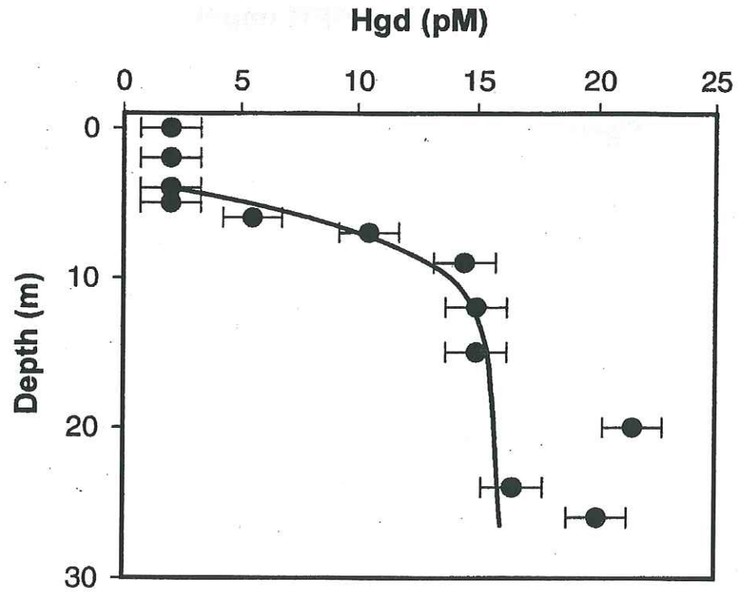

Figure 11

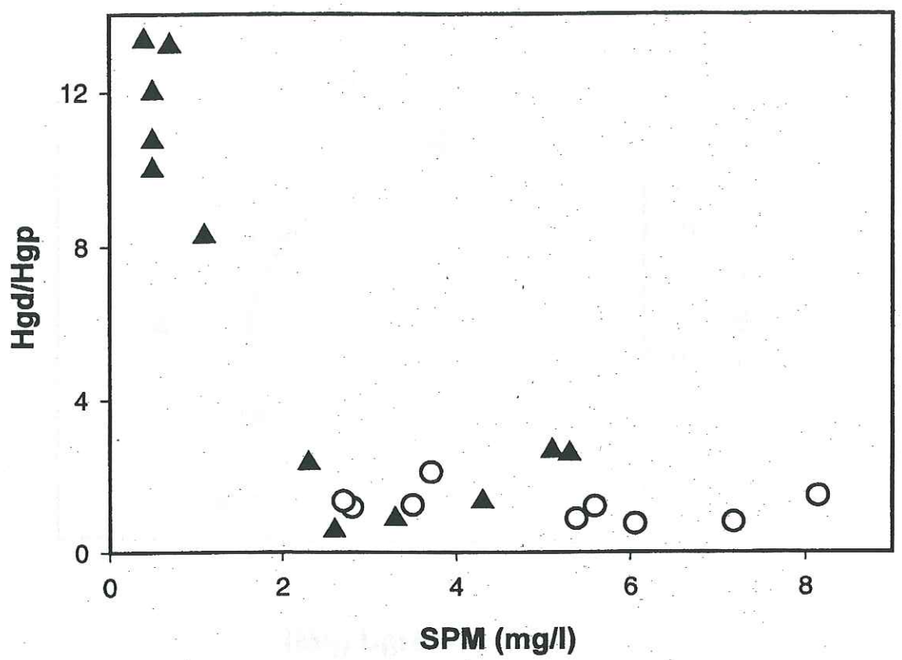

Figure 12

CHAPITRE 5

Production of gaseous mercury Hg ° in an anoxic environment: Petit Saut reservoir, French Guiana.

T. Peretyazhko, L. Charlet, D. Cossa, V. Kazimirov

INTRODUCTION

In natural waters, mercury is distributed among several chemical forms: elemental mercury, Hg°, a number of mercuric species, Hg(II), and organic mercury, chiefly methyl (CH_3Hg^+), dimethyl ($(CH_3)_2Hg°$), and some ethyl ($C_2H_5Hg^+$) mercury *(1)*. Elemental mercury plays an important role in the environmental mercury cycle. It represents nearly 95% of the atmospheric mercury and 10 to 50% of the dissolved mercury in lakes and the ocean *(2-5)*. The formation of Hg° can favor the removal of mercury from the natural system , through gas evasion. The volatilization of mercury reduces the Hg burden in surface waters and soils *(6)* and can be considered a natural attenuation process which limits the methylmercury production and accumulation in fish *(5)*.

The processes involved in the production of Hg° in natural waters are still subject of debate. In general, two types of reduction are considered: biotic and abiotic processes . The literature data show that abiotic reduction can be initiated by various photochemical processes: photoinduced reduction of mercury in lake water *(7, 8)* caused by direct photolysis *(5)* or by dissolved organic carbon (DOC) *(5, 9)*; photosensitized production by a chain DOC-dissolved oxygen - Hg(II)-Hg° *(5)*; sunlight Hg° production in the presence of ferric iron through photolysis of Fe(III)-organic acid coordination compound and subsequent reduction of Hg(II) to Hg° *(10)*. Biotic transformations may also play a significant part: reduction by algalphotosynthate, phytoplankton cultures, microbial communities *(11, 12)* were studied under laboratory conditions.

Elemental mercury was considered to be relatively unreactive *(1, 13)*, that is why Hg° chemical transformations have not been largely studied. As shown in recent publications *(13, 14)*, Hg° can undergo chemical transformations in natural waters which may be important in reducing fluxes of Hg out of aquatic systems: significant photooxidation rates of Hg° were found in aqueous samples from St Lawrence river *(13)*. Zhang and Lindberg *(10)* observed that storage of fresh lake water in the dark frequently caused Hg° decreases probably due to dark oxidation of Hg° to Hg(II) by some oxidants formed during sunlight exposure or adsorption of Hg° by suspended particles. These authors suggest that the observed Hg° in natural waters can represent the steady state values between reduction and oxidation processes.

In the present work, we studied the mechanisms controlling the formation and distribution of Hg° in a tropical artificial lake. Measurements of Hg° were carried out on the lake during dry season. Laboratory experiments with surface sediments were designed to

elucidate Hg(II) reduction pathways and to measure reduction rates in anoxic conditions. Experimental studies of Hg° production by Fe(II) in the presence of hematite particles were performed to study an abiotic process of Hg(II) reduction in oxygen depleted aquatic environments. Equilibrium modeling of mercury distribution between surface sediments and water was applied to evaluate the influence of mercury speciation on reduction phenomena. In order to interpret spatial distribution of elemental mercury in a tropical reservoir, Hg° production rate together with Hg° fluxes toward the oxycline, out of the dam, evasion to the atmosphere and ebullition were estimated.

EXPERIMENTAL METHODS

Sampling site

Reservoir Petit Saut is located on the Sinnamary river, French Guiana, South America. The construction of the dam took place from 1989 to 1995. The reservoir covers 80 km of the Sinnamary river course, flooding, at it maximal level, 35m, 360 km^2 of uncleared tropical rainforest *(15)*. The total water volume stored is $3.5 \cdot 10^9$ m^3 and the average residence time of water in the reservoir is 5 months *(16)*. Possible localized sources of mercury contamination include the upstream Saint Elie active gold-mining area and the impounded "Adieu Vat" former mining sites.

Water samples were taken at Roche Genipa (N4°56'474", W53°02'468") and Saint Eugene (N 4°51'250", W53°04'155") sites (Figure 1) during dry season in December 1999. The two sites are located respectively at the center (Roche Genipa site, max. depth 26m) and in a lateral branch(Saint Eugene site, max. depth 16m) of the lake.

Oxygen concentration drops sharply between 3 and 5 m at Roche Genipa sampling site and between 2.5 and 4 m at Saint Eugene sampling site. A well pronounced thermal stratification is detected at Roche Genipa site. However, at Saint Eugene sampling site temperature decreases gradually. Maximum temperature at the surface is 31°C, and temperature decreases to 25.4°C below 10 m. pH in the oxic part of the water column is circum neutral (pH 6.8), and becomes slightly acidic in anoxic waters with an average value for the hypolimnion of pH 5.8. Alkalinity increased strongly in hypolimnion up to 0.3 and 0.46 mM at the bottom layer at Roche Genipa and Saint Eugene sites, respectively. Similar to alkalinity, Fe(II) increase sharply in hypolimnion with maximum, 0.1 and 0.18 mM, at the

bottom layer at Roche Genipa and Saint Eugene sampling sites, respectively. Mean concentration of dissolved organic carbon in epilimnion is 8 mg/l and in hypolimnion is 6.2 mg/l.

Values of turbulent diffusion coefficient, K_z, estimated for hypolimnic waters differs strongly with depth in the water column during the dry season *(17)*. K_z increases steadily from $3.5 \cdot 10^{-6}$ m s^{-2} to $2.5 \cdot 10^{-4}$ m s^{-2} between 5 and 15 m and remains constant, $2.5 \cdot 10^{-4}$ m s^{-2}, from 15 m down to the lake bottom.

Water sampling and field analysis

Water samples for Hg° analysis were collected with a peristaltic Teflon pump in 500-ml Teflon bottles. All bottles were previously soaked in HNO_3 according the procedure described by Quémerais and Cossa *(18)*, then thoroughly rinsed with double-distilled water (Milli-Q water), filled with Milli-Q water and acidified by HCl ultra-pure (Merck) to 1% solution. The bottles were kept in double polyethylene bags until sampling. In addition, each bottle was first rinsed with lake water 3 times before filling. Polyethylene gloves were worn at all times.

Hg° was analyzed on-shore within 4-5 hours after sampling by cold vapor atomic fluorescence spectroscopy (CVAFS) *(19)*. Water was purged for 20 min with ultra pure Ar and Hg° concentration was determined after gold amalgamation. Blank was 14 pg l^{-1} and detection limit 10 pg l^{-1}.

The reactive mercury (Hg_R) analysis were performed in field laboratory as for Hg°. It was determined by reduction with 20% $SnCl_2$ (w/v). The sample was purged for 7 min immediately after adding $SnCl_2$ with ultra-pure Ar and mercury concentration was determined after gold amalgamation. Blank was 58 pg l^{-1} and detection limit was 35 pg l^{-1}.

Ex-situ Hg° production experiments with surface sediments

Black Teflon bottles previously acid washed were used in all experiments in order to create conditions close to natural and to avoid light penetration. 150 ml of sampled H_2O and 10 g w.w. (2.7 g d.w. or 18 g l^{-1}, determined by drying of 10 g w.w. sediments at 70°C) of sediments were added to each bottle. A pH value of 6 was maintained by addition of 0.1 M MOPS (Fisher Scientific) solution. Ultrapure argon was passed overnight through the suspension to eliminate dissolved oxygen. Then the samples were kept in N_2/H_2 atmosphere

during one week. Hg^0 was analyzed with CVAFS. The standard deviation of the bubbler blank was on average 8 pg l^{-1} resulting in detection limit (3*STD of blanks) of 24 pg l^{-1}.

For the kinetic experiment a 25 μM initial Hg(II) acidified to 1% with HNO_3 (Merck, Suprapur) was prepared from 5 mM Hg(II) stock solution before each experiment. At t = 0, an aliquot of Hg(II) initial solution was added to the suspension to obtain $[Hg(II)]_0$ = 4.4, 2.5 or 1.5 nM. To get $[Hg(II)]_0$ = 250 nM an aliquot of 5 mM Hg(II) stock solution was added. At fixed time intervals, the produced gaseous mercury was purged with ultra pure Ar, stored on the gold trap, and determined by CVAFS.

Some water and sediment samples were exposed to γ-ray irradiation (25 kGy) for 24 hr in order to sterilize the samples. Suspensions were then prepared according to the protocol described above and NaN_3 (Merck), 1%, was added to each suspension in order to stop any residual bacterial activity.

Hg° production experiments by Fe(II) in the presence of hematite particles

The suspension of hematite was obtained by adding $Fe(NO_3)_3 \cdot 9H_2O$ to boiling and vigorously stirred distilled water by the protocol described in details in *(20)*.

The initial concentration of hematite suspension was 0.68 g l^{-1}. A suspension of hematite was diluted with deoxygenated water to 5 mg l^{-1}. Then KOH (0.01 M) was added to adjust the pH. Ferrous sulfate was added to obtain an initial concentration of Fe(II) 1.5 μM. The reactor was purged continuously with ultrapure Ar to avoid oxidation of Fe(II) to Fe(III) by ultratraces of oxygen. The suspension was equilibrated for 24 h. Then the aliquot (50 ml) was transferred to a 125 ml Teflon bubbler and Hg° was analyzed with CVAFS using Tekran detector. The standard deviation of the bubbler blank was on average 12 pg l^{-1} resulting in detection limit (3*STD of blanks) of 36 pg l^{-1}.

For the kinetic experiment, a 10nM initial Hg(II) solution in 1% $HNO_3$was prepared from 2.5 μM Hg(II) stock solution before the experiment. At t = 0, an aliquot of Hg(II) initial solution was added to the Fe(II)/hematite suspension to get $[Hg(II)]_0$ = 20 pM. At fixed time intervals, produced gaseous mercury was purged with ultra pure Ar, stored onto gold trap, and determined by cold vapor atomic fluorescence spectroscopy. The experiments without hematite particles were also carried out with the same conditions as described above.

Other measurements

XRD patterns for total mineralogy analysis were recorded with SIEMENS D501 diffractometer using a 0.02° step size and 6 s counting time per step. Total elemental composition was determined by X- ray fluorescence. Concentration of organic carbon in sediments was analyzed calorimetrically after an oxidation in sulfochronic environment *(21)*.

RESULTS AND DISCUSSIONS

Hg° in Petit Saut reservoir

Vertical Hg° concentration profiles were measured at two sites in Petit Saut dam reservoir, French Guiana, and are given in Figure 2. In both sites, the highest Hg° concentrations (0.57 and 0.35 pM at Roche Genipa and Saint Eugene sampling sites, respectively) were detected at the bottom layer. In the water column the Hg° concentrations decreased continuously with decreasing depth down to 0.09 pM and 0.07 pM below the oxycline, i.e. at 7 m in Roche Genipa and 5 m in Saint Eugene sampling sites, respectively. Closer to the water/air interface, the Hg° concentrations increased again up to 0.2 pM (Roche Genipa) and 0.27 pM (Saint Eugene). At Roche Genipa site we also observed a local Hg° concentration peak of 0.31 pM at the oxycline.

The degree of saturation for Hg° in the lake relative to equilibrium with Hg° in the atmosphere was determined by the following equation

$$S = \frac{C_w * H}{C_g} \times 100 \qquad (1)$$

where C_w and C_g are the concentrations of Hg° in lake water (mol l^{-1}) and air (mol l^{-1}), respectively, and H is the Henry's law constant (Hg°(g)/Hg°(aq), dimensionless) corrected to ambient temperature *(22)*. The atmosphere average Hg° concentration is about 7.5 pmol m^{-3} *(23, 24)*. The waters were all supersaturated with Hg°, for both sites at all depths, and the level of saturation was more than two times higher in the O_2 depleted bottom waters than in the oxic surface waters.

Vertical variations of saturation index in water column of Petit Saut reservoir are summarized in Table 1. In order to compare Hg° distribution in lakes under temperate and tropical climates, we give in Table 1 the values reported for Pallette lake, Wisconsin, USA

(2). We chose this lake as a reference lake because the authors presented the results for different conditions of the lake with respect to thermal stratification, i.e. in March, when no temperature variation with depth is observed, and in August, when the lake was completely stratified. Several observations follow from Table 1. In Pallette lake, during the period of stratification, saturation index was seven times greater in epilimnion than in hypolimnion. During winter time, disappearance of thermal stratification leads to homogeneous distribution of Hg° in the water column due to water mixing throughout the water column. When lake is completely stratified, the principal zone of Hg° production is the epilimnion with only small input from deeper waters. Similar Hg° vertical profiles were also found in some Canadian lakes *(8)*, with maximum concentrations in the upper oxic part of water column. In surface waters, Hg° production has been shown by a variety of authors to be due to sunlight-mediated photochemical processes *(5, 7, 8, 10, 11, 14, 25, 26)*. In stratified Petit Saut reservoir, the saturation index in surface waters is of the same order of magnitude as in temperate lakes. Conversely, vertical Hg° concentration profiles are very different, with maximum production found in the bottom layer, where sediments appear to be a major source of Hg° in Petit Saut reservoir .

It follows from Figure 2 and Table 1, in the Petit Saut reservoir, three Hg° concentration peaks are observed: the photoinduced Hg(II) reduction peak at the lake surface *(27)*, Hg° peak at the oxycline (Roche Genipa sampling site), and the absolute maximum concentration observed at the bottom of lake (both sampling sites). A peak at the oxycline may be due to an increased bacterial activity at the oxic/anoxic interface. In fact, a maximum of bacteria concentration level was found exactly in this layer in Petit Saut reservoir in dry season *(28)*. Another pathway of Hg° production could be abiotic redox transformations in this zone. Since various redox transformations may occur at the oxycline layer, the Hg° formation may also be linked, as discussed below, to the Fe(II)- Fe(III) dynamic couple.

Comparison of Hg° in temperate and tropical lakes demonstrate a net Hg° production by the sediments which can be only observed in stratified tropical lakes. This may be explained by a temperature difference between the two types of water body, i.e. by a difference in reaction kinetics. Average temperature in temperate lake hypolimnion is 2 to 10°C whereas it is ~25 in Petit Saut lake hypolimnion. We can hypothesize that the difference in Hg° concentrations in the anoxic part of the lakes located in different climatic zones can be attributed to the increase of bacterial activity in sediments with increased temperature. Measurements of Hg° and physico-chemical parameters in other tropical freshwater systems should be carried out in order to verify the hypothesis. We could get some insights in the

mechanisms of Hg° production occurring at the bottom layer of Petit Saut reservoir by some laboratory experiments which were performed with water collected from bottom layer and surface sediments.

Production of Hg° in anoxic system: water/surface sediments

Figures 3 and 4 show a production in the dark of Hg° from anoxic suspensions of untreated surface sediment. In four hours reaction time, 3.2, 0.67, 0.52 and 0.33 % of the initial Hg(II) concentration (250 nM, 4.4 nM, 2.5 nM and 1.5 nM, respectively) was transformed in Hg°. These data demonstrate that the amount Hg° produced, C_{Hg° (in mol l^{-1}), depends on the initial spiked Hg(II) concentration $C_{Hg(II)}$(in mol l^{-1}) and decrease with decrease of Hg(II) input.

Our data can be fitted satisfactory well by both first- and second- order kinetics indicating the complex nature of the process. The same phenomena has been observed by Zhang and Lindberg, *(10)* in the Fe(III) - enhanced photochemical production of dissolved gaseous mercury. Since no information is available on the nature and concentration of the reductant, a pseudo-first-order kinetics is assumed. The values of first-order rate constants estimated for the four-hour reaction time, and values of half-time, are given in Table 2a. Elemental mercury formation rates in undisturbed sediment suspensions are the same range as formation rates in freshwater lakes reported in literature. Mass balance calculations and laboratory reduction experiments with various microorganisms demonstrate the rates of Hg° formation in the range between $3x10^{-6}$ and $18x10^{-5}$ min^{-1} *(11, 26)* (Table 2b).

In order to distinguish biotic from abiotic reduction mechanisms, some experiments were carried out with water and sediment samples previously irradiated with gamma-rays and treated with NaN_3. Production of gaseous mercury was only observed for the highest Hg(II) concentration (Figure 4), i.e. a 250 nM concentration. The total produced Hg° concentration never exceeded 26 pM after 2.5 h of reaction time, a value 300 times lower than the Hg° concentration recorded after reaction with untreated sediment. The observed rate constant for sterilized sample is two order of magnitude lower ($3x10^{-7}$ min^{-1}) than for non sterilized sample.

For all samples (treated and untreated) the highest Hg° production rate is observed during the first 20 minutes of reaction time. Afterwards, the reaction proceeds at a much slower rate (Figures 3 and 4).

The contrast between experiments run with sterilized sediments and raw sediments indicate that the reduction in the dark of Hg(II) in anoxic sediment suspensions is a biologically mediated phenomena. We can conclude that at the bottom layer of the tropical stratified reservoir Petit Saut, the Hg° formation mechanism is a biotically induced mechanism. A similar mechanism may operate below the oxycline, an area characterized by the maximum bacteria concentration in the water column *(28)* and a local Hg° concentration maximum (Figure 2a).

According to the relatively low reduction rate constants, production of Hg° comparing to initial Hg(II) is not intensive: in our experimental conditions only 0.3 - 1.5 % of mercury happens to be reduced in 4 hours. Although, this rate may appear to be low, it must be considered with respect to the water residence time. The lake average residence time is equal to six months and little sedimentation occurs in the lake *(29)*. So the aqueous Hg(II) residence time is of the same order as water residence time. Since the reaction time of reduction in aqueous suspension of nonsterilized sediments does not exceed 96 days (three months, Table 2a), all dissolved mercury which comes in contact with the sediment could be reduced by the sediment before it leaves the reservoir dam.

Mercury speciation in aqueous suspension of surface sediments

In order to understand the limited Hg° production, we estimated equilibrium speciation of mercury in our laboratory water- sediment suspensions.

As shown by Peretyazhko et al *(17)* the partition coefficients ($Kd_{(ml/g)}= Hg_P/Hg_D$) does not change with season, with $\log K_d$ equal to 5.27± 0.17 and 5.23± 0.27 in wet and dry season, respectively. We considered only hydroxocomplexes of mercury in the model. In this simple case, no dissolved organic ligand was included. Hence, all dissolved mercury could be related to reactive mercury, usually determined as an easily-reducible fraction of total mercury which corresponds, probably, to the inorganically bound fraction of Hg(II) *(1)*. Equilibrium constants for Hg(II) aqueous complexes are taken from *(30)*. As the $Hg(OH)_2°$ complex is predominant for Hg(II) complexes in fresh waters then the distribution coefficient can be handled just like any other equilibrium constant following the equation

$$Kd=[Hg(II)]_{ads}/[\ Hg(OH)_2°] \qquad (2)$$

or

$$Kd \times C_{part} = [Hg(II)]_{ads}/(K_{Hg(OH)2}[Hg^{2+}]/[H^+]^2) \qquad (3)$$

where C_{part} corresponds to the total concentration of particles (kg/l) and $K_{Hg(OH)2}$ is the $Hg(OH)_2°$ formation constant. Following equation (3) $[Hg(II)]_{ads}= 1.8*10^{-3}\ [Hg^{2+}]/[H^+]^2$. Calculations were performed for the conditions of the experiments: pH 6 , the $Hg(II)_{total}$ 250, 4.4, 2.5 and 1.5 nM, the total solid concentration 18g/l, and $\log K_d$ 5.25.

Computations predict 99.96 % of total mercury is complexed by the solid phase at equilibrium. Concentration of reactive mercury, i.e., the sum of all dissolved inorganic species ($[Hg^{2+}]$+[$Hg(OH)_2°$]), does not exceed 0.04% of the total mercury concentration. The calculated results correlate well with measured concentrations of reactive mercury in our experimental aqueous suspensions of surface sediments: for suspensions with $Hg(II)_{total}$ concentrations equal to 4.4, 2.5 and 1.5 nM the experimental reactive mercury (Hg_R) concentrations are equal to 1.25 ± 0.2 pM, 1.06 ± 0.2 pM and 0.92 ± 0.2 pM, while calculated Hg_R are 1.83, 0.95 and 0.62 pM, respectively.

Sediment bulk composition is presented in Table 3. The highest concentrations are found for Al, Si, Fe and C_{org}. X-ray powder diffraction spectra indicates that the inorganic fraction contains three main minerals: quartz (SiO_2), gibbsite ($Al(OH)_3$) and kaolinite ($Al_2Si_2O_5(OH)_4$) present as 352, 244 and 322 mol/kg of dry sediment according to elemental composition (Table 3). Iron hydroxides were not detected by XRD, but tropical ferralitic soils are rich in Fe-(hydro)oxides. As sediments in Petit Saut reservoir are flooded soils, then Fe(III) hydrooxides, quartz, gibbsite, kaolinite, together with organic matter and bacteria, are the main reactive surfaces towards Hg(II) adsorption.

In our experiments, a fast reduction step, occurring in the first 20 minutes reaction time is followed by a slower reduction step (Figure 3, 4). Different reduction mechanisms may be involved with reactive mercury as principal reactant in the reduction processes. First, a fast reduction of the available reactive mercury occurs. Then the total rate of reaction will depend on the availability of reactive mercury, i.e. on mercury desorption and organic matter decay, which may both be rate-limiting steps. The hypothesis is confirmed by a positive correlation between the rate of Hg° production (in pM min^{-1}) and measured reactive mercury concentration (pM): Rate = $0.2857C_{HgR} - 0.243$ ($R^2 = 0.9988$) .

We can schematize the total pathways of reaction as follows

$$\begin{array}{l} Hg^{2+} + [S] \underset{k_{-1}}{\overset{k_1}{\rightleftharpoons}} [S\text{-}Hg^{2+}] \\ \downarrow \\ Hg^{2+} + B + 2e^- \rightarrow Hg°\text{-}B \rightarrow Hg° + B \end{array} \qquad (4)$$

where [S] is an active site on inorganic sorbent or organic species ($R\text{-}O^-$, $R\text{-}S^-$, $R\text{-}COO^-$), B is a bacteria cell, Hg°-B is the precursor complex, k_1, k_{-1} are the rate constants of adsorption and desorption reactions, respectively.

As follows from equation (4), reduction of Hg(II) to Hg° requires two electrons to be transferred. The transformation

$$1/2Hg(OH)_2° + H^+ + e^- \rightarrow 1/2Hg°aq + H_2O \qquad (5)$$

has a pε°(W) value of 7.1 *(31)*. From a thermodynamic point of view the $Hg(OH)_2°/Hg°$ couple is able to oxidize any other system with a lower pε°(W) value, namely, Fe(II), S(-II) and organic matter. As mercury is present in aquatic systems at trace levels (typically Hg_D is 18 ± 0.003 pM in lake Petit Saut, *(24)*) and mainly complexed with organic matter, we can propose that the mercury reduction is a secondary process coupled with microbially mediated production of Fe(II), S(-II). Vandal et al *(2)* suggested that Hg° production in anoxic waters may be linked to the activity of sulfate reducing bacteria (SRB). However sulfate concentration is rather low in Petit Saut lake (21nM, *(16)*) . Hypolimnic waters contain little sulfide and they are always undersaturated with respect to FeS *(17)*. Sediments and suspended matter collected during field trips were light brown. Therefore the link between $Hg(OH)_2°$ and SO_4^{2-} reduction mechanism remains an open topic in sulfate depleted tropical surface waters. Since an intensive Fe-(hydro)oxides reductive dissolution by dissolved organic matter, observed in anoxic layer of Petit Saut reservoir during dry season *(17)*, leads to the release of reactive mercury into water body (Figure 2) we suggest that Hg° production may be linked to this redox transformation. At the oxycline layer Hg(II) reduction can be due to the oxidation of Fe(II). This phenomena has been studied in laboratory experiments which are discussed below.

Reduction of Hg(II) by Fe(II) in the presence of hematite

As demonstrated in Figure 2a, a sharp increase in Hg° concentration is observed, just below the oxycline, near 5 m depth at Roche Genipa site. At this layer, a rapid turnover of redox sensitive elements including iron takes place. Ferrous iron has been shown to provide an effective means for removing a variety of pollutants including nitrite, nitrate, chromium, selenate, uranium, pertechnetate, and nitrobenzene from aqueous solution *(20, 32-35)*. A common feature of these reductive transformation reactions is that surface ferrous iron is always much more reactive than dissolved iron (II). Indeed, rates of homogeneous reduction by dissolved Fe(II) are exceedingly slow (Figure 6a, filled circles). Surface Fe(II) complexes

formed with hydrous iron oxides, silicates and sulfides, are on the other hand very efficient reductants from a thermodynamic (Figure 5) as well as from a kinetic point of view *(36)*.

Hence, it is possible that together with the biotic production of Hg°, an abiotic reduction pathway involving ferrous iron sorbed on suspended particles, may occur. In order to verify this hypothesis, experiments with suspensions of hematite nanoparticles were performed. In these experiments, the concentration of Fe(II), Hg(II) and particles were chosen to be close to the ones observed in Petit Saut reservoir.

Figure 6a shows a typical example of Hg° production in a system containing aqueous Hg(II) and Fe(II) together with hematite particles. The reactivity of the system was studied at three different pH values (pH 6, 7.4, 7.8). Fe(II) adsorption varies dramatically in this pH range *(20)*. There is virtually no production of Hg° in pure 1.5 μM Fe(II) solution, i.e. without hematite (Figure 6a).

During the entire length of the experiments (about 120 min) the formation of Hg° follows an apparent first order kinetic law (Figure 6b):

$$\ln\left(\frac{[Hg(II)]_t}{[Hg(II)]_o}\right) = -k_{obs}t \qquad (6)$$

where $[Hg(II)]_t$ and $[Hg(II)]_0$ are the Hg(II) concentrations at time t and time 0, respectively, and k_{obs} is the observed pseudo first order rate constant under the prevalent conditions. The pseudo-first-order rate constant values are equal to 0.002 min^{-1} at pH 6, 0.003 min^{-1} at pH 7.4 and 0.006 min^{-1} at pH 7.8 (Table 2b).

These data demonstrate that the amount Hg° produced, $C_{Hg°}$, depends on the initial pH and increases with pH increase. This observation correlates well with the adsorption of Fe(II) onto hematite particles *(20)*. Thus, we could suggest that reduction of Hg(II) is coupled to the oxydation of Fe(II) adsorbed on particles, as demonstrated before in the case of micaceous particles *(37)*.

Estimated fluxes of Hg°

The deeper water of the reservoir have been shown to have the highest turbulent diffusion coefficient, with values up to $2.5*10^{-4}$ m^2s^{-1} on h = 11 m during the period of dry season. With the average concentration of reactive mercury in these waters, we can estimate

the rate of production, R_p, (mol m^{-2} d^{-1}) of Hg° at the bottom layer of the Petit Saut reservoir by the following equation

$$R_p = k \times h \times C_{HgR} \qquad (7)$$

where k is the rate constant, $1.3*10^{-5}$ min^{-1}, a mean value of rate constants (Table 2a) of Hg° production in aqueous suspension of surface sediments with Hg(II) total concentrations of 4.4, 2.5 and 1.5 nM , C_{HgR} is an average concentration of reactive mercury, on h equal to 11 m from the bottom.

Hg° produced by the sediments has several possible fates: evasion to the atmosphere, export out of the dam or reoxidation, which we shall explore now.

The output flux of Hg° out of the dam is equal to

$$F_{out} = C_{Hg^\circ} \times F_{H2O} \qquad (8)$$

where F_{H2O} is a water flux (m s^{-1}) obtained as a ratio of turbine flow (m^3s^{-1}) to reservoir surface area (m^2), estimated from total volume (m^3) and lake average depth (m). In December 1999 the turbine flow and average depth were 144 m^3s^{-1} and 10 m, respectively (Sissakian, personal communication). Thus, the water flux, F_{H2O}, is equal to $4.1 \cdot 10^{-7}$ m s^{-1} in dry season. C_{Hg° is an average Hg° concentration in hypolimnion (mol m^{-3}).

The value of flux toward the oxycline is estimated by

$$F_{oxycline} = K_z*(\Delta C/\Delta h) \qquad (9)$$

where K_z is a turbulent diffusion coefficient at the oxycline layer ($4.35 \cdot 10^{-6}$ m^2s^{-1}), $\Delta C/\Delta h$ is Hg° concentration gradient (mol m^{-4}).

The evasion of Hg° to the atmosphere is approximated using the thin film gas exchange model given below:

$$F_e = K(C_a*H^{-1} - C_w) \qquad (10)$$

here C_a and C_w are the concentrations of Hg° in the air and water, respectively; H is a Henry's law constant, K, the transfer velocity (cm hr^{-1}), is estimated from the empirically derived relationship $K(600)=0.45*w^{1.64}$ *(38)* and is dependent on the Schmidt number (i.e. 600) which is a function of temperature and diffusivity and wind speed (w) at 10 m above the ground. The value of transfer velocity was estimated on the basis of a wind speed of 5 m s^{-1} *(16)*.

The ebullition of Hg° gas from the bottom layer is defined as

$$F_{eb} = \varepsilon C_{Hg^\circ}/(P_h K_H) \qquad (11)$$

where K_H represents the Henry's constant (0.128 M atm^{-1} at 25°C), P_h is the hydrostatic pressure (atm) at the given depth h (m), C_{Hg° is Hg° concentration at the bottom, ε is a rate of ebullition (mol m^{-2} d^{-1}) *(39)*. The rate of ebullition was estimated from the measured value of

CH_4 bubbling flux reported for the Petit Saut reservoir *(16)*. From the bubbling flux of 15 mol m^{-2} d^{-1}, determined at the layer from 7 to 9 m, the rate of ebullition of 0.061 mol m^{-2} d^{-1} was obtained.

Estimated values of production rate and fluxes toward the oxycline, export out of the dam, evasion to the atmosphere and ebullition fluxes at Roche Genipa and Saint Eugene sampling sites are summarized in Table 4. Evasion of Hg° to the atmosphere from the surface waters is of the same order of magnitude as Hg° production rate at the bottom layer. According to the Table 4, evasion of Hg° due to ebullition from the hypolimnic waters is negligible with respect to Hg° production in the surface sediments, i.e. only 0.025 – 0.05 % of R_p. Hg° diffusion flux toward the oxycline together with export out of the dam constitute 25 and 11 % of production rate, R_p, at Roche Genipa and Saint Eugene sampling sites, respectively. Consequently, Hg° evasion from the hypolimnetic waters (the sum of F_{out} and F_{ox}) does not completely compensate the production of Hg° at the bottom layer and Hg° evasion to the atmosphere. Thus, the venting of Hg° to the atmosphere from the surface water is almost due to photochemical processes and not due to the input from the hypolimnion. The difference between Hg° production rate in surface sediments and Hg° evasion from the hypolimnetic waters suggests that back oxidation of Hg° may take place in the deeper waters which decrease Hg° volatilization from the hypolimnion. The reaction mechanism of Hg° oxidation is not clear. Recent laboratory experiments demonstrated that in oxygenated solutions, i.e., surface waters Hg° photooxidation takes place. In order to understand a fate of elemental mercury, Hg°, in anoxic tropical water the laboratory experiments should be carried out.

CONCLUSIONS

In tropical stratified Petit Saut reservoir we found the increase of Hg° concentrations in the surface waters and at the bottom layers at the both studied sites and near the oxycline at Roche Genipa sampling site. Comparison of Hg° in temperate and tropical lakes showed that visible Hg° production by the sediments can only be observed in stratified tropical lakes.This can be explained by a temperature difference between the two water bodies (2-10°C in hypolimnion of temperate lakes and 25 - 26°C in Petit Saut lake hypolimnion).

Laboratory experiments with surface sediments indicate that Hg° production at the bottom layer of Petit Saut reservoir is biologically mediated. Calculations of mercury

distribution between surface sediments and aqueous phase predict that almost all mercury is complexed by solid phase at equilibrium. The principal sorbents could be kaolinite, quarts, gibbsite, Fe (hydro)oxides and organic matter. According to kinetic experiments and equilibria calculations, the total rate of reaction depends on the availability of reactive mercury, Hg_R, and the processes of desorption and degradation of organic matter may be the rate-limiting steps. As mercury is presented in natural aquatic systems always at nano-gram level, we can propose that the mercury reduction is mainly a secondary process of microbially mediated redox transformations. Since an intensive reductive dissolution of Fe-(hydro)oxides by dissolved organic matter, observed in anoxic layer of Petit Saut reservoir during dry season, leads to the release of reactive mercury into water body, we suggest that Hg° production may be linked to this redox transformation.

Production found at the oxycline layer could be due to biotic Hg_R reduction and also abiotic reduction by Fe(II) in the presence of particulate matter. Laboratory experiments on Hg° production by Fe(II) in the presence of hematite particles suggest that reduction of Hg(II) is coupled to the oxidation of Fe(II) adsorbed on particles.

Calculated Hg° production rate in the surface sediments together with Hg° fluxes toward the oxycline, out of the dam, evasion to the atmosphere, demonstrate that production rate at the bottom layer is not completely compensated by Hg° evasion due to the fluxes toward the oxycline and out of the dam, suggesting the possibility of Hg° back oxidation in hypolimnion of the tropical reservoir. Hg° ebullition out of the deeper waters is negligible with respect to Hg° production rate. The venting of Hg° to the atmosphere from the surface water is almost due to photochemical processes and not to the input from the hypolimnion.

FIGURE CAPTIONS

Figure 1. Map of Petit Saut reservoir with marked sampling sites.

Figure 2. Vertical profiles of gaseous mercury, Hg°, (○) and reactive mercury, Hg_R, (□) at Roche Genipa (a) and Saint Eugene (b) sampling sites in dry season (December 1999).

Figure 3. Cumulated Hg° production in aqueous suspension of 18 g l^{-1}(d.w.) untreated surface sediment at pH 6 with three initial Hg(II) total concentration: 1.5 nM (Δ), 2.5 nM (□) and 4.4 nM (○).

Figure 4. Hg° concentration in aqueous suspension of 18 g l^{-1}(d.w.) untreated (in black) or γ-ray and NaN_3 treated (in white) surface sediments at pH 6 and 250 nM Hg(II) initial concentration.

Figure 5. Eh values computed for various Fe(II)/Fe(III) couples *(36)* and Hg(II)/Hg° at pH 7.0.

Figure 6. In situ measurement of Hg° production by an aqueous solution containing 1.5 μM Fe(II), 20 pM Hg(II), and 5 mg L^{-1} hematite (a) suspension of hematite with Fe(II) and Hg(II) pH 6(○), 7.4(Δ) and 7.8(■),●- solution of Fe(II) and Hg(II) without hematite at pH 7.8, (b) Natural logarithm of the relative concentration (C/C_0) for Hg(II) vs. time. Solid line is the linear regression through the data.

Table 1. Levels of Hg° concentrations in Petit Saut and Pallette *(2)* lakes .

		Hg° (pM)	S (‰)	t°C
Petit Saut reservoir, French Guyana (dry season)	epilimnion	0.19 - 0.27	664 - 915	~ 31
	metalimnion	0.07 - 0.31	430 - 876	27.5
	hypolimnion (mean)	0.26 - 0.4	1143 - 1742	25.4
	bottom layer	0.35 - 0.57	1522 - 2453	
Pallette lake, USA (March, 1989 , no stratification)	epilimnion	0.12	360	2.0
	metalimnion	0.12	360	2.8
	hypolimnion	0.15	460	3.0
Pallette lake, USA (August, 1989 , stratification)	epilimnion	0.26-0.35	930 - 1180	19.5
	metalimnion	0.06	140	6
	hypolimnion	0.075	170	6

Table 2a. Summary of observed first- order rate constants, k_{obs} of Hg° production.

Aqueous suspension of surface sediments		
$Hg(II)_{initial}$ (nM)	k_{obs} (R^2)[c] (min^{-1})	$t_{1/2}$ (days)
250[a]	$7 \cdot 10^{-5}$ (0.89)	7
250[b]	$3 \cdot 10^{-7}$ (0.96)	1600
4.4[a]	$2 \cdot 10^{-5}$ (0.99)	24
2.5[a]	$1 \cdot 10^{-5}$ (0.89)	48
1.5[a]	$1 \cdot 10^{-5}$ (0.99)	48
Aqueous suspension of hematite particles[d]		
pH	k_{obs} (R^2) (min^{-1})	$t_{1/2}$ (hr)
6	$2 \cdot 10^{-3}$ (0.99)	6
7.4	$3 \cdot 10^{-3}$ (0.99)	4
7.8	$6 \cdot 10^{-3}$ (0.99)	2

[a] Untreated suspension of 18 g l^{-1} (d.w.) surface sediments at pH 6.

[b] Suspension of surface sediments of 18 g l^{-1} (d.w.), pH 6 treated by γ-ray and NaN_3 (1 %).

[c] Regression of $\ln([Hg(II)]_{initial} - [Hg°]_t)$ vs t, where t is whole time interval of kinetic experiment.

[d] Suspension of 5 mg l^{-1} hematite, 1.5 μ Fe(II), 20 pM Hg(II).

Table 2b. Summary of first order rate constants of Hg° production, reported for different aquatic environments.

	k_{obs} (min^{-1})
Pallette Lake,USA[a]	
Epilimnion (1-3m)	$6 \cdot 10^{-6} - 17.4 \cdot 10^{-5}$
Metalimnion (9m)	$2.7 \cdot 10^{-5} - 4 \cdot 10^{-5}$
Heat sterilized	$7.2 \cdot 10^{-6} - 1.2 \cdot 10^{-5}$
Marine microorganisms[b]	$2.8 \cdot 10^{-6} - 6.7 \cdot 10^{-5}$
Upper Mystic lake, USA[b] surface waters	$4.9 \cdot 10^{-6} - 3.7 \cdot 10^{-5}$
Aqueous suspension of phlogopite with Fe(II)[c]	0.0116

[a] Vandal et al, *(26)*.

[b] Mason et al, *(11)*.

[c] Suspension of 3 mg l^{-1} phlogopite, pH 7.5, 10 μM Fe(II), 50 pM Hg(II), *(37)*.

Table 3. Bulk composition of sediments collected at St Eugene site.

Element	(g kg^{-1})	(mol kg^{-1})
Si	246	8.7
Al	205	7.6
Fe	84	1.5
C_{org}	50	
Ti	8.8	0.2
Mg	0.84	0.03
Ca	0.72	0.018
K	0.4	0.01
Mn	0.3	0.005
P	0.8	0.03

Table 4. Hg° production rates (R_p), export out of the dam (F_{out}), flux toward oxycline ($F_{oxycline}$), evasion to the atmosphere (F_e) and ebullition (E_{eb}) (in mol m^{-2} d^{-1}).

	Roche Genipa	Saint Eugene
R_p	$3.2 \pm 1.3 \cdot 10^{-10}$	$1.23 \pm 1.3 \cdot 10^{-10}$
F_{out}	$1.3 \pm 0.2 \cdot 10^{-11}$	$0.8 \pm 0.2 \cdot 10^{-11}$
$F_{oxycline}$	$6.7 \pm 0.7 \cdot 10^{-11}$	$0.6 \pm 0.2 \cdot 10^{-11}$
F_e	$2.9 \pm 0.2 \cdot 10^{-10}$	$4.1 \pm 0.2 \cdot 10^{-10}$
F_{eb}	$7.6 \cdot 10^{-14}$	$6.5 \cdot 10^{-14}$

REFERENCES

(1) Morel F.M.M., Kraepiel A.M.L., Amyot M., (1998). *The chemical cycle and bioaccumulation of mercury.* Annual Reviews Ecol.Syst., 29: p. 543-566.

(2) Vandal G.M., Mason R.P., Fitzgerald W.F., (1991). *Cycling of volatile mercury in temperate lakes.* Water, air and soil pollution, 56: p. 791-803.

(3) Kim J.P.,Fitzgerald W., (1986). *Sea-air partitioning of mercury inthe equatorial pacific ocean.* Science, 231(03): p. 1986.

(4) Fitzgerald W.,Mason R., *The global mercury cycle: oceanic and anthropogenic aspects*, in *Global and regional mercury cycles: sources, fluxes and mass balances*, e.a. Baeyens W., Editor. 1994. p. 85-108.

(5) Nriagu J.O., (1994). *Mechanistic steps in the photoreduction of mercury in natural waters.* The science of the total environment, 154: p. 1-8.

(6) PeretyazhkoT., Charlet L., Grimaldi M., (2002). *Production of gaseous mercury in hydromorphic soils.* European journal of soil science (in prep.).

(7) Amyot M., Mierle G., Lean D.R., McQueen D.J., (1994). *Sunlight-induced formation of dissolved gaseous mercury in lake waters.* Environmental science and technology, 28: p. 2366-2371.

(8) Amyot M., Mierle G., Lean D., McQueen D.J., (1997). *Effect of solar radiation on the formation of dissolved gaseus mercury in temperate lakes.* Geochimica et cosmochimica acta., 61(5): p. 975-987.

(9) Allard B.,Arsenie I., (1991). *Abiotic reduction if mercury by humic substances in aquatic system- an important process for the mercury cycle.* Water Air and Soil Pollution, 56: p. 457-463.

(10) Zhang H.,Lindberg S.E., (2001). *Sunlight and iron(III)-induced photochemical production of dissolved gaseous mercury in freshwater.* Environmental science and technology., 35: p. 928-935.

(11) Mason R. P., Morel F. M. M., Hemond H. F., (1995). *The role of microorganisms in elemental mercury formation in natural waters.*

(12) Barkay T., Liebert C., Gillman M., (1989). *Environmental significance of the potential for mer(Tn21)-mediated reduction of Hg2+ to Hg0 in Natural waters.* Applied and environmental microbiology, 55(5): p. 1196-1202.

(13) Lalonde J.D., Amyot M., Kraepiel A.M.L., Morel F.M.M., (2001). *Potooxidation of Hg(0) in artificial and natural waters.* Environmental science and technology., 35: p. 1367-1372.

(14) Amyot M., Gill G.A., Morel F.M.M., (1997). *Production and loss of dissolved geseous mercury in coastal seawater.* Environ. Sci. Technol., 31: p. 3606-3611.

(15) Sissakian C., (1992). *Présentation de la retenue de Petit saut en Guyane Française: cartographie- partition de la retenue- volumes et surfaces- intégration paysagère.* Hydroécol. Appl., 1: p. 121-132.

(16) Galy-Lacaux C., Delmas R., Jambert C. , Dumestre J.-F., Labroue L., Richard S., Gosse P., (1997). *Gaseous emissions and oxygen consumption in hydroelectric dams: A case study in French Guyana.* Global biogeochemical cycles, 11(4): p. 471-483.

(17) Peretyazhko T., Van Cappellen P., Coquery M. , Meile C., Musso M. , Regnier P. , Charlet L., (2002). *Biogeochemistry of tropical reservoir lake(Petit Saut, French Guiana): implications for mercury cycle.*

(18) Quémerais B.,Cossa D., *Procedures for sampling and analysis of mercury in natural waters..* 1997, Environmental Canada-Québec Region, Environmental Conservation, St Laurence Centre. Scientific and technical report. p. 36.

(19) Bloom N.S.,Fitzgerald W.F., (1988). *Determination of volatile mercury species at the picogram level by low-temperature gas chromatography with cold-vapor atomic fluorescence detection.* Anal. Chim. Acta., 208: p. 151-161.

(20) Liger E., Charlet L., Van Cappellen P., (1999). *Surface catalysis of uranium(VI) reduction by iron(II).* Geochimica et cosmochimica Acta., 63(19/20): p. 2939-2955.

(21) Vogel A.I., (1989). *Vogel's textbook of quantitative chemical analysis.* Longman Scientific and technical. 877 p.

(22) Samemasa I., (1975). *The solubility of elemental mercury vapor in water.* Bulletin of the chemical society of Japan, 48(6): p. 1795-1798.

(23) Amouroux D., Wasserman J., Tesseir E., Donard O., (1999). *Elemental mercury in the atmosphere of a tropical amazonian forest (French Guyana).* Environmental science and Technology.

(24) Programme mercure en Guyane: region de Saint Elie et retenue de Petit Saut.. 2001.

(25) Xiao Z., Stromberg D., Lindqvist O., (1995). *Influence of humic substances on photolysis of divalent mercury in aqueous solution.* Water, air and soil pollution, (80): p. 789-798.

(26) Vandal G.M., Fitzgerald W.F., Rolfhus K.R., Lamborg C.H., (1995). *Modeling the elemental mercury cycle in Palette lake, Wiskonsin, USA.* Waater, air and soil pollution., 80: p. 529-538.

(27) Beucher C., Wong Wah Chung P., Richard C., Mailhot G., Bolte M., Cossa D., (2002). *Hg° formation under irradiation of unamended waters from French Guiana.* Environmental science and technology (in prep.).

(28) Dumestre J.F., Labroue L., Galy-Lacaux C., Reynouard C., Richard S., (1997). *Biomasses et activites bacteriennes dans la retenue et a l'aval du barrage de Petit Saut (Guyane): influence sur les emissions de methane et la consommation d'oxygene.* Hydroecologie appliquee, 9(1-2): p. 139-167.

(29) Sissakian C., (1997). *Présentation général de l'aménagement hydroélectrique de Petit Saut (Gyuane française) et du programme de suivi écologique lié à sa mise en eau.* Hydroecologie appliquée, 9(1-2): p. 1-21.

(30) Tiffreau C., Lutzenkirchen J, Behra P., (1995). *Modeling the adsorption of Hg on (Hydr)oxides.* Journal of colloid and interface science, 172: p. 82-93.

(31) Stumm W.,Morgan J.J., (1996). *Aquatic chemistry.* John Wiley&Sons. 1022 p.

(32) Klausen J., Tröber P.T., Haderlein S.B., Schwarzenbach R.P. , (1995). *Reduction of substituted nitrobenzenes by Fe(II) in aqueous mineral suspensions.* Env. Sci. Technol., 29: p. 2396-2404.

(33) Cui D.,Eriksen T.E., (1996). *On the reduction of pertechnetate by derrous iron in solution; influence of soebed and precipitated Fe(II).* Environmental science and technology.

(34) Myrreni S.C.B., Tokunaga T.K., Brown Jr. G.E., (1997). *Abiotic selenium redox transformations in the presence of Fe(II, III) oxides.* Science, 278: p. 1106-1111.

(35) Buerge I.J.,Hug S.J., (1999). *Influence of mineral surfaces on chromium(VI) reduction by Fe(II).* EnvironSci. Technol., 33: p. 4285-4291.

(36) Stumm W.,Sulzberger B., (1992). *The cycling of iron in natural environments; considerations based on laboratory studies of heterogeneous redox processes.* Geochim. Cosmochim. Acta, 56: p. 3233.

(37) Charlet L., Bosbach D., Peretyashko T., (2002). *Natural attenuation of TCE, As, Hg linked to the heterogeneous oxidation of Fe(II): an AFM study.* Chemical geology (submitted).

(38) Wanninkhof R., (1992). *Relationship between wind speed and gas exchange over the ocean.* Journal of geophysical research, 97(C5): p. 7373-7382.

(39) Morel F.M.M.,Hering J.G., (1993). *Principles and applications of aquatic chemistry.* Wiley Interscience. 588 p.

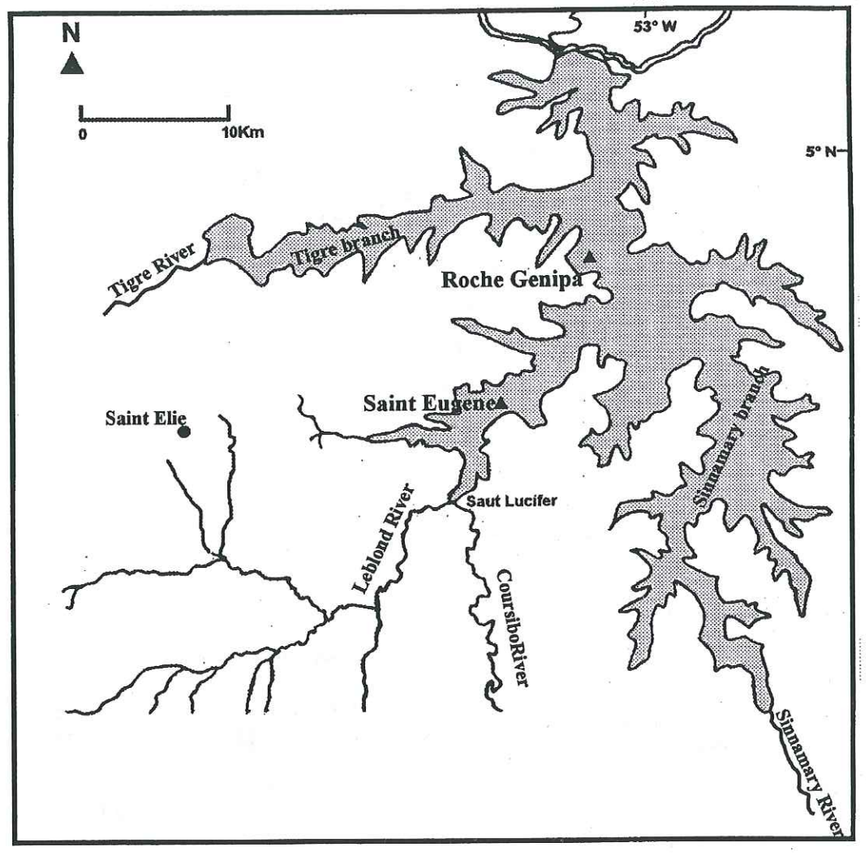

Figure 1

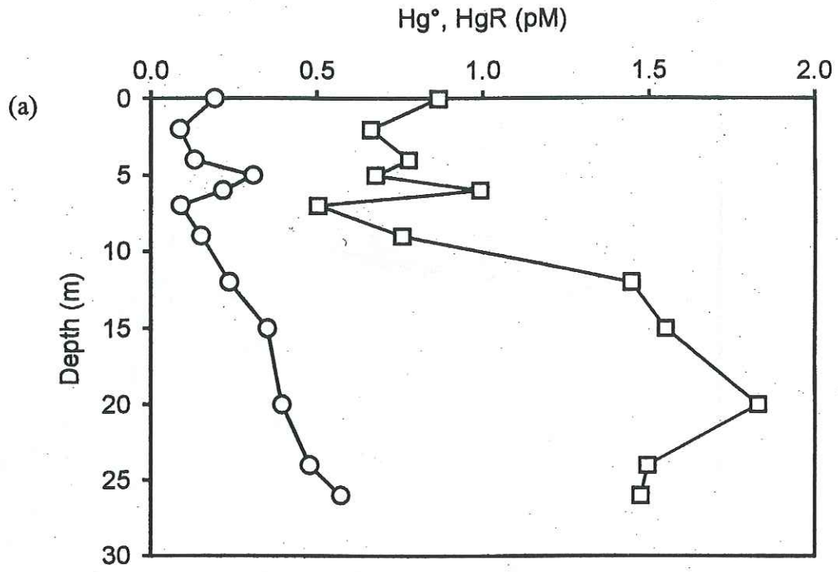

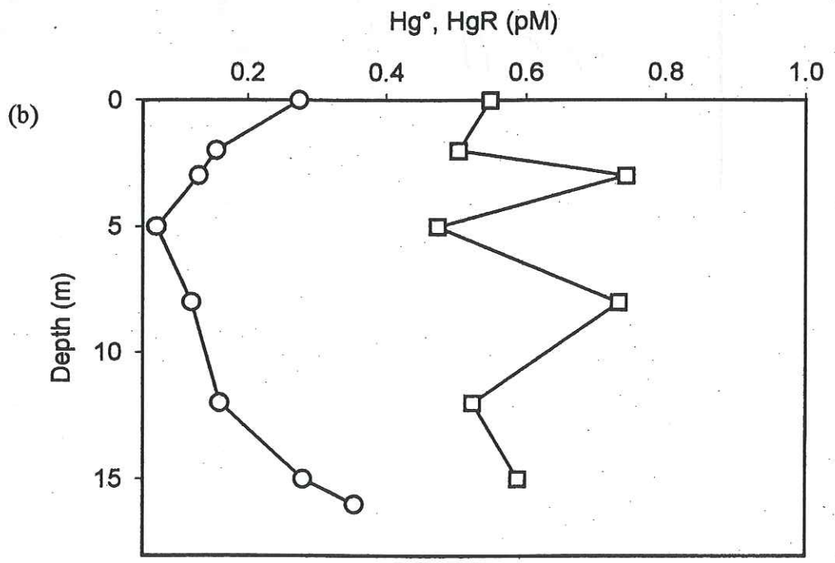

Figure 2

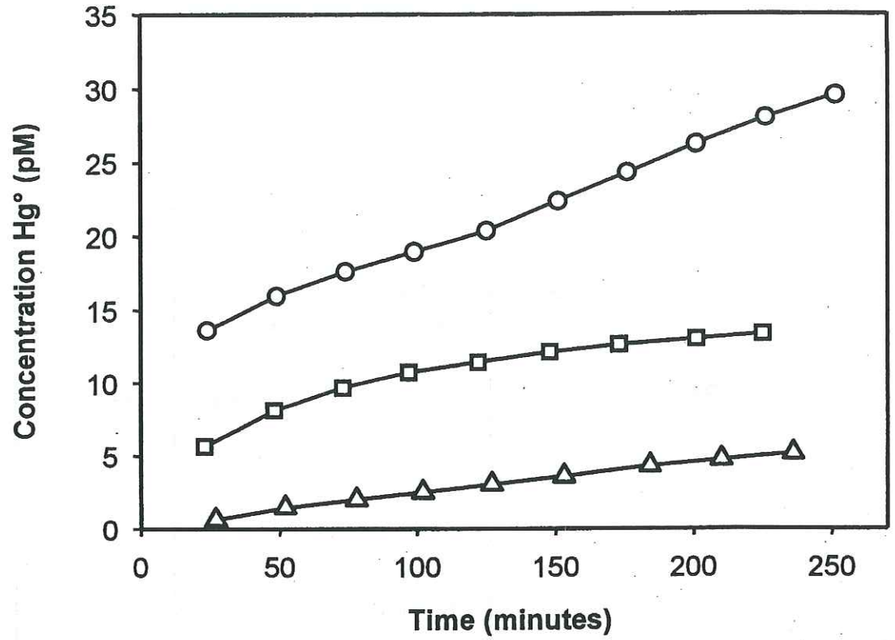

Figure 3

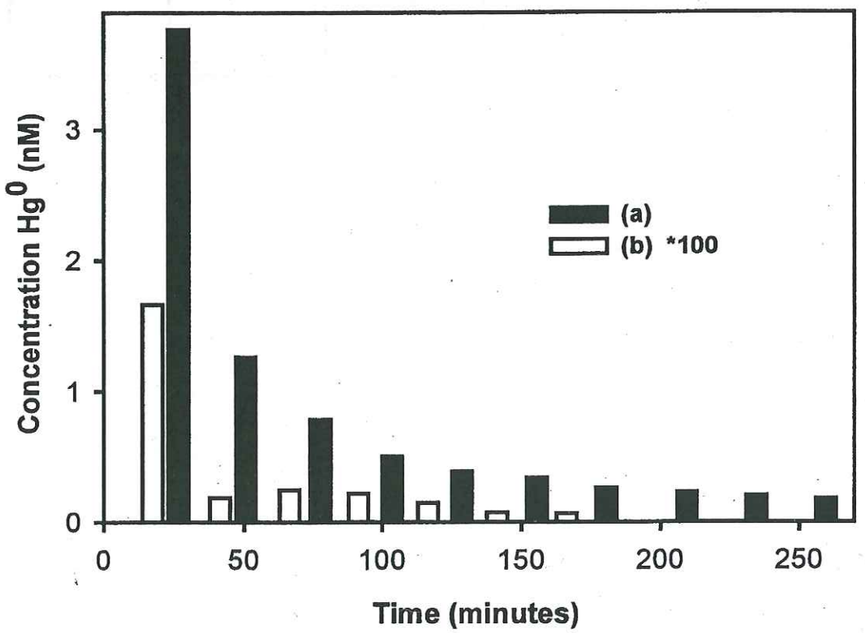

Figure 4

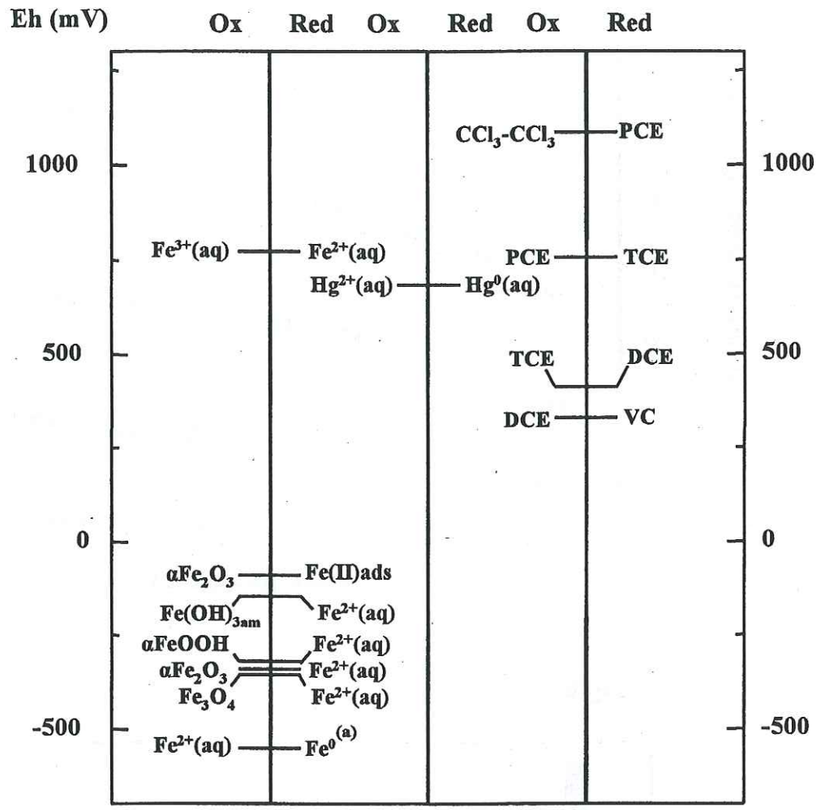

Figure 5

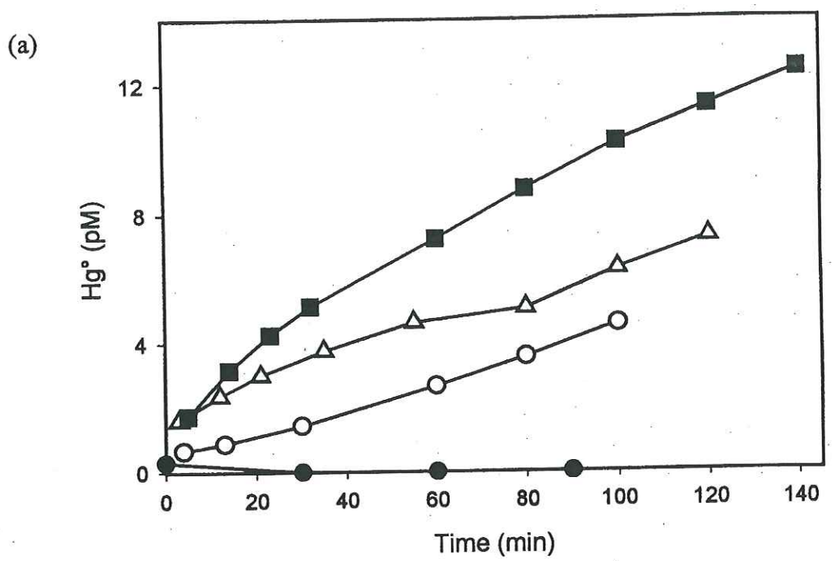

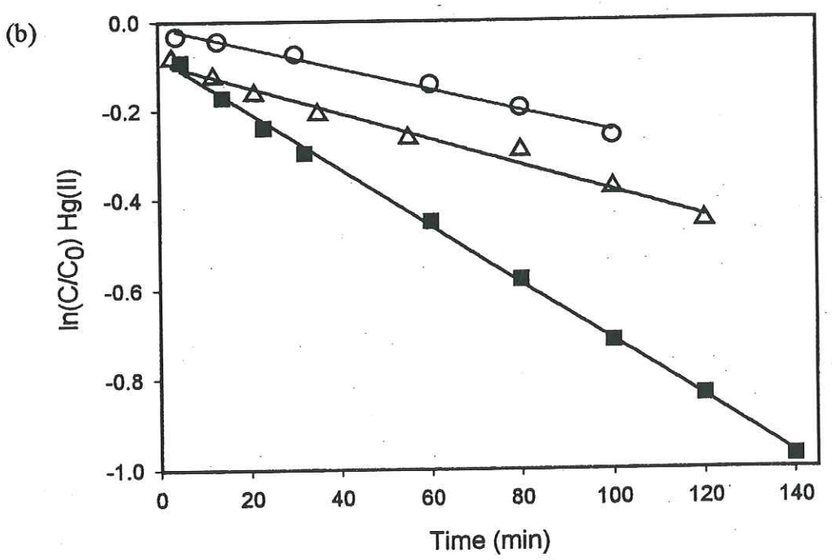

Figure 6

INTRODUCTION

Mercury contamination is considered one of the worst environmental problems affecting the tropical ecosystems in the South America. Among the evidences of such contamination are the high mercury contents found in the fish fauna and riverine inhabitants whose diet is based exclusively on fish protein *(1, 2)*. The principal anthropogenic source of mercury is gold mining activity. The annual average losses of mercury to the atmosphere is about 137 tons $year^{-1}$ and to rivers about 44 tons $year^{-1}$ in the Amazon region due to gold mining *(3)*. Soils are considered to be one of the important natural sink of released mercury *(4)*. Ferralitic soils, widespread in tropical climate, are particularly efficient traps of mercury due sorption phenomena *(5)*. However, recent calculations of Roulet and co-workers, *(6)* of the anthropogenic contribution to the overall content of mercury in Amazonian soils demonstrate that only 3 % of the Hg present in the surface horizons of soils are from gold mining sources. According to these authors, mercury would have been accumulated mainly through natural pedogenetic processes. Degradation of ferralitic soils (including soil deforestation, erosion, flooding, cultivation) represents a natural source of mercury contamination in the Amazon ecosystems.

Highly- weathered tropical ferralitic soils consist of mainly the following inorganic components: Fe and Al hydrous oxides and clay minerals such as kaolinite *(7)*. As shown by many researches, mercury has high affinity to inorganic adsorbents *(8)*. Free Hg ions can be adsorbed by iron (hydro)oxides (goethite *(9)*, ferrihydrite *(10)*), clay minerals *(11)* and quartz *(12)*.

Another well-documented component that significantly affects mercury adsorption in soil is organic matter. Kerndorff and Schnitzer *(13)* investigated the adsorption of 11 metals (Hg, Fe, Pb, Cu, Al, Ni, Cr, Zn, Cd, Co and Mn) by soil humic acid, and reported that among these metals, Hg and Fe exhibited the strongest affinity for humic acid. The presence of organic matter in solution was also reported to inhibit the adsorption of Hg(II) on mineral surfaces *(8)*. It has been experimentally shown that Hg has a greater affinity for fulvic acid organic ligand, than for inorganic ligands such as chloride and hydroxide ions *(8, 14)*.

The general vertical distribution pattern of mercury in acid forest soils under temperate climate is closely related to the distribution of organic matter. For instance, in Swedish podsols, the concentration of mercury is maximal in the organic (A) surface horizon (40-200 ng/g), low in the eluvial (E) horizon (20-40 ng/g), again high in the illuvial (B) horizon (40-80

ng/g) where some organic matter has been flocculated , and then is usually of low concentrations in the parent material (30 ng/g) *(15)*. In tropical ferralitic soils, the absence of a well developed organic layer coupled with the rapid turnover of any accumulated organic matter appears to limit superficial Hg accumulation. In these soils, mainly oxy-hydroxide levels (Fe and Al) control the Hg content along depth profiles *(16)* and the Hg concentrations are elevated (88- 209 ng/g) in comparison to values reported for temperate environments *(16)*. The flooding of these soils and the development of hydromorphy leads to the release of a significant amount of Hg into aqueous environment and to a decrease of Hg content in soils. This observation is generally interpreted in terms of Fe (hydro)oxides reductive dissolution and migration of the released mercury to downstream aquatic ecosystems *(5)*.

In the present work, we were interested in checking another possible mechanism which can decrease the concentration of mercury in hydromorphic soil, namely the reduction of Hg(II) to gaseous mercury, Hg°. In surface waters, photochemically induced mercury reduction is considered to be the principal mechanism of Hg° formation *(17-20)*. In anoxic systems such as anoxic sediments and lake hypolimnium, the biotic reduction of Hg(II) and the reduction of Hg(II) by adsorbed Fe(II) are also important processes of Hg° production *(21, 22)*. As shown in *(23)*, dissolved humic substances can also participate in abiotic reduction processes.

Here we investigate the reduction of Hg(II) as one of the pathway leading to the decrease of mercury concentration in tropical hydromorphic soils. Laboratory experiments were carried out with/and without iron(III) citrate complexes in order to determine whether Fe(II), produced by the biotic reduction of Fe(III), could participate to the transformation of Hg(II) to Hg°.

STUDY SITE

The study site is a 300 m long toposequence located on the left bank of the Leblond River, one of the inflows rivers into Petit Saut reservoir, French Guiana, South America (Figure 1a). The geological substrate is made up of granitoïds . The toposequence includes a clayey oxisol (S1) on the top of the hill, grading downslope towards ultisols (S2, S3, S6) on steep slopes and hydromorphic soils (S4, S5, S7) on gentle slopes (mid-slope terrace or bottom land) (Figure 1b).

The soil samples were collected from auger-boring in 0.1m increments. For mercury analysis, samples were digested in a 10 :1 solution of nitric and hydrochloric acids. Total mercury concentrations were then determined by cold vapor atomic fluorescence spectrometry *(24)*. The analysis were performed in Laboratoire Central d'Analyses of CNRS. Amorphous Fe(III) oxides were analyzed by ascorbate extraction according to the method of Kostka and Luther III *(25)* (data provided by L. Spadini).

LABORATORY STUDY

Reduction experiments were carried out with three samples of the hydromorphic soil S5 taken at the following depths: 30-40, 60-70 and 90-100cm. The clay fraction (<2 μm) of a 30 g subsample was separated by suspension of the soil centrifugation in 500 ml Milli-Q water at 700 rpm during 10 min and collection of the aqueous suspension upper 8 cm. Calcium chloride was then added to the suspension to reach a 1 N $CaCl_2$ concentration and to flocculate the particles. After several days the solid sample was washed several times with Milli-Q water to remove Cl^- by centrifugation at 6000 rpm during 30 min and freeze-dried.

A 60 mg aliquot of the obtained clay fraction of soil was added to 150 ml of deoxygenated water (final concentration 0.4 g l^{-1}), 16 ml of 0.1 M MOPS deoxygenated solution in a 200 ml titration reactor. The initial pH of the suspension was 7.0. Afterwards Fe(III) citrate ($FeC_6H_5O_7 \cdot H_2O$, hereafter denoted FeCit) was added to obtain an initial concentration of $1 \cdot 10^{-3}$ M. The samples without FeCit were prepared in a similar way. All samples were kept in a N_2-flushed glove box during one week.

For the kinetic experiment, a 2.5 μM initial Hg(II) solution was prepared from 5mM Hg(II) stock solution and acidified by HNO_3 before each experiment. At t = 0, an aliquot of Hg(II) stock solution was added to the suspension to get $[Hg(II)]_0$ = 2.5 nM. At fixed time intervals, the produced gaseous mercury was purged with ultra pure Ar, stored onto gold trap, and determined by cold vapor atomic fluorescence spectroscopy *(24)*. After one hour reaction, time a suspension aliquot was sampled, filtered through a 0.45 μm Milli-pore filter and analyzed for Fe(II) content in solution using the 1,10-phenantroline method *(26)*.

RESULTS AND DISCUSSIONS

Hydromorphic soils

The hydromorphic soils at Leblond pedosequence are gleysols, characterized by fluctuations of the water table level, which may rise up to the soil surface, and development of reducing conditions due to water saturation. In the uphill hydromorphic soils (S5) the effect of hydromorphy is detected from the surface layer down to the alterit layer located at 1.5 m.

The pedological profile shows, under a humic dark grayish brown horizon, a set of yellowish brown horizons with millimeter to centimeter gray and red mottles, sandy clayey (depth < 0.4 m) to clayey sandy (> 0.4 m). The soil changes at a depth of 1.2 m to a red yellowish, sandy clayey horizon, rich in ferruginous coarse particles (sand and gravel size), above a dark red alterite of low water conductivity which appears at 1.5 m in depth.

In the hydromorphic soil S5 under study, the concentration of organic matter is high below 50cm depth compared to the oxisol (Table1, Figure 2) as a result of poor decomposition of organic matter and production of organic acids. Acidic conditions (pH between 4.6 and 5) and organic acids favor the leaching of aluminum and iron from the upper horizons downwards and lead to a decrease in clay content in these soils (Figure 2). The metals released from clay mineral dissolution can be complexed by organic matter and move downward. Accumulation occurs at the middle layer between 1.2 and 1.5m where precipitation of (hydro)oxides takes place. These processes explain well the observed increase of amorphous Fe(III) oxides, as measured by ascorbate extraction, in the layer between 1 and 1.5 m (Figure 2).

During wet season, when a heavy precipitation takes place, water saturation cause the development of anoxic conditions due to the complete consumption of dissolved oxygen by aerobic respiration. Oxygen deficiency favors the development of anaerobic microorganisms responsible of diverse redox transformations. One of the most important transformations is the reductive dissolution of Fe oxyhydroxides which has strong influence on the immobilization/mobilization of many other elements. This transformation can be mediated by microbial catalysis, i.e., by dissimilatory Fe-reducing bacteria. Dissimilatory Fe-reducing bacteria obtain energy by coupling the oxidation of organic matter to the reduction of Fe(III) to Fe(II) *(27)*. Reduction of Fe(III) leads to the formation of soluble Fe(II)-organic complexes, adsorbed Fe(II), and Fe(II)- Fe(III) minerals, such as "green rust"*(28)*. As FeCit was added to the clay suspensions, significant Fe(III) reduction took place. The concentrations of dissolved Fe(II) are $5.2 \cdot 10^{-4}$, $2.6 \cdot 10^{-4}$ and $2.5 \cdot 10^{-4}$ M in the samples taken

from 30-40, 60-70 and 90-100 cm layers, respectively. Without FeCit, we did not observe the formation of any Fe(II).

Mercury in oxisol and hydromorphic soils

Mercury vertical distribution in the oxisol (S1), ultisol (S3) and hydromorphic soil (S5) is shown in Figure 3. The results demonstrate that the total mercury content in pedosequence varies strongly with soil type. The highest concentrations are found in oxisol, where it varies in a broad interval, with a mean value of 236 ± 107 ng/g and two 2100 and 500 ng/g maxima at the surface and at near 1m depth, respectively. The transition to ultisol is characterized by a decrease in total mercury content, with an average concentration of 138 ± 58 ng/g and a 250 ng/g maximum observed at 35 cm. The hydromorphic soil (S5) is characterized by the lowest Hg concentration with a mean value of 80 ± 40ng/g. A maximum concentration of 170ng/g is found near 1.35m, the level where a maximum in amorphous iron (hydro)oxide content is also observed (Figure 2). At the depths where samples were taken for the reduction experiments, total mercury concentrations are 74.5, 100.5 and 62.5ng/g, at 30-40, 60-70 and 90-100cm, respectively.

In the oxisol located at the top of the slope, a positive correlation between mercury concentration and clay fraction distribution has been observed *(29)*. In opposite, in the hydromorphic soil under study, no correlation between mercury concentration and clay fraction distribution is found. As suggested in *(5)*, the distribution of Hg is controlled by its transport in soil profiles and, i.e., by the mobility of humic-Hg complexes. Hence, in hydromorphic soil under study, mercury distribution is mainly controlled by migration of mercury associated with organic molecules and accumulation during hydroxides precipitation between 1 and 1.5 m.

The decrease of total mercury concentration observed between oxisol and hydromorphic soils clearly demonstrates that the principal reason is the development of anoxic conditions in hydromorphic soils. Under ambient reducing conditions, Fe(III) (hydr)oxides are dissolved. The reduction of Fe(III) leads to a decrease in the adsorption capacity of the soil. Mercury released from Fe(III) (hydro)oxides reductive dissolution may be complexed by humic substances, following its release from plant organic matter, and is thus further leached out from the profile as suggested by the low mercury content in these soils.

We suggest that along with leaching processes, reduction of Hg(II) to its gaseous form, Hg°, may take place. The reduction to gaseous mercury will decrease the pool of Hg presented in soils due to the low solubility of Hg° and its degassing to the atmosphere *(30)*. In studied hydromorphic soil, several potential reductants (bacteria, Fe(II) and humic substances) of Hg(II) are present, suggesting that production of Hg° may take place in anoxic conditions, when water saturation is observed. In order to check the hypothesis of reduction of Hg(II) to Hg°, the laboratory experiments where carried out with clay fraction of hydromorphic soils with and without FeCit. FeCit was used as a nutrient for the bacteria and a source of ferrous iron.

Production of Hg° in hydromorphic soils

Figure 4 shows the production of Hg° in anoxic suspension of hydromorphic soil samples taken at various depths. The experiments demonstrate that production of Hg° may take place in presence of FeCit with all samples taken from the hydromorphic tropical soil . After one hour reaction time, the highest Hg° production was observed for the soil sample taken at 90 to 100 cm depth. Total accumulated concentration of Hg° produced by this sample is 850 pM, while with 30-40 and 60-70 cm depth samples only 208 pM and 40 pM of Hg° was produced, respectively. Thus 8 %, 1.6 % and 34 % of the mercury initially injected in the suspensions was reduced by with 30-40, 60-70 and 90-100 cm soil samples, respectively, after one hour reaction time. Some kinetic experiments were carried out without addition of FeCit in order to observe the effect of soil constituents on their own Hg° production. Production by the 30-40 cm sample suspension does not exceed 20 pM at every time of Hg° sampling against a 97 pM production in the first minutes after Hg(II) addition in the sample with FeCit (Figure 5a). At 60-70 cm level, no production of Hg° in the absence of FeCit addition is found (Figure 5b). A significant production of Hg° is observed for the sample collected at 90-100 cm in the absence of FeCit although the initial observed kinetics is much slower. We found that presence of FeCit may enhance production of gaseous mercury. Concentration of Hg° is in general twice as large with FeCit, than without it (Figure 5c).

Our data can be fitted satisfactory well by first – order kinetics. The values of first-order rate constants are given in Table 2. The rate constant is constant in the upper horizons of the soil profile and increases an order of magnitude in the bottom horizon. Rate constants of elemental mercury formation, measured in the present work in aqueous suspensions of hydromorphic tropical soils, are significantly higher than the ones reported for the biotic

reduction in aqueous systems *(20, 31)* and anoxic suspensions of surface sediments *(21)*. Hg° production rate constants in these studies were in the range between $3 \cdot 10^{-6}$ and $18 \cdot 10^{-5}$ min^{-1} . These results suggest that some abiotic processes may contribute to the Hg° reduction in our system. In fact, rate values measured for Hg redox transformation by near 1m deep soil sample are close to the rate constants obtained for abiotic Hg(II) reduction by Fe(II) in the presence of hematite (0.002 min^{-1} at pH 6, 0.003 min^{-1} at pH 7.4 and 0.006 min^{-1} at pH 7.8) or phlogopite (0.0116 min^{-1} at pH 7.5).

No Fe(II) was present in the suspension before FeCit addition, while Fe(II) concentration was about 0.5mM afterwards. The presence of Fe(II) just after FeCit addition suggest the presence of Fe(III)-reducing microorganisms at all depths. Observed variation in Fe(II) concentration among samples can be explained by different dissimilatory reducing bacteria density, different reduction rates or different Fe(II) adsorptive properties. The high Hg° production in the sample taken at 90 to 100 cm depth without adding FeCit suggest the presence of either Fe(II) rich minerals in this horizon or specific anaerobic microorganisms. Due to the long phase of water saturation (nine months of wet season) intense mineralogical transformation may occur in this horizon although clay fraction XRD spectra are dominated by kaolinite and Al oxide diffraction peaks. Several reasons may create favorable conditions for bacterial growth. First, anoxic conditions developed in hydromorphic soils during wet season may last longer in the deeper horizons. Dissimilatory iron reducing bacterial growth can be influenced by longer phases of water saturation comparing to the upper horizons and limited oxygen diffusion. Also migration of humic substances downward may create a constant supply of nutrients to the microorganisms. In such hydromorphic soils, Fe(III) is typically transported downward, complexed with humic acids. It may then precipitate between 1 and 1.5 m depths as (hydro)oxides and could be an electron-accepter in microbially mediated redox processes. These considerations suggest that the 1 m deep horizon is the horizon where most of the redox reactions occur. As shown in Figure 3, concentration of total mercury decrease from 100 at 65 cm layer to 60 ng/g at 95 cm depth. This decrease may thus not be due to Hg(II) elution but to Hg(II) reduction and Hg° volatilization. The rate constants obtained in this study are of the same order of magnitude as the ones obtained for the reduction of Hg(II) by Fe(II) in presence of the mineral particles. Thus, in this horizon, bacterial reduction acts together with abiotic reduction by Fe(II) to reduce Hg(II) stored in similar – non hydromorphic – soils, such as the oxisol located above in the pedosequence. The small difference in Hg° production between sample with and without FeCit addition could be explained by the presence of large amounts of microorganisms and by the presence

of Fe(II) in clay fraction *(32)*. The smaller production at lower depth (30-40 and 60-70cm) could be due to a decrease in bacterial activity and a limited availability of Fe(II) to redox transformation. Slower organic matter degradation by microorganisms causes the increase of mercury complexation and consequently a decrease in its availability to reduction. In order to verify this hypothesis and to determine the contribution of each mechanism, more detailed laboratory research should be performed.

CONCLUSIONS AND PERSPECTIVES

Laboratory experiments were performed with clay fraction of some hydromorphic tropical soils. They demonstrate that reduction of Hg(II) to Hg° takes place in these soils. Hence, two processes lead to the decrease of the total mercury content observed when comparing oxisol and hydromorphic soils located on a same slope: leaching and reduction. The complexity of the system does not permit to determine the exact mechanism of Hg° production in hydromorphic soils. We can hypothesize that in hydromorphic tropical soils at near 1 m depth and below, various anaerobic microorganisms may develop in pronounced anoxic and permanent nutrient supply conditions. Biotic reduction, together with abiotic reduction by Fe(II) adsorbed on the particles, is responsible for mercury redox transformation and evasion. The lower production measured in the upper layers could be due to a decrease in bacterial activity and in Fe(II) available for Hg(II) reduction. In the surface horizon, slower organic matter degradation by microorganisms causes the increase of mercury complexation and consequently further decrease its availability to reduction.

Mercury availability to redox transformation clearly depends on its complexation with organic matter. The reductive dissolution of Fe (hydro)oxides by dissimilatory Fe reducing bacteria will promote not only the leaching of mercury from the soils but also its release from the consumed organic substances and its availability to reduction reaction. An important question remains the study of Fe(III) reduction rates in tropical soils and how they relate to Fe reducing bacteria. The compared rates of biotic reduction and abiotic reduction by adsorbed Fe(II) should be further investigated. What forms of Fe(II) participate in reaction? Could it include "green-rust" minerals? All these questions still remain open and require detailed studies.

Table 1. Characteristics of oxisol (S1) and hydromorphic soil (S7) of toposequence located on the Leblonde river *(29)*.

	Oxisol			Hydromorphic soil		
	30-40cm	60-70cm	90-100cm	30-40cm	60-70cm	90-100cm
pH	5.1	5	5.1	4.7	5	4.9
Clay (g/kg)	482	532	562	267	313	287
Silt (g/kg)	129	158	150	169	205	472
Sand (g/kg)	368	308	274	554	472	496
C_{org} (g/100g)	20.9	6.7	4.6	10.2	10.5	8.1
Fe_{asc}(g/kg)	4.5	1.2	0.2	4.2	4.2	4.7

Table 2. Apparent first-order rate constants for the production of Hg° in hydromorphic soil samples.

Sample	R^2	$k(min^{-1})$
Experiments with FeCit		
30-40cm	0.997	$3.0 \cdot 10^{-4}$
60-70cm	0.991	$3.0 \cdot 10^{-4}$
90-100cm	0.943	$5.1 \cdot 10^{-3}$
Experiments without FeCit		
90-100cm	0.865	$2.9 \cdot 10^{-3}$

FIGURE CAPTIONS

Figure 1. Study area of Petit Saut reservoir, French Guyana (a), and schematic diagram of sampling site situated at the Leblond river (b).

Figure 2. Profiles of clay fraction (○) and Fe_{asc} concentrations (□) in hydromorphic soil (S5). (*(29)*, Fe_{asc} data provided by L. Spadini)

Figure 3. Profiles of Hg concentration in oxisol,S1, (○), ultisol, S3, (□) and hydromorphic soil, S5, (▲). *(29)*

Figure 4. Cumulated Hg° production in suspensions of 0.4 g l^{-1} hydromorphic soil samples at pH 7, initial Hg(II) total concentration 2.5 nM and FeCit $1 \cdot 10^{-3}$ M: 30-40 cm (●), 60-70c m (■), 90 –100 cm (▲).

Figure 5. Hg° concentration in suspensions of 0.4 g l^{-1} hydromorphic soil samples at pH 7, initial Hg(II) total concentration 2.5 nM, with and without FeCit $1 \cdot 10^{-3}$ M: (a) 30-40 cm , (b) 60-70 cm, (c) 90 –100 cm. In (b) in absence of FeCit addition, in all samples Hg° produced was below detection limit (< 0.17 pM).

REFERENCES

(1) Akagi H., Malm O., Branches F.G.P., Kinjo Y., Kashima Y., Guimara J.R.D., Oliveira R.B., Haraguchi K., Pfeiffer W.C., Takizava Y., Kato H., (1995). *Human exposure to mercury due to goldmining in the tapajos river basin, Amazon, Brazil: speciation of mercury in human hair, blood and urine.* Water, Air, and Soil Pollution, 80: p. 85-94.

(2) Guimamaraes J.R.d., Fostier A.-H., Forti M.C., Melfi J.A., Kehrig H., Mauro J.B.N., Malm O., Krug J.F., (1999). *Mercury in human and environmental samples from two lakes in Amapa, Brazilian Amazon.* Ambio, 28(4): p. 296-301.

(3) Lacerda L.D.,Salomons W., (1998). *Mercury from gold and silver mining: a chemical time bomb?* Springer. 146 p.

(4) Mason R.P., Fitzgerald W.F., Morel F.M.M., (1994). *The biogeochemical cycling of elemental mercury: Anthropogenic influences.* Geochimica et Cosmochimica Acta, 58(15): p. 3191-3198.

(5) Roulet M.,Lucotte M., (1995). *Geochemistry of mercury in pristine and flooded ferralitic soils of a tropical rain forest in French Guiana, South America.* Water, Air and Soil Pollution, 80: p. 1079-1088.

(6) Roulet M., Lucotte M., Farella N., Serique G., Coelho H., Soussa Passos C.J., De Jesus Da Silva E. , Scavone De Andrade P., Mergler D., Guimaraes J.-R. D., A. A., (1999). *Effects of recent human colonization on the presence of mercuty in amazonian ecosystem.* Water, Air and Soil Pollution, 112: p. 297-313.

(7) *Soil taxonomy*, (1975). 754 p.

(8) Schuster E., (1991). *The behavior of mercury in the soil with special emphasis on complexation and adsorption processes- a review of the literature.* Water, Air, and Soil Pollution, 56: p. 667-680.

(9) Bonnissel-Gissinger P., Alnot M., Lickes J.-P., Ehrhardt J.-J., Behra P., (1999). *Modeling the adsorption of mercury(II) on (hydr)oxides II: a- FeOOH(goethite) and amorphous silica.* Journal of Colloid and Interface Science., 215: p. 313-322.

(10) Tiffreau C., Lutzenkirchen J, Behra P., (1995). *Modeling the adsorption of Hg on (Hydr)oxides.* Journal of colloid and interface science, 172: p. 82-93.

(11) Sarkar D., Essington M.E., Misra K.C., (2000). *Adsorption of mercury(II) by kaolinite.* Soil Sci. Soc.Am.J., 64(november-december): p. 1698-1975.

(12) Sarkar D., Essington M.E., Misra K.C., (1999). *Adsorption of mercury(II) by variable charge surfaces of quartz and gibbsite.* Journal of american society of soil science, 63: p. 1626-1636.

(13) Kerndorff H.,Schnitzer M., (1980). *Sorption of metals on humic acid.* Geochimica et cosmochimica acta, 44: p. 1701-1708.

(14) Xu H.,Allard B., (1991). *Effects of a fulvic acid on the speciation and mobility of mercury in aqueous solutions.* Water, Air and Soil Pollution, 56: p. 709-717.

(15) Lee Y-H., Borg G.C., Iverfeldt A., Hultberg H., *Fluxes and turnover of methyl mercury: mercury pools in forest soils.*, in *mercury pollution: toward integration and synthesis.*, H.J. Watras C.J., Editor. 1994, Lewis Publ. p. 329-341.

(16) Roulet M., Lucotte M., Saint-Aubin A., Tran S., Rheault I., Farella N., De Jesus Da Silva E., Dezencourt J., Sousa Passos C.-J., Santos Soares G., Guimaraes J.-R., Mergler D., Amorim M., (1998). *The geochemistry of mercury in central Amazonian soils developed on the Alter- do- Chao formation of the lower Tapajos River Valley, Para state, Brazil.* The sience of the total environment, 223: p. 1-24.

(17) Amyot M., Mierle G., Lean D.R., McQueen D.J., (1994). *Sunlight-induced formation of dissolved gaseous mercury in lake waters.* Environmental science and technology, 28: p. 2366-2371.

(18) Nriagu J.O., (1994). *Mechanistic steps in the photoreduction of mercury in natural waters.* The science of the total environment, 154: p. 1-8.

(19) Zhang H.,Lindberg S.E., (2001). *Sunlight and iron(III)-induced photochemical production of dissolved gaseous mercury in freshwater.* Environmental science and technology., 35: p. 928-935.

(20) Mason R. P., Morel F. M. M., Hemond H. F., (1995). *The role of microorganisms in elemental mercury formation in natural waters.*

(21) Peretyazhko T., Charlet L., Cossa D., Kazimirov V., (2002). *Production of gaseous mercury Hg° in an anoxic environment: Petit Saut reservoir, French Guiana.* Environmental science and technology (in prep.).

(22) Charlet L., Bosbach D., Peretyashko T., (2002). *Natural attenuation of TCE, As, Hg linked to the heterogeneous oxidation of Fe(II): an AFM study.* Chemical geology (submitted).

(23) Allard B.,Arsenie I., (1991). *Abiotic reduction if mercury by humic substances in aquatic system- an important process for the mercury cycle.* Water Air and Soil Pollution, 56: p. 457-463.

(24) Bloom N.S.,Fitzgerald W.F., (1988). *Determination of volatile mercury species at the picogram level by low-temperature gas chromatography with cold-vapor atomic fluorescence detection.* Anal. Chim. Acta., 208: p. 151-161.

(25) Kostka J.E.,Luther III G.W., (1994). *Partitioning and speciation of solid phase iron in saltmash sediments.* Geochimica and cosmochimica acta, 58(7): p. 1701-1710.

(26) Vogel A.I., (1989). *Vogel's textbook of quantitative chemical analysis*. Longman Scientific and technical. 877 p.

(27) Lovley D.R., (1993). *Dissimilatory metal reduction.* Annu. Rev. Microbiol., 47: p. 263-290.

(28) Cornell R.M.,Schwertmann U., (1996). *The iron oxides*. VCH. 573 p.

(29) Programme mercure en Guyane: region de Saint Elie et retenue de Petit Saut.. 2001.

(30) Samemasa I., (1975). *The solubility of elemental mercury vapor in water.* Bulletin of the chemical society of Japan, 48(6): p. 1795-1798.

(31) Vandal G.M., Fitzgerald W.F., Rolfhus K.R., Lamborg C.H., (1995). *Modeling the elemental mercury cycle in Palette lake, Wiskonsin, USA.* Waater, air and soil pollution., 80: p. 529-538.

(32) Mueller-Vonmoos M.,Kahr G., *Mineralogische von Wyoming Bentonit MX-80 und Montigel*. 1983: Technischer Bericht 83-12, Institut fur Grundbau und Bodenmechanik, ETH Zuerich, Zuerich. p. 15.

(a)

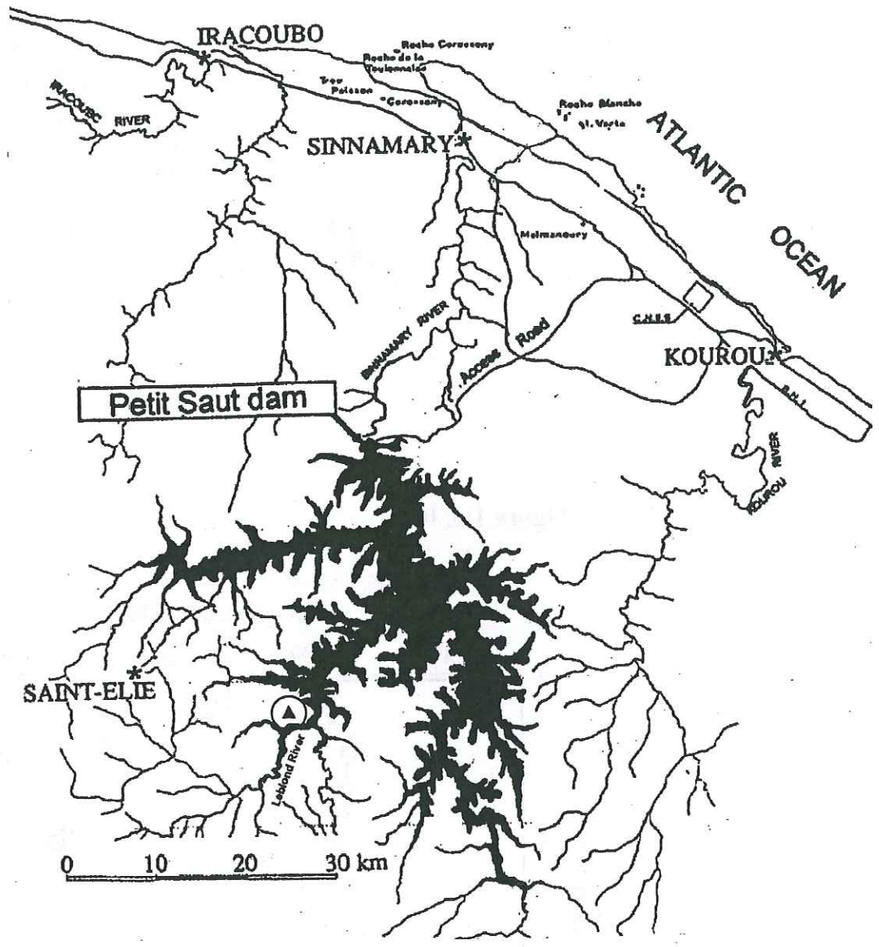
IRACOUBO
Roche Corossony
Roche de la Poulonnais
Roche Blanche
Pte Pelosse
Corossony
IRACOUBO RIVER
SINNAMARY
ATLANTIC OCEAN
Malmanoury
C.N.E.S
SINNAMARY RIVER
Access Road
KOUROU
Petit Saut dam
KOUROU RIVER
SAINT-ELIE
Jolicoeur River
0 10 20 30 km

(b)

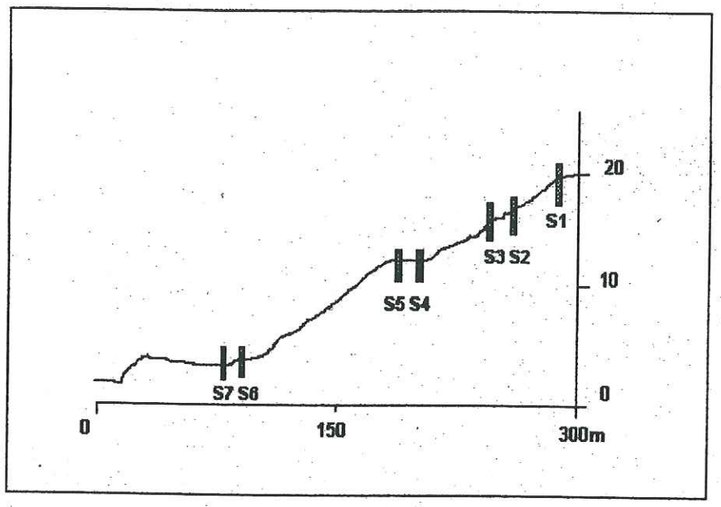

Figure 1 a, b

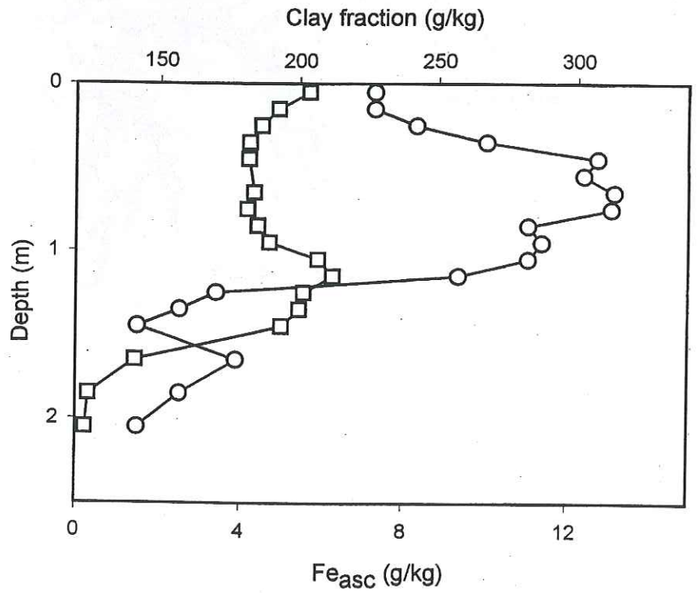

Figure 2

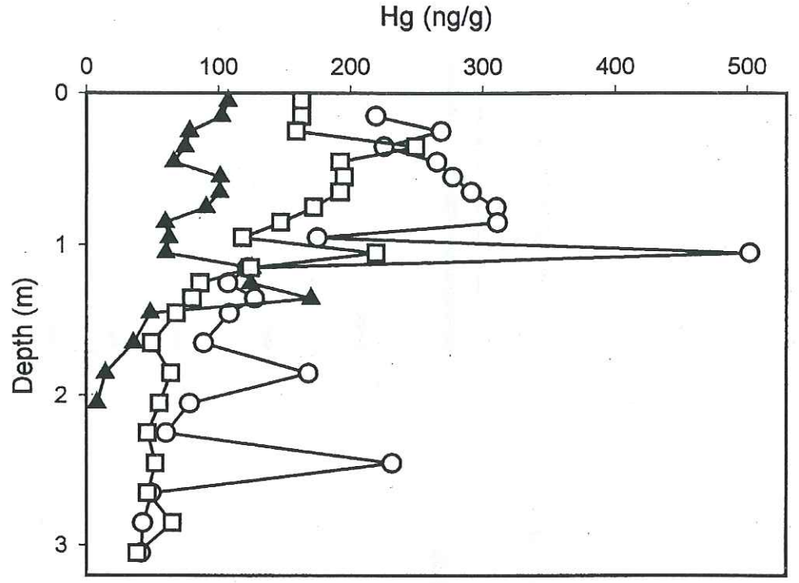

Figure 3

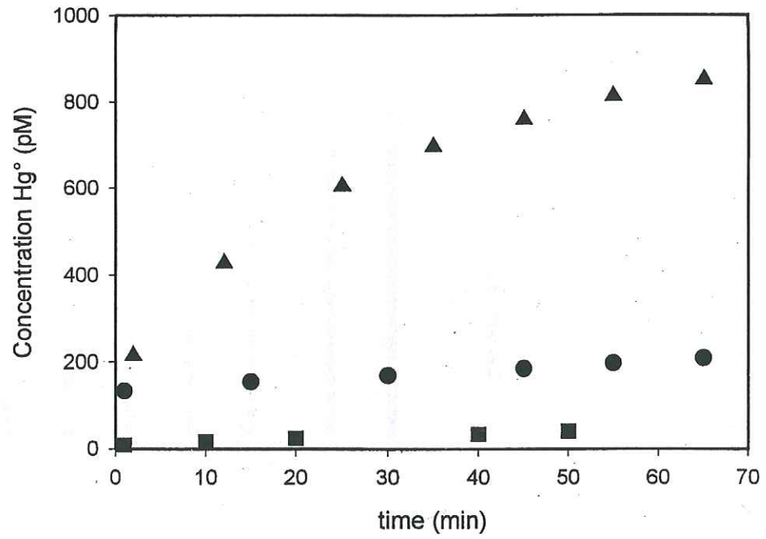

Figure 4

(a)

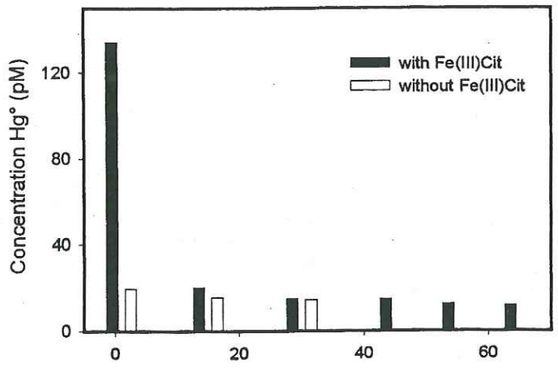

(b)

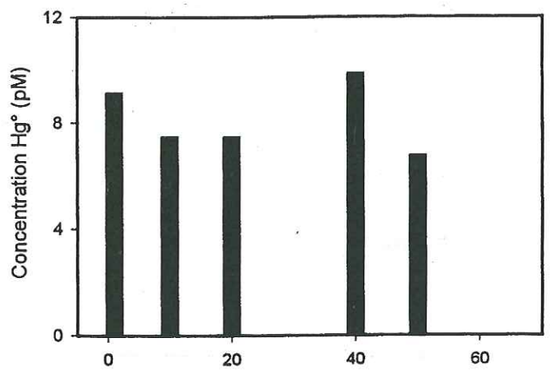

(c)

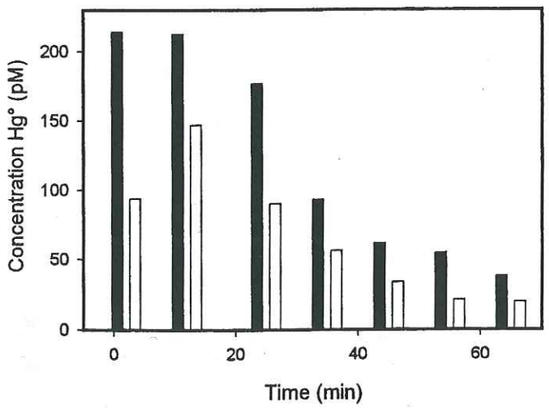

Figure 5

CHAPITRE 7

Conclusions et perspectives

CONCLUSIONS

Cette étude a été orientée sur deux grands axes : la biogeochimie du lac tropical en prêtant une attention particulière sur le cycle du mercure et des mécanismes de production de Hg° dans des milieux anoxiques. Dans le but de développer le premier axe, des travaux de terrain ont été réalisés sur le réservoir tropical artificiel de Petit Saut, en Guyane Française, Amérique du Sud. Concernant le deuxième axe, les objectifs de nos recherches ont été étudiés: (i) la distribution verticale de mercure élémentaire (Hg°) et réactif (Hg_R) dans le réservoir de Petit Saut, (ii) de l'interpréter en termes de mécanismes de production de Hg° en milieu anoxique, mécanismes à l'œuvre tant dans l'hypolimnion de ce lac et que dans les sols tropicaux hydromorphes.

Le travail de terrain réalisé durant la saison sèche et la saison humide démontre une stratification thermique permanente et le développement de conditions anoxiques dans le réservoir Petit Saut. La présence permanente de larges concentrations de NH_4^+ , CH_4 et CO_2 dans l'hypolimnion indique une dégradation des matières organiques venant de la végétation submergée et de la biomasse des algues. Cette dégradation des matières organiques est un facteur clé dans des transformations redox apparaissant dans l'hypolimnion et dans le niveau d'oxycline. Ainsi, la consommation principale d'oxygène dissout est due aux décompositions biologiques des matières organiques. La dissolution réductive d'oxy(hydroxy)de de fer par des matières organiques dissoutes est l'un des facteurs responsable de l'accroissement de l'alcalinité observée dans les parties anoxiques du réservoir Petit Saut à la saison sèche.

Des variations saisonnières dans les concentrations des espèces réduites sont observées dans l'hypolimnion: les concentrations augmentent pendant la saison sèche et diminuent pendant la saison humide. Ceci peut s'expliquer par des phénomènes soit de dilution soit d'oxydation. Dans l'hypolimnion, les flux les plus importants résultent des apports d'eau par les affluents et les eaux de pluies, conduisant à un meilleur mélange en saison humide qu'en saison sèche. Les transports causés par ce phénomène ont une grande influence sur la distribution des espèces chimiques dans l'hypolimnion. Pendant la saison humide, à cause de la turbulence qui se développe au fond du lac, des sédiments sont réintroduits dans la colonne d'eau. En conséquence, les teneurs en espèces réduites augmentent par la réduction des oxy(hydroxy)des de fer couplée à la décomposition de la matière organique.

Les phénomènes de mélanges gouvernent la distribution verticale du mercure dissout (Hgd) dans l'hypolimnion du lac artificiel. Les principales sources de mercure dissout sont le

fond du lac, les sédiments composés par les sols inondés lors de la mise en eau, et la fine couche de sédiments déposée depuis.

Dans les lacs tempérés, les concentrations maximum en mercure élémentaire (Hg°) sont plus fortes au-dessus de l'interface air-eau, que dans l'hypolimnion. Dans le réservoir tropical de Petit Saut, la concentration maximum de Hg° se trouvent au fond du lac. Les expériences de laboratoire sur la production de Hg° avec des suspensions de sédiments prélevés dans le réservoir de Petit Saut, démontrent que cette production est essentiellement d'origine biologique. La vitesse de production de Hg° dépend de la présence de mercure réactif. Ainsi les facteurs cinetiquement limitant sont la désorption de particules inorganiques (hydroxydes de Fe(III), Al , etc…) et la dégradation de la matière organique.

Un des mécanismes abiotiques responsable de la production de Hg° en milieu anoxique est la réduction de Hg(II) par le Fe(II) en présence de particules (hématite, mica). Cette hypothèse est confirmée par nos expériences de laboratoire menées sur la production de Hg° par le Fe(II) en présence de particules d'hématite suggèrant que la réduction de Hg(II) est accompagnée d'une oxydation du Fe(II) adsorbé sur les particules.

Nos calculs montrent que la production de Hg° au fond du lac n'est pas complètement compensée par le flux de Hg° vers l'oxycline et vers l'aval du barrage. Ceci semble suggérer la possibilité que Hg° soit oxydé réversiblement dans l'hypolimnion du réservoir tropical. A partir de ces données nous avons démontré que le dégazage de Hg° des eaux profondes est négligeable par rapport a la vitesse de production de Hg° , et que l'évaporation de Hg° vers l'atmosphère depuis la surface est essentiellement due à des procédés photochimiques et non à des contributions de l'hypolimnion.

Nos expériences de laboratoire avec des sols tropicaux hydromorphes démontrent que la réduction de Hg(II) par Fe(II) en Hg° peut aussi avoir lieu dans ces sols. Ainsi, deux procédés mènent à la diminution du contenu total de mercure observé dans les sols hydromorphes comparés au oxisols de la même toposéquence: la lixiviation et l'évaporation après la réduction. La complexité du système ne permet pas de déterminer le mécanisme exact de la production de Hg° dans les sols hydromorphes. En nous basant sur nos expériences de laboratoire, deux mécanismes conduisent à la transformation redox et donc son évaporation: la réduction biotique, ainsi que la réduction abiotique par le Fe(II) adsorbé sur les particules.

PERSPECTIVES

Ce travail a contribué à une meilleure connaissance du cycle du mercure en milieu tropical, par des études sur la transformation du mercure dans un réservoir tropical stratifié ainsi que dans des sols hydromorphes. Les résultats obtenus posent de nouvelles questions, ouvrant donc sur de nouvelles perspectives.

Dans notre modélisation du transport du mercure incluant seulement les phénomènes de mélange, on ne décrit pas de manière satisfaisante la distribution de certaines espèces chimiques dans le réservoir de Petit Saut. Il semble donc qu'il faille en premier lieu développer un modèle dynamique du lac qui prendrait en compte tant la physique du lac que les réactions chimiques nécessaires, et ce afin de décrire correctement les principaux procédés se déroulant dans le réservoir et leurs variations saisonnières. Pour développer une meilleure connaissance des transformations du mercure en milieu tropical, il faudrait aussi appliquer ce modèle au cycle du mercure dans d'autres lacs tropicaux, et axer cette application sur le methylmercure, espèce du mercure la plus dangereuse pour la santé humaine, mais aussi espèce aqueuse la plus difficile à mesurer. Le prélèvement, par les organismes aquatiques, du methylmercure provenant des différentes couches de la colonne d'eau (oxycline, eaux du fond, eaux oxique) doit être étudié ainsi que les variations saisonnières de cette bioamplification. Il s'agit à terme de pouvoir répondre à la question suivante: les réservoirs artificiels tropicaux sont-ils une source importante de methylmercure, comme cela a été démontré précédemment en ce qui concerne les gaz à effet de serre ?

Il n'y a à ce jour que très peu de travaux visant à étudier la production de mercure gazeux dans des milieux anoxiques tropicaux. Nos expériences en laboratoire ont montré que les principaux mécanismes de production de Hg° dans des sédiments anoxiques et dans la colonne d'eau sont tout autant biotiques (réduction microbienne dans le sédiment) que abiotiques (réduction par le Fe(II) adsorbé). Il me paraît judicieux d'envisager une série d'étude sur le destin du Hg° produit dans l'hypolimnion d'un lac tropical. Parmi les questions non résolues par la présente étude, il y a la nature du piège à Hg° observé au-dessous de l'oxycline et, au niveau des bilans, le pourcentage de mercure total susceptible de s'échapper de la colonne d'eau sous la forme Hg°. Il faudrait aussi étudier si une oxydation réversible de Hg° a lieu. Il me semble intéressant de vérifier s'il y a un lien entre le procédé de methylation et la production de Hg° via, par exemple, l'activité de bactéries sulfato – réductrices (BSR). Celles-ci sont supposées être responsables de la methylation du mercure, et il faut étudier si

HS^- produit par les BSR est aussi capable de réduire le mercure en Hg°. Plus d'informations sont nécessaires pour comprendre comment l'activité bactérienne va changer avec le milieu (changement de pH, de température).

Les expériences de réduction réalisées sur sols hydromorphes démontrent que la formation du mercure élémentaire peut avoir lieu et que la disponibilité du mercure pour cette transformation redox dépend essentiellement de sa complexation avec des matières organiques. Ainsi, la réaction de réduction d'oxy(hydroxy)de de fer par les bactéries présentes dans des sols va favoriser non seulement la lixiviation du mercure hors du sol mais aussi sa libération par dégradation microbienne des substances organiques et donc sa disponibilité vis à vis de la réduction en Hg°. Il est donc nécessaire pour comprendre les mécanismes de la production de Hg° d'étudier la vitesse de réduction des oxyhydroxides de Fe(III) dans les sols tropicaux et le lien entre ces vitesses et l'activité des bactéries fer-réductrices. Il me semble important de mettre en évidence et de comparer plus en détail les vitesses de Hg(II) réduction biotique et de réduction abiotique par le Fe(II) adsorbé sur des particules de sols. Une des questions liées à l'étude de la production de Hg° est de déterminer les formes de Fe(II) participant à la réaction et, par exemple, de savoir si elles incluent des minéraux de type rouille – vertes.

Pendant le procédé d'amalgamation, une quantité variable de mercure métallique est rejetée et accumulée dans les sols adjacents. Malgré sa faible réactivité, le mercure pourrait être lentement transformé sous forme labile et transporté vers les systèmes aquatiques. Il faudrait envisager des expériences de traçage (aquatique et atmosphérique) avec des isotopes du mercure. Il faudrait aussi, pour comprendre les transformations du mercure métallique dans un sol tropical étudier la surface des billes de mercure métallique (MEB, XPS), et le changement de la surface de ces particules. Ces études permettront de caractériser la couche de corrosion de métal, couche faite d'oxydes, d'hydroxydes ou de sulfures. La dissolution de ces particules, induite par les exsudats organiques de type sidérophore, pourrait contrôler le transport et à terme la biodisponibilité du mercure dans le milieu naturel.

ANNEXE 1

Natural attenuation of TCE, As, Hg linked to the heterogeneous oxidation of Fe(II): an AFM study

Laurent Charlet, Dirk Bosbach and Tanya Peretyashko

To be published in Chemical Geology (accepted)

Abstract

Hydrous ferric oxide (HFO) colloids formed, in strictly anoxic conditions upon oxidation of Fe^{2+} ions adsorbed on mineral surface, were investigated under *in situ* conditions by contact mode atomic force microscopy (AFM). Freshly cleaved and acid etched large single crystals of near endmember phlogopite were pre-equilibrated with dissolved Fe(II) and then reacted with Hg(II), As(V) and trichlorethene (TCE)-bearing solutions at 25°C and 1 atm. HFO structures are found to be of nanometer scale. The As(V)-Fe(II) and Hg(II)-Fe(II) reaction products are round (25 nm) microcrystallites located predominantly on the layer edges and are indicative of an accelerated Fe(II) oxidation rate upon formation of Fe(II) innersphere surface complexes with the phyllosilicate edge surface sites. On the other hand, TCE-Fe(II)-phlogopite reaction products are needle shape (45 nm long) particles located on the basal plane along the Periodic Bond Chains (PCBs) directions. Experiments with additions of sodium chloride confirm the importance of the Fe(II) adsorption step in the control of the overall heterogeneous Fe(II)-TCE electron transfer reaction.

Kinetic measurements at the nano molar level of Hg° formed upon reduction of Hg(II) by Fe(II) in presence of phlogopite particles provide further convincing evidence for reduction of $Hg(II)_{aq}$ coupled to the oxidation of Fe(II) adsorbed at the phlogopite-fluid interface, and indicate that indeed sorption of Fe(II) to mineral surfaces enhances the reduction rate of Hg(II) species. The Hg(II) reduction reaction follows a first order kinetic law. Under our experimental conditions, which were representative of many natural systems, 80% of the mercury is transferred to the atmosphere as Hg° in less than 2h.

The reduction of a heavy metal (Hg), a toxic oxyanion (arsenate ion) and a chlorinated solvents (TCE) thus appear to be driven by the high reactivity of adsorbed Fe(II). This is of environmental relevance since these three priority pollutants are that way reductively transformed to avolatile, a immobilizable and a biodegradable species, respectively. Such kinetic data and reaction pathways are important in the evaluation of natural evaluation scenarios, in the optimization of Fe(II)/mineral mixtures as reductants in technical systems, and in general, in predicting the fate and transport of pollutants in natural systems.

Keywords

Ferrous iron, natural attenuation, clay edges, mercury, AFM.

Introduction

Ferrous iron has been shown to provide an effective means for removing a variety of pollutant including nitrite, nitrate, chromium, selenate, uranium, vanadate, pertechnetate, and nitrobenzene from aqueous solution (Schwertmann and Pfad, 1994; Klausen et al., 1995, Cui and Eriksen, 1996; Ottey et al., 1997; Myrreni et al., 1997; Buerge and Hug, 1998; Liger et al., 1999). A common feature of these reductive transformation reactions by ferrous iron is that sorbed ferrous iron is always much more reactive than dissolved iron (II) present in the background electrolyte solution. Indeed, rates of homogeneous reduction by dissolved Fe(II) are exceedingly slow. Surface Fe(II) complexes formed with hydrous iron oxides, silicates and sulfides, are on the other hand very efficient reductants from a thermodynamic (Figure 1) as well as from a kinetic point of view (Stumm and Sulzberger, 1992).

The reductive transformation of an oxidized species *ox* by surface Fe(II) may be written:

$$n(Fe^{II})_{sorbed} + ox = nFe(OH)_3(s) + red \qquad (1)$$

where n is the number of electrons which must be transferred to *ox* in order to produce *red* (e.g. n = 2, 3 and 6 for U(VI), Cr(VI) and nitrobenzene, respectively). However, the reaction rate is not a direct function of the total sorbed Fe(II) concentration. Instead, it has been shown by Charlet et al. (1998b) to be proportional to the concentration of the $>FeOFe^{II}OH^{\circ}$ hydroxylated surface complex of Fe(II), a complex formed with one surface functional group $>FeOH^{\circ}$, one Fe^{2+} ion and two hydroxyl ions. Reaction (1) has been also shown to follow a 2nd-order rate law (Charlet et al., 1998; Buerge and Hug, 1999; Liger et al., 2000), and the observed rate to be a function of $>FeOFe^{II}OH^{\circ}$ as well as oxidant concentration according to:

$$-\frac{d[Ox]}{dt} = k[> FeOFe^{II}OH^{O}][Ox] \text{ with Ox} = \text{U(VI), Cr(VI) or } ArNO_2 \qquad (2)$$

Equation (2) indicates that, among the electrons transferred in reaction (1), only the first electron transfer is rate limiting (Charlet et al., 1998).

The reduction mechanism outlined in equations (1) and (2) can be further compared to the homogeneous oxidation of Fe(II) by oxygen. The oxygenation is routinely used in a number of European countries in *in situ* iron removal procedures (Appello et al., 2000).

Electron transfer takes place between the dissolved oxygen present in injection water and the dissolved Fe(II) species originally present in ground water. Both dissolved $OH^-(aq)$ and surface hydroxyl groups facilitate the electron transfer to O_2, as the OH^- ligands donate electron density to Fe(II) through both σ and π systems, which results in metal basicity and increased reducing power (Luther, 1990). Above pH 5.0, the homogeneous oxygenation of Fe(II) in solution follows a rate law (Stumm and Sulzberbger, 1992) similar to equation (2):

$$-\frac{d[Fe(II)]}{dt} = k[Fe(OH)_2^O]P_{O_2} \qquad (3)$$

In comparison to oxidation in homogeneous solution, sorption of Fe(II) to mineral surfaces enhances the oxygenation of sorbed Fe(II) species. This has been demonstrated for Fe(II) present on Fe-oxyhydroxide surfaces (Tamura et al., 1980) as well as on clay mineral surfaces. This reaction can lead to autocatalytic processes. Upon oxidation of a Fe(II) surface species, Fe-oxyhydroxide precipitates. As a consequence of the formation of a new phase, new mineral surface area is generated which serves as a substrate for further Fe(II) sorption. Therefore, as the reaction proceeds, the heterogeneous precipitation of Fe-oxyhydroxides leads to the formation of new sites for Fe(II) sorption, and the reaction rate speeds up. After the initial injection of a defined volume of oxygenated water, subsequently larger volumes of ground water can then be pumped with a lower iron concentration than is found in native ground water (Appelo et al., 2000).

Natural attenuation is defined by EPA (1997) as "a variety of processes that act without human intervention to reduce the toxicity, mobility and concentration of contaminants in soils or groundwater". Surface Fe(II) is shown by the above mentioned studies to be a natural mean to remove priority compounds from groundwater and its efficiency may be compared to that of Fe°, which has been used in engineered barriers to remove Cr(VI), U(VI) and chlorinated solvent from contaminated groundwater (Orth and Gillham, 1996). This efficiency of surface Fe(II) has been verified in a number of field studies. For instance in aquifers located below a source of organic carbon, e.g. below a waste dumping site, the organic matter input induces the formation of a large Fe reduction zone, where only 2% of the total Fe(II) is present as dissolved Fe(II), up to 20% is present as exchangeable sorbed Fe(II), the remainder being in a solid form (pyrite and "AVS") (Heron and Christensen, 1995). Sorbed Fe(II) is very effective in aquifers to remove nitrate (Ernstsen, 1996; Vanek, 1990), nitrite (Sorensen and Thorling, 1991) and chlorinated aliphatics (Christensen et al., 1994)

from groundwater. This has important consequences for strategies to improve ground water quality in such environments.

Macroscopic experimental approaches, where the fluid composition during experiments is monitored, have provided detailed information about the heterogeneouos oxidation of Fe(II) surface species. However, the actual reactive sites and products of reaction (1) have not yet been identified simultaneously and unambigously. Atomic Force Microscopy (AFM) has proven to be a powerful technique for the characterization of clay mineral surface microtopography (Bickmore et al., 1999) and the identification of reactive surface area (Rufe & Hochella 1999, Bosbach et al., 2000) at molecular scales. One of the greatest strengths of AFM is that it can characterize surface microtopography directly in solutions so it can track *in-situ* and in real-*time* the dissolution of clay minerals (Bosbach et al., 2000; Bickmore et al., 2001), the adsorption of small polymers or humic acids on a flat mineral surfaces (Plaschke et al., 1999), or the oxygenation of dissolved Fe(II) and subsequent crystal growth of (100) and (110) faces of goethite (Weidler et al., 1998).

In this study, we expand upon the oxygenation experiments described above to further test the hypothesis that in the presence of $[Fe(II)]_i$ = 10 to 250 μM, the Fe(II) oxidation by various priority pollutants occurs primarily through heterogeneous reactions at the clay mineral/water interface. The initial Fe(II) concentration range was chosen for three reasons: (i) Buerg and Hug (1998) have shown that at $[Fe(II)]_i >> 2.5\ 10^{-4}$ M, the reaction would become too rapid for in-situ imaging with AFM. (ii) At lower initial Fe(II) concentrations, reaction products would be too sparse to be detected even by a high resolution microscopic technique, such as AFM. (iii) The chosen Fe(II) concentration window represents the ferrous iron concentration of many reducing natural environments, such as aquifers (McArthur et al., 2000, Gale and Smedley, 1989), lake hypolimnion (Cossa et al., 1994) and sediments (Davison et al., 1991). Although in nature, oxygen, nitrate and manganese oxides are often the most abundant electron acceptors, we chose to use Hg, As and Trichlorethene (trichlorethylene or TCE) because their reduction by surface Fe(II) leads to products belonging to three different thermodynamic phases, i.e. to gas ($Hg^{\circ}(g)$), solid ($Fe(OH)_3(s)$ coprecipitated with As) and liquid (DCE(aq)) phases, respectively. The ferric (hydr)oxide phase formed in the course of the reaction at the phlogopite/water interface may therefore be drastically different.

Materials and Methods

Materials

Large phlogopite single crystals, several cm in diameter and up to two mm in thickness, were provided by the Mineral Museum of the University of Münster. Phlogopite - $(K,Na)_{x-y}((Mg^{2+}, Fe^{2+})_{3-y}\ (Fe^{3+})_y)(Si_{4-x}Al_x)O_{10}(OH)_2$ - as a trioctahedral mica contains Mg as the dominating cation in the octahedral sites. Only minor amounts of Fe(II) and Fe(III) are present. Since it has a perfect cleavage parallel to (001), single crystals were cleaved by using a scotch-tape. Freshly cleaved phlogopite surfaces consist of large atomically flat terraces. The occurrence of molecular steps is rare. In order to study reaction at layer broken edges, we have induced the formation of etch pits and consequently the formation of molecular steps by the following procedure. A small (36 mm^2) square of a freshly cleaved phlogopite sample was etched for 2 min in concentrated distilled HF at room temperature and rinsed with a stream of deionized water.

Iron (II), Arsenic(V) and mercury(II) stock solutions at concentrations of 10^{-3}M Fe(II), $5x10^{-4}$ M As(V) and 10^{-2} M Hg(II) were prepared from $FeSO_4 \cdot 7H_2O$(Merck), $Na_2HAsO_4x7H_20$(Fluka) and $HgCl_2$(J.T. Baker), using boiled and degassed Milli-Q deionized water (BDDIW), acidified with ultrapure HNO_3. The $1gl^{-1}$ TCE stock solution was made in two steps. First a known weight of TCE is dissolved in methanol, second an aliquot of this solution is dissolved in BDDIW to $5x10^{-3}$ M TCE. The ionic strength was adjusted with a 1 M NaCl solution. The pH in our experiments was controlled by reagent grade MOPS buffer (Fisher Scientific). 0.1 M MOPS solution was titrated to pH 7.5 with reagent-grade NaOH solution.

Macroscopic kinetic experiments

60 μg of phlogopite was added to 150 ml of deoxygenated water and 29 ml of buffer in a 200 ml titration reactor. Ferrous sulfate was added to obtain a $1.0\ 10^{-5}$M Fe(II) initial concentration. The initial pH of the suspension was 7.5. The reactor was purged continuously with ultrapure Ar to avoid oxidation of Fe(II) to Fe(III) by ultratraces of oxygen. The suspension was equilibrated for 24h. A 50 ml aliquot was then transferred to a 125 ml Teflon bubbler, and mixed at t = 0 with an aliquot of a 0.25 μg l^{-1} stock Hg(II) solution, to get a 50 pM initial Hg(II) concentration in the suspension. This very low concentration is representative (and even larger) than most Hg(II) dissolved concentrations found in polluted surface waters (e.g. Cossa et al., 1994). At fixed time intervals, produced gaseous mercury

was purged with ultra pure Ar, stored onto gold trap, and determined by cold vapor atomic fluorescence spectroscopy (CVAFS) using Tekran detector (Bloom and Fitzgerald,1988). The standard deviation of the bubbler blank was on average 1.4 pg resulting in detection limit (3xSTD of blanks) of 4.2 pg.

Atomic Force Microscopy (AFM)

The small (36 mm^2) square of a freshly cleaved phlogopite was introduced in a vial, together with aliquots of the iron (II), oxidant (As, Hg or TCE) and MOPS stock solutions. The total concentration was equal to 2.5 10^{-4} M for Fe(II), 5 10^{-4} M for As(V) and 10^{-3} M for TCE. In the case of Hg(II) *ex-situ* experiment the total concentration was equal to 1 10^{-5} M for Fe(II) and 3 10^{-5} M for Hg(II). In order to be able to observe Reaction (1) solid products, a high Hg(II) total concentration had to be used, which is 10^3 higher than the concentration used in the kinetic experiment. Total volume was equal to 10 ml. The solution was flushed with argon before closing the vial tightly. Further, in order to ensure that no oxygen could access the solution, the vial was wrapped with teflon tape. The vials were shaken and then stored in an evacuated dessicactor. Some samples had their ionic strength set up equal to 0.1 M NaCl. Reaction time ranged from 30 min to 5 days.

After the desired reaction time, the phlogopite slides were removed with Teflon tweezers, gently flushed with a stream of BDDIW for 5 min, and oven dried at 45°C for 10 min. It was then mounted with double-sided sticky tape to the AFM sample holder.

We have used a Digital Instruments Nanoscope III AFM. Images were taken in air in contact mode (CM) as well as in tapping mode (TM). Oxide sharpened Si_3N_4 Twin tips (Digital Instruments) Cantilevers with integrated pyramidal Twin Tips and with a force constant of 0.12 N/m were used for CM measurements and etched Si probes (Olympus) with a force constant of about 40 N/m and a resonance frequency of about 300 kHz were used for TM measurements. All images shown in this paper were taken in contact mode. Although tapping mode ensures significantly lower tip - sample loading forces we obtained significantly better images in contact mode. Particle diameter and height data were obtained independently using the Digital Instruments software.

Results

Reduction of Hg(II) by Fe(II) in the presence of phlogopite

Figure 2a shows a typical example of the reactivity of a system containing Hg(II) at pH 7.5 in aqueous Fe(II) solutions with and without suspended phlogopite. There is virtually no change in the Hg(II) oxidation state in pure 10 mM Fe(II) solution (without suspended phlogopite). There is also no Hg(II) reduction in pure phlogopite suspension (without additional Fe(II)), although the reduction of Hg(II) with minerals containing traces of Fe(II) is thermodynamically possible at neutral pH (Figure 1). Apparently, either there is not enough Fe(II) present in our phlogopite sample or the reduction of Hg(II) with reduced electron donors that may be part of the phlogopite lattice – or which are present in solution - is a rather slow process.

However, in suspensions of phlogopite that also contain additional Fe(II), significant amounts of Hg(II) become reduced. Clearly, the adsorption of Fe(II) to the phlogopite surface creates highly reactive sites for the reduction of Hg(II). During the entire length of the experiments (140 min), i.e. up to the disappearance of nearly 80% of initial mercury from solution, the formation of Hg° follows an apparent first order kinetic law (Figure 2b):

$$\ln\left(\frac{[Hg(II)]_t}{[Hg(II)]_o}\right) = -k_{obs}t \qquad (4)$$

where $[Hg(II)]_t$ and $[Hg(II)]_0$ are the Hg(II) concentrations at time t and time 0, respectively, and k_{obs} is the observed pseudo first order rate constant under the prevalent conditions. The pseudo-first-order rate constant value is equal to 0.0116 min^{-1}, and the half time of Hg(II) in the suspension is 58 min.

With respect to natural situations, this attenuation mechanism is remarkably efficient. Although the Fe(II) and phlogopite concentrations were rather low (10 µM and 3 mg l^{-1}, respectively), 80% of the mercury could be transformed from an aqueous species (predominantly $Hg(OH)_2°(aq)$) to a gaseous species (Hg°(g)) and be subsequently transferred to the atmosphere within 2h. Therefore clay minerals do not act only as a storage facility for contaminants; they serve also as a template for heterogeneous decontamination reactions. This is especially important since mercury present in anoxic environment may otherwise be microbiologically transformed to methyl mercury which is much more toxic and bioaccumulate in the trophic chain.

AFM observation of unreacted phlogopite (001)

In order to characterize the reactivity of phlogopite surfaces and to identify reactive sites for the heterogeneous oxidation of adsorbed Fe(II) we have treated freshly cleaved phlogopite with HF. Up to 10^9 cm^{-2} etch pits formed on the (001) basal surface upon HF treatment (Figure 3a). The depth of the etch pits was up to 5 molecular TOT layers. However, etch pits with a depth of one TOT layer (=10.2 Å) were by far the most abundant ones. The etch pit morphology is defined by step edges parallel to <100> and <110> (Figure 3b), which one would expect for a mica (001) surface according to PBC theory (Hartmann, 1983, White & Zelazny, 1988). The dissolution rate of the step edges in pure water at pH 7.5 is small. Rufe & Hochella (1999) found that the retreat velocity of molecular steps on a phlogopite (001) surface at pH 6 is 4 10^{-5} nm/s. Therefore, within the timeframe of our experiments there will be no change in microtopography on our samples.

The microtopography generated by HF treatment turned out to be a suitable substrate for the characterization of the reactivity of the basal surface as well as step edges, which represent {hk0} crystal faces.

AFM observation of Hg(II) reacted phlogopite (001)

After reacting a phlogopite single crystal with a Fe(II) solution no changes in microtopography can be identified, indicating that no precipitation of e.g. Fe-(hydr)oxide occured. This observation agrees with our macroscopic experiments.

However, after adding Hg(II) to the Fe(II) solution with phlogopite single crystal we found significant changes in microtopography (Fig. 4b). Although the etch pits, which where generated by HF treatment can still be recognized, small 25 nm wide microprecipitates of presumably Fe-(hydr)oxide have formed (Table 1). Nuclei appeared on the (001) surface after approximately 1 hour and remained to the end of the experiment. Unfortunately, no reliable data were obtained during the experiment for the changes of the length in the direction of the c-axis of the crystal.

AFM observation of As(V) reacted phlogopite sample

Figure 5 shows AFM images of iron (hydr)oxide particles formed on a HF treated phlogopite (001) surface after various reaction times of As(V) with the phlogopite previously

equilibrated with Fe(II). Although some nuclei are found at random on the (001) face of phlogopite after 30 min, the distribution of particles start to be well organized after 2h reaction time. Later on, the size of the globular nuclei does not change with time and remains closed to 24 nm (Table 1). Figure 6 depicts how the width, length and height reported in Table 1 for these microcristallites are recorded.

With time, more and more of these nanoparticles are formed along the walls of the etch pits, while the particle density on the (001) phlogopite plane remained constant. This behavior is clearly illustrated in Figure 5, which is a time series of AFM images taken during the precipitation of iron (hydr)oxide crystallites in pH 7.5 solution. The reaction fronts at broken edges appear to offer very reactive defect sites.

AFM observation of TCE reacted phlogopite sample

Ferric hydrous oxides formed at the phlogopite surface upon oxidation of surface Fe(II) by TCE are shown in Figure 7a and 7b. In the presence of high background ionic strength, nearly no particles are formed (Figure 6c and 6d). This demonstrates that Fe(II) must be first adsorbed on the phlogopite particles in order to be later oxidized by TCE. The morphology of these precipitates differ significantly from those particles formed upon Hg(II), or As(V), oxidation of Fe(II). In the case of TCE elongated particles (50 nm long) with an aspect ratio of approximately 2.5 are formed after 5 days reaction time (Figure 8 and Table 1).

Furthermore, the elongated precipitates are distributed randomly over the phlogopite (001) terraces, instead of being preferentially located on the clay edges. The morphologic difference between the elongated particles, formed upon TCE reduction, and the amorphous-like circular ferric particles, formed upon Fe(II) oxidation by As or Hg, could be due to electron transfer kinetics. Iron hydroxides formed from Fe(II) are known to be lepidocrocite at intermediate oxidation rate, ferrihydrite at fast oxidation rate or goethite at slow oxidation rates (Cornell and Schwertman, 1996). Arsenic(V) and mercury(II) are expected to be specifically adsorbed on clay edge surface sites, together with Fe(II). A fast inner-sphere electron transfer could then occur and lead to a ferrihydrite precipitation process. The presence of silicic acid, released upon dissolution of phlogopite etch pits, would further inhibit Fe(III) polymerisation (Doelsch et al., 2000) and lead to the preferential precipitation of small ferrihydrite particles (Karim, 1984). TCE on the contrary has been reported not to form inner-sphere complexes, neither with Fe(II) nor with mineral surface functional groups. As in the case of nitrobenzene (Charlet et al., 1998b; Schultz and Grundl, 2000), this could

lead to slow redox kinetics, and thus to the heterogeneous formation of goethite-like surface precipitates.

The orientation of the elongated needles sitting on the clay (001) terraces is not random. Three distinct preferential orientations can be easily recognized (Figure 6a,b), which coincide with the crystallographic direction of periodic bond chains in the phlogopite structure, as indicated in figure 3. At this stage it is not clear whether the preferential orientation of the Fe-precipitates is a consequence of an epitaxial overgrowth. However, the Fe hydroxide particles were not wiped away during the contact mode AFM imaging procedure, which indicates that the precipitates are tightly bound to the phlogopite basal surface.

Discussion

Mechanisms of adsorption on phlogopite

Adsorption of cations on phyllosilicates results from the formation of two different types of surface complexes, with two different surface functional groups. First, heteroionic cationic substitutions impart to phyllosilicates a permanent negative structural charge, which is compensated by the adsorption of cations on basal planes. In natural phlogopite, these cations are K^+ ions which may have lost part of their hydration shell. However, the acid treatment imposed on our phlogopite sample upon etching must have released a large part of these potassium ions, which were replaced first by protons, and second by Na^+, introduced together with the MOPS pH buffer. Sodium ion forms outer-sphere (OS) surface complexes (Sposito et al., 1999) and are easily exchanged with solute ions (e.g. $Fe(H_20)_6^{2+}$) by varying the cationic composition of the solution. In this adsorption mechanism, the sorbate cation (Na^+, Fe^{2+}) is held in the vicinity of the sorbent surface without loosing its hydration shell. In such a complex, ferrous ion is not expected to undergo hydrolysis at pH 7.5 (pK_1 = 10.1 for the first Fe(II) first hydrolysis; Stumm and Sulzberger, 1992). The rate of electron transfer between $Fe(H_20)_6^{2+}$ and an oxidant species will then be slow with neutral species (e.g. $Hg(OH)_2°(aq)$ or $O_2(g)$) and very slow for anionic species (e.g. $HAsO_4^{2-}(aq)$) which are electrostatically repulsed from the negatively charged phlogopite surface.

Besides these cation exchange properties, phyllosilicates also possess pH- dependent sorption properties. Trioctahedral smectites (e.g. hectorite) and micas (e.g. phlogopite) are built of layers made by the condensation of one central magnesian octahedral sheets and two tetrahedral sheets. The pH-dependent sorption was inferred to take place at layer edges, where truncation of the bulk structure leads to the formation of oxygen dangling bonds. The edge surfaces and their broken bonds are characterized by a well-known tendency to form inner-sphere complexes with protons and other cations (e.g. White and Zelazny, 1988; Zachara and McKinley, 1993; Charlet *et al.*, 1994; Schlegel *et al.*, 1999). The formation of these inner-sphere (IS) surface complexes involves the creation of chemical bonds between the sorbate and the surface oxygens of the sorbent (Cases et al., 2000). Surface cations of the sorbent thus enter the second coordination sphere of the sorbate. Thanks to Polarized EXAFS spectroscopy, divalent cations (e.g. Co^{2+} and Zn^{2+}) were shown to form IS complexes with the edges of the hectorite platelets, in the prolongation of the octahedral sheet. The cation octahedra share one or several edges with structural octahedra and one or several corners with Si tetrahedra, like in a clay structure (Schlegel et al., 1999, 2000). Excess of divalent cations can lead to the formation of octahedral sheets parrallel to the ab plane of hectorite crystallites, and if present these polymers may incorporate Si to form clay minerals (Schlegel et al, 2001).

Reduction mechanism

Divalent cation sorption on silica and (hydr)oxides lead to their enhanced hydrolysis, compared to solution (Schindler, 1991). Similarly, sorption of Fe(II) on the edges of phlogopite platelets, i.e. on the walls of etch pits, is expected to lead to the formation of reactive $>SOFe^{II}(OH)_i^{1-i}$ with surface species (with S = Mg or Si and i = 0 or 1). Hydroxyl groups will in turn facilitate the electron transfer to the oxidant species, as the OH^- ligands donate electron density to Fe(II) through both σ and π systems. A kinetic mechanism consistent with our results involves: (i) rapid adsorption of Fe(II) and formation of reactive $>SOFe^{II}(OH)_i^{1-i}$,(ii) oxidation of Hg(II) or As(V) by $>SOFe^{II}(OH)_i^{1-i}$ through formation of an activated surface complex or an outer-sphere complex, and (iii) precipitation of $Fe(OH)_3(s)$.

We shall first discuss in detail the reduction of Hg(II) by surface Fe(II). The experimental results obtained in the present study (Figure 2a) show the

formation of gaseous mercury immediately after Hg(II) addition. This suggests the principal "supply " of mercury to be dissolved mercury presented in the aqueous layer in the vicinity of surface rather than sorbed mercury. Thermodynamic calculations demonstrate the dominant solution species at pH>4 to be $Hg(OH)_2°$ in the absence of chloride- ion. Production of Hg° involves formation of an activated "outer-sphere" complex between $>SOFe^{II}(OH)_i^{1-i}$ and $Hg(OH)_2°$, the OH^- groups mediating the hydrogen bridging through which electron transfer occurs. The proposed mechanism includes the following steps:

(i) $$>SOH° + Fe^{2+} + iH_2O \xleftrightarrow{K_1} >SOFe^{II}(OH)_i^{1-i} + (i+1)H^+$$

(ii) $$2>SOFe^{II}(OH)_i^{1-i} + Hg(OH)_2^0 \underset{k_{-2}}{\overset{k_2}{\rightleftharpoons}} \left[>SOFe^{II}(OH)_i \cdots HOHg^{II}OH \cdots (HO)_iFe^{II}OS<\right]$$

(iii) $$\left[>SOFe^{II}(OH)_i \cdots HOHg^{II}OH \cdots (HO)_iFe^{II}OS<\right] \xrightarrow{k_3} 2>SOFe^{III}(OH)_{i+i}^{1-i} + Hg°$$

(iv) $$>SOFe^{III}(OH)_{1+i}^{1-i} + (2-i)H_2O \xrightarrow{k_4} >SOH° + Fe(OH)_{3(s)}^0 + (1-i)H^+$$

where K_1 is an intrinsic equilibrium constant; k_2, k_{-2}, k_3 and k_4 are rate constants. k_2 corresponds to the formation of precursor complexes, k_{-2} relates to the inverse rate, k_3 is the Hg° rate formation constant out of the transition complex and k_4 corresponds to the formation of a new $Fe^{III}(OH)_{3(s)}^0$ solid phase at the surface of phlogopite.

From the model given in Equations (i-iv) a complete rate-law expression, more complex than Equation 4, is derived. After applying the steady-state principle to the formation of the precursor complex and suggesting that $k_{-2} << k_3$ (Cervini-Silva et al., 2000) and that $C_{Hg2+}=C_{Hg(OH)20}$ the rate-law expression is given by

$$\frac{dC_{Hg^{2+}}}{dt} = -\frac{k_2 K_1^2 C_{0>SOH0}^2 C_{Fe2+}^2}{C_{H+}^{2(i+1)}\left(1+\frac{K_1 C_{Fe2+}}{C_{H+}^{i+1}}\right)^2} C_{Hg2+} \qquad (5)$$

where $C_{0>SOH}$ is a total concentration of surface sites. For our experimental conditions, i.e. at pH=7.5 and at an initial Fe^{2+} concentration C_{Fe2+}equal to 10 μM, the term $\frac{K_1 C_{Fe2+}}{C_{H+}^2}$ is smaller than 1 when $K_1<10^{-10}$. This value of the order of intrinsic equilibrium constants measured for the surface complexation of Fe(II) with other mineral surfaces (Zhang et al., 1992; Liger et al, 1999).

As the initial concentration of Fe(II) (10 μM) is much greater than the initial Hg(II) concentration (50 pM), the speciation of >SOH°, Fe(II) and $>SOFe^{II}(OH)_i^{1-i}$ is expected not to vary much within the course of Hg° formation and Equation 6 can be rewritten as a pseudo-first-order reaction with respect to Hg(II), with an observed rate constant (Equation 4):

$$k_{obs} = \frac{k_2 K_1^2 C_{0>SOH°}^2 C_{Fe^{2+}}^2}{C_{H^+}^{2(i+1)}} = k_2 \frac{C_{0>SOH°}^2}{C_{>SOH°eq}^2} C_{>SOFe^{II}(OH)_i^{1-i}}^2 \qquad (6)$$

It follows that the formation of the precursor complex is a rate-limiting step and that k_{obs} depends on the surface speciation of Fe(II) and on the concentration of $>SOFe^{II}(OH)_i^{1-i}$ surface complexes. The variability of k_{obs} due to changes in abundance of hydroxo surface complex $>SOFe^{II}OH^*$ has been documented for the reduction of inorganic compounds (U(VI), Liger et al, 1999) and organic species (4-chloronitrobenzene) (Charlet et al, 1998b).

The same oxidation mechanism is expected to apply to the two other oxidants, namely to $HAsO_4^{2-}$ and TCE. However, the type of $>SOH^0$ surface site involved in these reactions may vary. Oxyanions, such as arsenate, are repelled from the structural negative charge bearing phlogopite basal plane, but may form, as for chromate, inner-sphere complexes with mica book edges, as shown by XPS spectroscopy, and, when micas contain structural Fe(II) books, to enhance this way the Fe(II)-Cr(VI) electron transfer (Ilton and Veblen, 1994). Furthermore, arsenate has been shown by EXAFS spectroscopy to form with $>Fe^{III}OH$ surface sites a bidentate mononuclear surface complex (Manceau, 1995) . In the present case $HAsO_4^{2-}$ is expected to form in equation (ii) a $[>SOFe^{II}]_2As^VO_3^{2-}$ activated surface complex. Equation (iii) would lead to a mixed

As(III)-As(V) coprecipitate with $Fe(OH)_{3(s)}$. Similar mixed coprecipitates have been observed in the reduction of U(VI) by surface Fe(II) (Liger, 1996; Liger et al, 1999).

The TCE case differs from the Hg(II) and As(V) cases in as much as TCE is a neutral hydrophobic species. The clay surface exhibits hydrophilic properties for molecules whose adsorption does not lead to the removal of the charge-compensating cations, but hydrophobic properties for molecules which replace the charge- compensating cations, since the siloxane layer- in absence of charge compensating cations, is characterized exclusively by charge-satisfied extremely stable siloxane bonds (White and Zelazny, 1988; Stauton and Quiquampoix, 1994, Sposito et al., 1999). Cations with high hydration enthalpy, such as Fe^{2+}, are expected upon adsorption in the interlayer domain to remain fully hydrated. Thus no enhancement of electron transfer via hydrolysis is expected for these cations. However, the pre-etching of phlogopite surfaces with HF may have created zones of mechanical weakness within micas which have been often shown to run parallel to the preferred growth faces (Bloss *et al.*, 1959; Klein and Hurlbut, 1993).

Rufe and Hochella (1999) and Bosbach et al (2000) recently examined with *in situ* AFM the dissolution behavior of phlogopite etch pits and hectorite platelets, respectively, in HCl solutions. The phlogopite etch pits and hectorite dissolution features were essentially euhedral along the preferred growth faces (Figure 3). Since crystal growth is approximated as the formation of strong bonds between growth units of stoichiometric composition (Grim and Güven, 1978), and since growth faces are observed to lie parallel to one or more continuous chains of strong bonds within the crystal structure, called Periodic Bond Chains (PBCs), the dissolution of phlogopite must be initiated by precusors in which the basal plane siloxane bonds are weakened along PBCs. Grimand Güven (1978) and Hartman (1982) showed that the PBCs in phyllosilicates are along the <110> and <100> directions, so that "pseudohexagonal" stepped (110), (010) and (110) edge faces are predicted to be the dominant dissolution (Figure 3). Surface oxygen atoms at these weakened sites may complex Fe(II) and polarize surrounding water molecules which will in turn be bridging, in an outer-sphere complex, the surface Fe(II) with TCE. Similarly, H_2O molecules mediating in an outer-sphere complex the hydrogen bridging between Si-O basal groups and an organic molecule have been shown to promote dehydrochlorination reaction, e.g. that of

pentachloroethane (5CA) by clay structural Fe(II) (Cervini-Silva et al., 2000). In our case, a hydrogen bridging is expected to be formed between TCE and Fe(II) complexed with free coordination sites located on the siloxane basal plane along PCB directions. These surface sites were not active for the two other oxidants which co-adsorb, and readily react, with Fe(II) on step surface sites. Surface atoms present at the weakened sites along PCB directions are characterized by a ligand sphere that differs from both that in the basal plane siloxane plane bulk, and that on the etch pits.

Environmental significance

The present experiments have shown that solid phases, i.e. mineral surfaces have a strong influence on the reductive transformation of some priority pollutants. The kinetic study of this and two accompanying papers on the pH dependence of Hg reduction in presence of synthetic and natural particles (Peretyashko et al., 2001a,b) help us to assess the redox behavior of mercury in natural environments. For example in eutrophic lakes (Peretyashko, 2001b) or hydromorphic soils (Peretyashko et al., 2001c), surface reaction can be expected to dominate, whereas biotic Hg reduction will likely occur in oxic environments (Mason et al, 1995).

Reduction of As(V) and TCE which are both frequent groundwater contaminants (McArthur et al., 2000; Christensen et al., 1994) lead to their natural attenuation and to hydrous ferric oxide reactions products localized in different structural features of the etched phlogopite/water interface. This leads to insights on their respective reduction mechanisms. As(V) is likely, like Cr(VI), to form inner-sphere surface complexes at the edges and etch pits walls of micas particles (Ilton and Veblen, 1994; Xu et al., 1988), and to react there with sorbed Fe(II). On the other hand, reduction of TCE by Fe(II) is likely to occur by outer sphere complex formation. It reacts with Fe sorbed on basal plane surface sites located along the weakened bonds between bond chains.

Detailed surface studies help to optimize the application of Fe(II)/mineral mixtures as reductants of pollutants in technical systems. In-situ remediation of contaminated soil and water by addition of soluble Fe(II) salts may be a cheap alternative to pump and treat remediation or to permeable, reactive Fe° barriers which might become less reactive with time because of surface passivation. The relative reactivities of the different surface Fe(II) species

towards the three contrasted species chosen for this study are possibly transferrable to predict the reduction of a number of other compounds.

Finally, this study provides compiling evidence that so called surface coatings of clay particles frequently encountered in soils may not be formed by transfer to the surface of homogeneously formed Fe(III) hydroxides (Hendershot and Lavkulich, 1983), but rather as a product of the heterogeneous oxidative precipitation of iron by a variety of natural electron acceptors. Electron micrographs of kaolinite and goethite association indicate goethite particles to be either associated with kaolinite basal plane (Tandy et al., 1988), as in the case of our TCE experiment, or to be located on clay edges (Muller and Bocquier, 1986), as in the case of our Hg(II) and As(V) experiments.

Conclusion

Our results confirm that Fe oxide coatings, often found in soil and aquifer materials at the surface of sand and clay particles (Cornell and Schwertmann, 1996), may not result from the homogeneous precipitation of Fe(III), but rather from the enhancement by the mineral surface of the rate of ferrous iron oxidation by a variety of oxidants. The *in situ* result show that although iron oxyhydroxides may precipitate in solution, the tiny (roughly 25 nm in diameter) particles observed in the present study are closely associated with topographical steps, i.e. with broken edges of the clay crystal. Therefore ferrous iron ions were sorbed and oxidized by Hg(II) and As(V) on surface edge sites. These results are consistent with macroscopic measurements and ex situ atomic force microscopy of Fe(II) reactions products with other oxidants at the surface of iron oxides (Weidler et al., 1998, Liger et al., 1999). Thus some extrapolation to a broader range of mineral surfaces and oxidants seems warranted.

While this study and previous ones show that at least some As is sequestrated by the nucleation and precipitation of a ferric solid phase, there are some inherent limitations to the methods used in this study. For example, AFM was not capable of atomic-scale resolution; hence we could not rule out a coprecipitation of As(V) or As(III) within the ferric oxyhydroxides nanoparticles precipitated on the phlogopite edges. Likewise, AFM is a surface-sensitive method, so that we could not rule out the possibility of reaction between TCE and structural Fe(II), a reaction suggested by the nanoparticles lining up along crystallographic axis. Structure-sensitive and depth-sensitive measurements (i.e. X-ray absorption spectroscopy, and Mössbauer spectroscopy) are presently being obtained and will

be presented in a future publication to address these issues. Nevertheless, the imaging of chemisorbed Fe(II) permits an interpretation of elementary steps in important catalytic reactions at an atomic level. This type of study should encourage surface science research further towards investigations into dynamic processes occurring on clay surfaces.

Acknowledgments. L.C. gratefully acknowledges partial support of this work by the program "Mercury in French Guyana" (CNRS-MATE-FEDER), the Indian-French Center for Advanced Research ("Geochemistry of Arsenic in Ganga River sediments" Project), and ADEME (V. Barbu scholarship). L.C. and D.B. acknowledge the Franco-German "Procope" project #9915, and T.P the support of a fellowship from the French Ministry for Foreign Affairs.

References

Appelo, C.A. J., Drijver, B., Hekkenberg, R. and De Jonge, M., 2000. Modeling In Situ Iron Removal from Ground Water, Ground Water 37, 811-817.

Appelo, C.A.J. , Van der Weiden, M.J.J., Tournassat, C. and Charlet, L., 2001. Some effects of surface complexation of ferrous iron and carbonate on ferrihydrite. Env. Sci. Technol. (submitted)

Bickmore B.R., Bosbach D., Hochella M.F. Jr., Charlet L., Rufe E. ,2001. *In situ* atomic force microscopy study of hectorite and nontronite dissolution: Implications for phyllosilicate edge structures and dissolution mechanisms. Am. Mineral. (in press)

Bickmore, B.R., Hochella, M.F., Bosbach, D., Charlet L.,1999. Atomic force microscopic imaging of minutes particles in aqueous solutions. Microscopy Today, 99(9), 14-18.

Bickmore, B.R., Hochella, M.F., Bosbach, D., Charlet L., 1999. Methods for performing atomic force microscopy imaging of clay minerals in aqueous solutions. Clays Clay Min. 47, 573-581.

Bloom N.S., Fitzgerald W.F., 1988. Determination of volatile mercury species at the picogram level by low-temperature gas chromatography with cold-vapor atomic fluorescence detection. Anal. Chim. Acta. 208,151-161.

Bloss, F.D., Sherkarchi, E. Shell, H.R. 1959. Hardness of synthetic and natural micas. Am. Mineral. 44, 33-48.

Bosbach D., Charlet L., Bickmore B., Hochella Jr. M.F., 2000. The dissolution of hectorite: In-situ, real-time observations using Atomic Force Microscopy. Am. Mineral., 85, 1209-1216

Buerge, I.J., Hug, S.J., 1999. Influence of mineral surfaces on chromium(VI) reduction by Fe(II). Environ. Sci. Technol. 33,4285-4291.

Cases, J.M., Villiéras, F., Michot, L., 2000. Adsorption, exchange and retention phenomena at the solid-aqueous interface. 1. Influence of structural, textural and superficial properties of solids. C.R. Acad. Sci. Paris, Earth Pl. Sci. 331, 763-773.

Cervini-Silva, J., Wu, J., Stucki, J.W. , Larson, R.A., 2000. Adsorption kinetics of pentachloroethane by iron-bearing smectites. Clays Clay Min. 48(1), 132-138.

Charlet, L., Schindler, P.W., Spadini, L., Furrer, G., Zysset, M., 1993. Cation adsorption on oxides and clays: The aluminum case. Aquatic Sci., 55, 291-303.

References

Appelo, C.A. J., Drijver, B., Hekkenberg, R. and De Jonge, M., 2000. Modeling In Situ Iron Removal from Ground Water, Ground Water 37, 811-817.

Appelo, C.A.J. , Van der Weiden, M.J.J., Tournassat, C. and Charlet, L., 2001. Some effects of surface complexation of ferrous iron and carbonate on ferrihydrite. Env. Sci. Technol. (submitted)

Bickmore B.R., Bosbach D., Hochella M.F. Jr., Charlet L., Rufe E. ,2001. *In situ* atomic force microscopy study of hectorite and nontronite dissolution: Implications for phyllosilicate edge structures and dissolution mechanisms. Am. Mineral. (in press)

Bickmore, B.R., Hochella, M.F., Bosbach, D., Charlet L.,1999. Atomic force microscopic imaging of minutes particles in aqueous solutions. Microscopy Today, 99(9), 14-18.

Bickmore, B.R., Hochella, M.F., Bosbach, D., Charlet L., 1999. Methods for performing atomic force microscopy imaging of clay minerals in aqueous solutions. Clays Clay Min. 47, 573-581.

Bloom N.S., Fitzgerald W.F., 1988. Determination of volatile mercury species at the picogram level by low-temperature gas chromatography with cold-vapor atomic fluorescence detection. Anal. Chim. Acta. 208,151-161.

Bloss, F.D., Sherkarchi, E. Shell, H.R. 1959. Hardness of synthetic and natural micas. Am. Mineral. 44, 33-48.

Bosbach D., Charlet L., Bickmore B., Hochella Jr. M.F., 2000. The dissolution of hectorite: In-situ, real-time observations using Atomic Force Microscopy. Am. Mineral., 85, 1209-1216

Buerge, I.J., Hug, S.J., 1999. Influence of mineral surfaces on chromium(VI) reduction by Fe(II). Environ. Sci. Technol. 33,4285-4291.

Cases, J.M., Villiéras, F., Michot, L., 2000. Adsorption, exchange and retention phenomena at the solid-aqueous interface. 1. Influence of structural, textural and superficial properties of solids. C.R. Acad. Sci. Paris, Earth Pl. Sci. 331, 763-773.

Cervini-Silva, J., Wu, J., Stucki, J.W. , Larson, R.A., 2000. Adsorption kinetics of pentachloroethane by iron-bearing smectites. Clays Clay Min. 48(1), 132-138.

Charlet, L., Schindler, P.W., Spadini, L., Furrer, G., Zysset, M., 1993. Cation adsorption on oxides and clays: The aluminum case. Aquatic Sci., 55, 291-303.

Charlet, L., Silvester, E.J., Liger, E., 1998b. N-compound reduction and actinide immobilisation in surficial fluids by Fe(II): The surface equivalent to $>Fe^{III}OFe^{II}OH°$ degrees species as major reductant. Chem. Geol., 151, 85-93.

Charlet, L., Liger, E., Gerasimo, P., 1998a. Decontamination of TCE and uranium-rich waters by granular iron: Role of sorbed Fe(II). J. Env. Eng., 124, 25-30.

Christensen, T.H., Kjeldsen, P., Albrechtsen, H.J., Nielsen, P.H., Bjerg, P.L., Holm, P.E. 1994. Attenuation of landfill leachate pollutants in aquifers. Critical Rev. In Env. Sci. Technol. 24 (4), 119-202.

Cornell, R. M., Schwertmann, U., 1996. The iron oxides. Weinheim (D), VCH Verlag.

Cossa, D., Mason, P.P., Fitzgerald, W.F. 1994. Chemical speciation of mercury in a meromictic lake In: Mercury Pollution, Integration and Synthesis, C.J. Watras Ed., Lewis Publ., Boca Raton.

Cui, D., Eriksen, T.E. 1996. On the reduction of pertechnetate by derrous iron in solution; influence of soebed and precipitated Fe(II). Env. Sci. Technol.

Davison, W., Grime, G.W., Morgan, J.A.W., Clarke, K. 1991. Distribution of dissolved iron in sediment pore waters at submillimeter resolution. 352, 323-325.

Doelsch E., Rose, J., Masion, A., Bottero, J.Y., Nahon,D. and Bertsch, P.M. 2000 Speciation and crystal chemistry of iron(III) chloride hydrolyzed in the presence of SiO_4 ligands. 1. An FeK-edge EXAFS study. Langmuir 16 (10) , 4726-4731.

Eggleston, C.M., Stumm, W. 1993. Scanning tunneling microscopy of Cr(III) chemisorbed on α-Fe_2O_3(001) surfaces from aqueous solution: direct observation of surface mobility and clustering. Geochim. Cosmochim. Acta . 57, 4843-4850.

Environmental Protection Agency. 1997. Use of monitored natural attenuation at Superfund, RCRA Corrective Action, and underground storage tank sites. Directive 9200, 4-17P, 32pp., Office of Solid Waste and Emergency Response, Washington D.C.

Ernstsen, V. 1996. Reduction of nitrate by Fe^{2+} in clay minerals. Clays Clay Min. 44, 599-608.

Hartman, P., 1973. Structure and morphology. In P. Hartman, Ed., Crystal Growth: An Introduction, p.367-402. North Holland Publishing Company, Amsterdam.

Hendershot, W.H., Lavkulich, L.M., 1983. Effect of sequioxide coating on surface charge of standard mineral and soil samples. Soil Sci. Soc. Am. J. 47: 1252-1260.

Heron, G., Christensen, T.H., 1995. Impact of sediment bound iron on redox buffering in a landfill leachate polluted aquifer(Vejen, Denmark). Env. Sci. Technol. 29(1), 187-192.

Hug, S.J., Johnson, A. Friedl, G. Lichtensteiger, T., Belevi, H. and Sturm, M. 1997. Characterization of environmental solid and surfaces. Chimia 51, 884-892.

Ilton, E.S. and Veblen, DS.R. 1994. Chromium sorption by phlogopite and biotite in acidic solutions at 25°C: insights from X-ray photoelectron spectroscopy and electron microscopy. Geochim. Cosmochim. Acta 58 (13), 2777-2788.

Karim, Z., 1984. Characteristics of ferrihydrites formed by oxidation of $FeCl_2$ solutions containing different amounts of silica. Clays Clay Min. 32(3), 181-184.

Klausen, J., Tröber, P.T., Haderlein, S.B., Schwarzenbach, R.P. 1995. Reduction of substituted nitrobenzenes by Fe(II) in aqueous mineral suspensions. Env. Sci. Technol. 29: 2396-2404.

Klein, C., Hurlbut, C.S. 1993. Manual of Mineralogy, 21st ed., 681p. John Wiley & Sons, New York.

Liger, E., Charlet, L., Van Cappellen, P. ,1999. Surface catalysis of uranium (VI) reduction by iron(II). Geochim. Cosmochim. Acta. 19/20, 2939-2956

Liger E. 1996. Role catalytique des oxyhydroxydes de Fe(III): réduction de U(VI) par le Fe(II) adsorbé. PhD diss. Univ. Grenoble, France.

Luther G.W., 1990. The frontier-molecular-orbital theory approach in geochemical processes. In Aquatic chemical kinetics, W. Stumm, Ed., Wiley-Interscience, New-York, 173-198.

Manceau, A., 1995. The mechanism of anion adsorption on Fe oxides: Evidence for the bonding of arsenate tetrahedra on free $Fe(O,OH)_6$ edges. Geochim. Cosmoch. Acta.59, 3647-3653.

Mason R. P., Morel F. M. M., Hemond H. F. ,1995. The role of microorganisms in elemental mercury formation in natural waters. Water, air and soil pollution. 80, 775-787.

McArthur, J.M., Ravenscroft, P., Safiullah, S., Thirlwall, M.F. 2000. Arsenic in groundwater: testing pollution mechanisms for sedimentary aquifers in Bangladesh. Water Resources Research 37(1): 109-117.

Myrreni, S.C.B., Tokunaga, T.K., Brown, Jr. G.E., 1997. Abiotic selenium redox transformations in the presence of Fe(II, III) oxides. Science. 278, 1106-1111.

Orth W.C., Gillham R.W., 1996. Dechlorination of trichloroethene in aqueous solution using Fe(0). Env. Sci. Technol. 30, 66-71.

Ottley, C.J., Davison, W., Edmunds, W.M. 1997. Geochim. Cosmochim. Acta 61:1819-1828.

Peretyashko, T., Charlet, L., Cossa, D., 2001a Production of gaseous mercury in anoxic environments: reservoir Petit Saut, French Guyana. (in prep.)

Peretyashko, T., Charlet, L., Cossa, D., Kazimirov, V., 2001b. Mechanism of Hg° production by heterogeneous oxidation of Fe(II).(in prep.)

Peretyashko, T., Charlet, L., Grimaldi, M.2001c. Production of gaseous mercury in flooded hydromorphic soils.(in prep.)

Plaschke, M., Römer, J., Klenze, R. and Kim, J.I. 1999. In situ AFM study of sorbed humic acid colloids at different pH. Colloids and Surfaces A. 160, 269-279.

Ramsden, J.J., Mate, M. 1998. Kinetics of monolayer particle deposition. J. Chem. Soc. Faraday Trans. 94, 783-788.

Rufe, E., Hochella, M.F. Jr. 1999. Quantitative assessment of reactive surface area of phlogopite dissolution during acid dissolution. Science. 285: 874-876.

Sarkar, D., Essington, M.E., Misra, K.C. 2000. Adsorption of mercury(II) by kaolinite. Soil Sci. Soc. Am. 64, 1968-1975.

Schindler P. W., 1991. A solution chemists view of surface chemistry. Pure and Applied Chemistry. 63, 1697-1704.

Schultz, C.A. and T.J. Grundl. 2000 pH dependance on reduction rate of 4-Cl-Nitrobenzene by Fe(II)/montmorillonite systems. Env. Sci. Technol. 34, 3641-3648.

Schlegel M.L., Manceau A., Chateigner D., Charlet L. 1999. Sorption of metal ions on clay minerals. I. Polarized EXAFS evidence for the adsorption of Co on the edges of hectorite particles. J. Colloid Interf. Sci. 215, 140-158.

Schlegel M.L., Charlet L., Manceau A. 2000. Sorption of metal ions on clay minerals. II. mechanism of Co sorption on hectorite at high and low ionic strength, and impact on the sorbent stability J. Colloid Interf. Sci. 220, 392-405.

Schlegel M.L., Manceau A., Charlet L. Hazemann, J.L. 2001. Adsorption mechanism of Zn on hectorite as a function of time, pH and ionic strength. Am. J. Sci. (submitted)

Schwertmann, U. and G. Pfab. 1994. Structural vanadium in synthetic goethite. Geochim. Cosmochim. Acta 58(20), 4349-4352

Sorensen, J., Thorling, L., 1991. Stimulation of lepidocrocite (γ-FeOOH) of Fe(II)-dependent nitrite reduction. Geochoim. Cosmochim. Acta. 55, 1289-1294.

Sposito, G., Skipper, N.T., Sutton, R., Park, S-H., Soper A. & J.A. Greathouse, 1999, Surface geochemistry of the clay minerals, Proc. Nat. Acad. Sci., 96, 3358-3364

Stumm, W., Sulzberger, B., 1992. The cycling of iron in natural environments; considerations based on laboratory studies of heterogeneous redox processes Geochim. Cosmochim. Acta. 56, 3233.

Staunton, S., Quiquampoix, H. 1994. Adsorption and conformation of bovine serum albumin on montmorillonite : modification of the balance between hydrophobic and electrostatic interactions by protein methylation and pH variation. J. Colloid. Interf. Sci. 166, 89-94.

Zachara, J. M., McKinley, J. P., 1993. Influence of hydrolysis on the sorption of metal cations by smectites: importance of edge coordination reactions. Aquatic Science. 55(4), 250-261.

Tamura, H., Kawamura, S., Nagayama, M. 1980. Acceleration on the oxidation of Fe^{2+} by Fe(III) oxyhydroxides. Corrosion Sci. 20, 963-971.

Vanek V., 1990. In situ treatment of iron-rich groundwater by the addition of nitrate. Rep. Lunds Universitet, 33 pp.

Wanner H., Albinsson Y., Karnland O., Wieland E., Wersin P., Charlet L. ,1994. The acid base chemistry of montmorillonite. Radiochimica. 66/67, 157-162

Weidler, P.G., Hug, S.J., Wetche, T.P., Hiemstra, T., 1998. Determination of growth rates of (100) and (110) faces of synthetic goethite by scanning force microscopy. Geochim. Cosmochim. Acta, 62, 3407–3412.

White, G. N., Zelazny, L. W., 1988. Analysis and implication of the edge structure of dioctaedral phylosilicates. Clays and Clay Minerals. 36(2), 141-146.

Xu, H., Allard, B. Grimvall, A. 1988 Influence of pH and organic substance on the adsorption of As(V) on geological materials.

Zhang,Y., Charlet, L., Schindler, P.W., 1992. Adsorption of protons, iron(II) and aluminum(III) on lepidocrocite. Colloids & Surfaces. 63, 259-268.

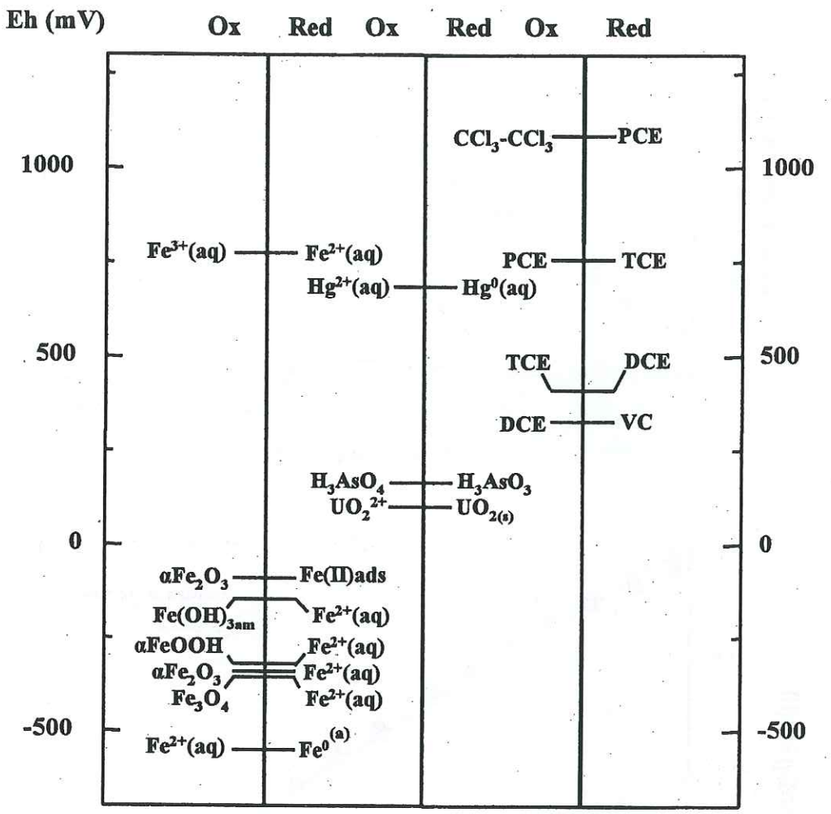

Charlet et al., Figure 1

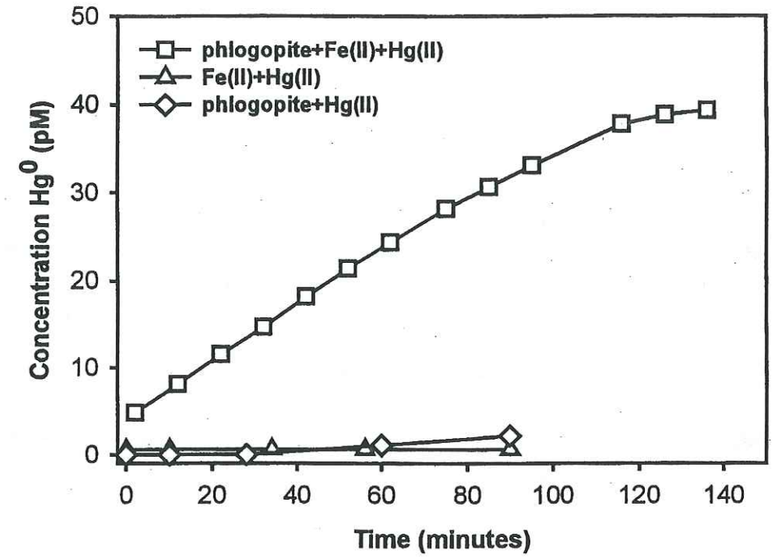

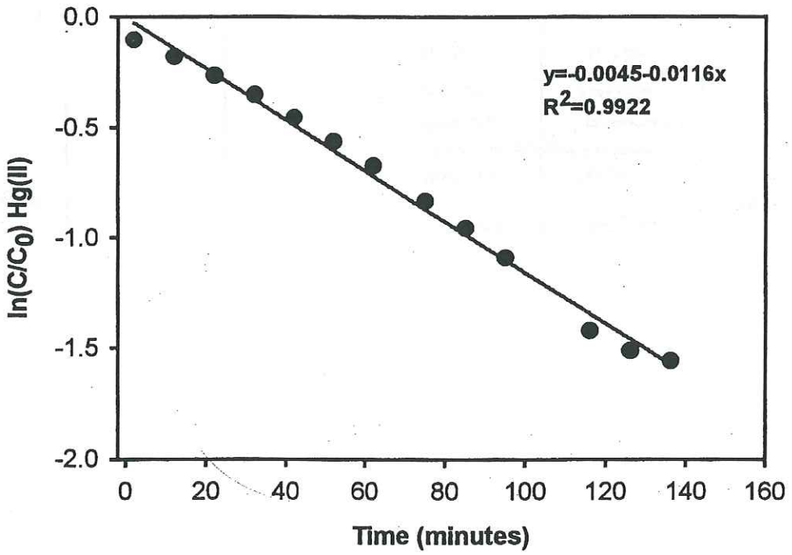

Charlet et al., Figure 2

a

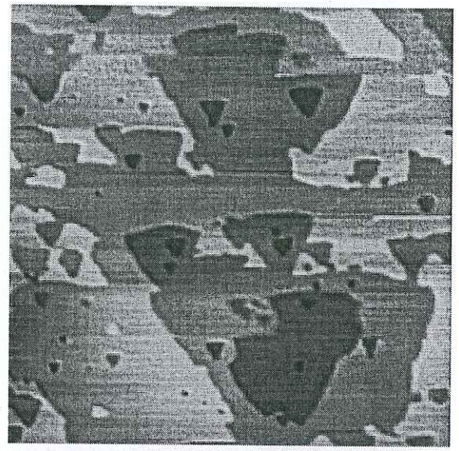

b

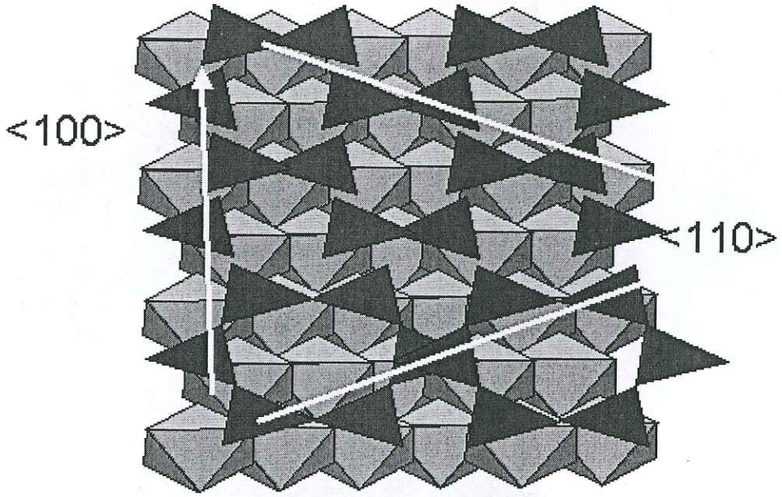

Charlet et al., Figure 3

a

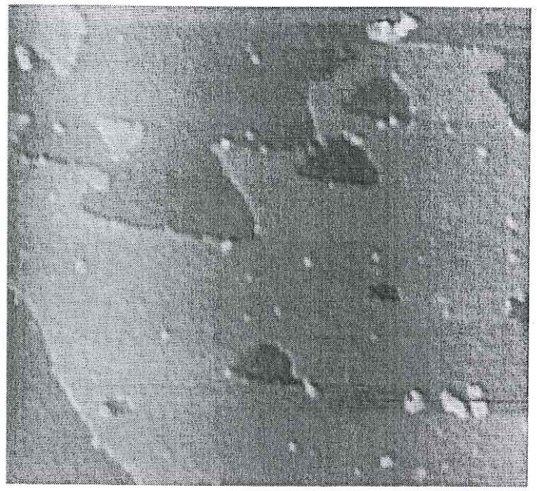

900 x 900 nm

b

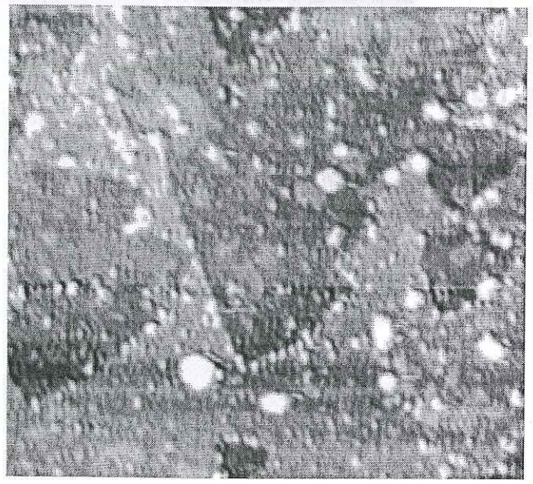

850 x 850 nm

Charlet et al., Figure 4

a

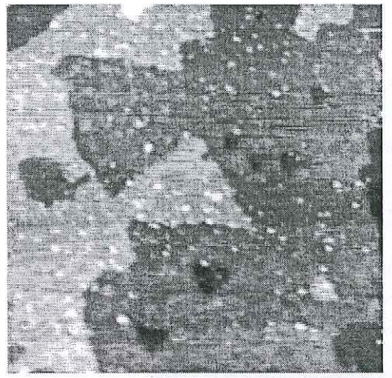

b

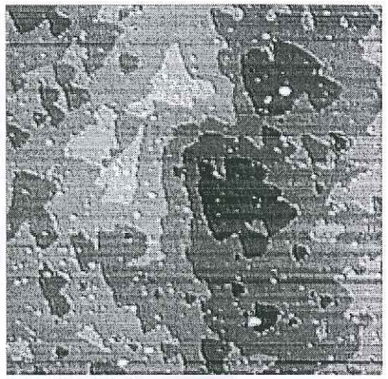

c

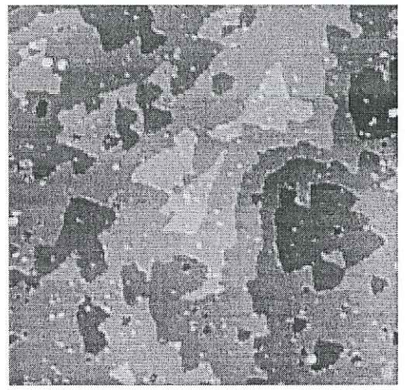

d

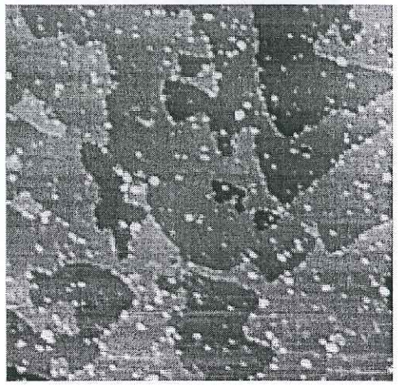

Charlet et al., Figure 5

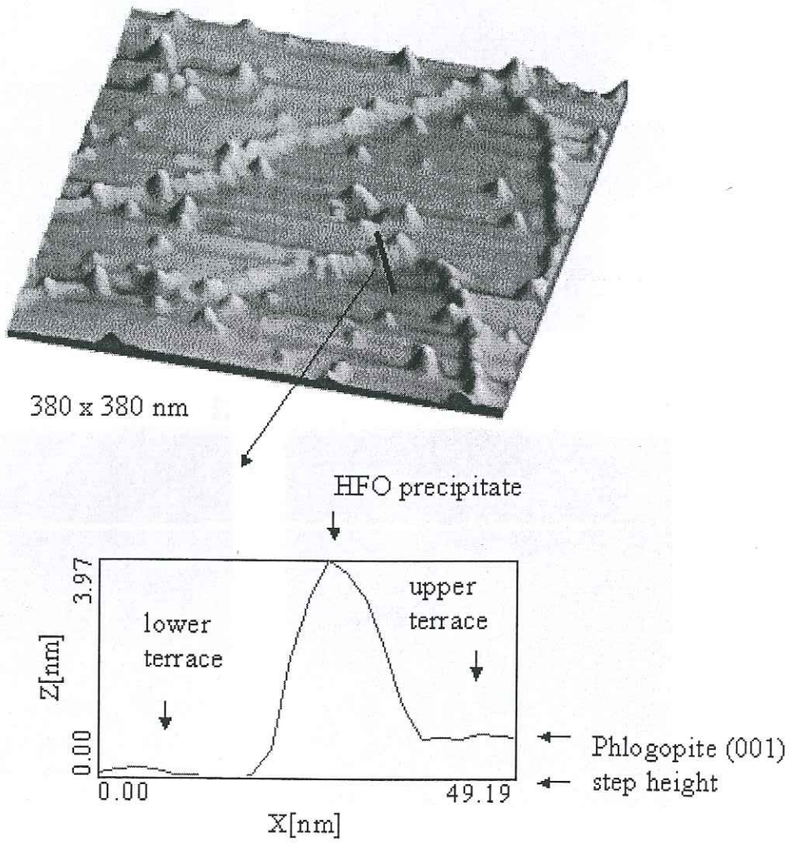

Charlet et al., Figure 6

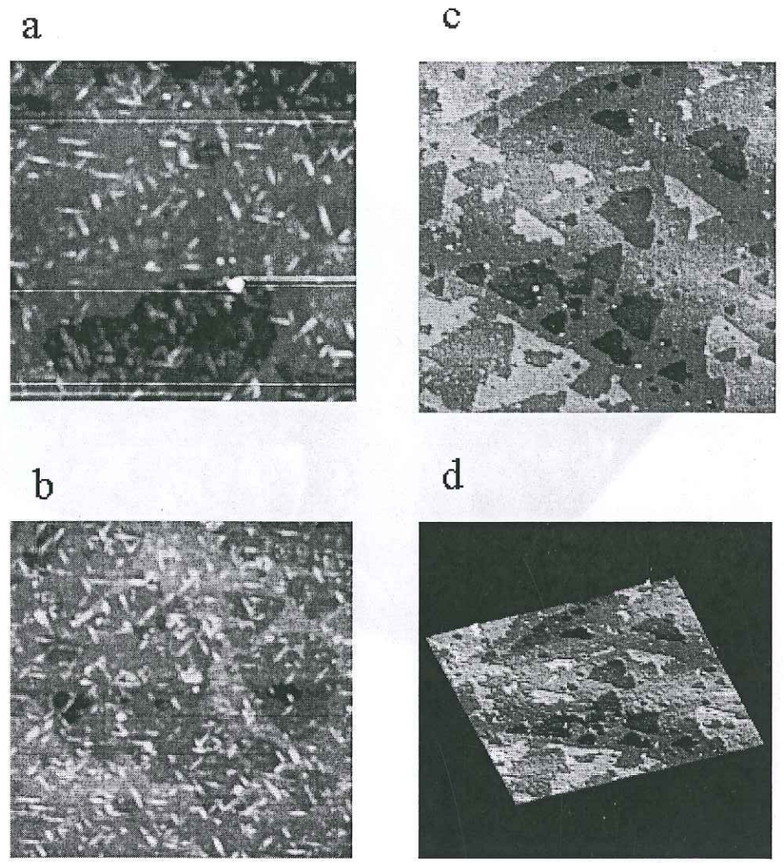

Charlet et al., Figure 7

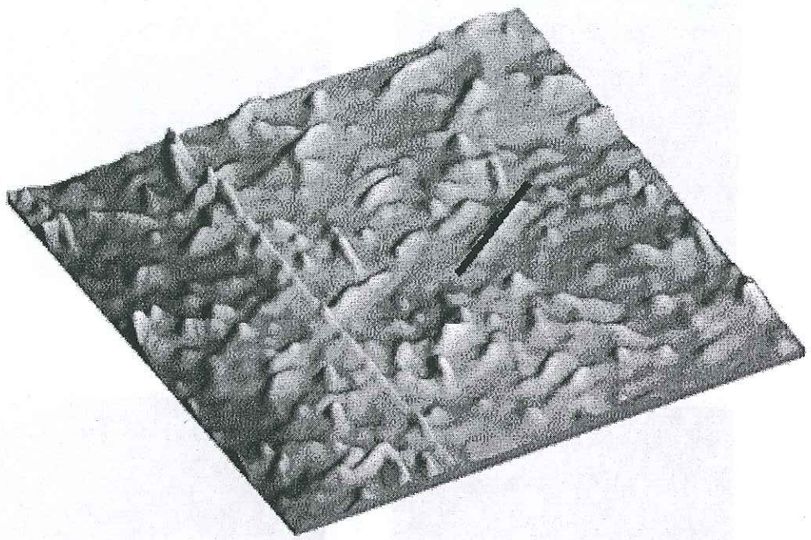

Charlet et al., Figure 8

Thèse de doctorat de l'Université Joseph Fourier Grenoble I

Titre de l'ouvrage :
Formation de Hg° dans des milieux anoxiques tropicaux (lac, sol)

Nom de l'auteur :
Tanya PERETYAZHKO

Résumé : Les mécanismes de production de Hg° dans des milieux anoxiques ont été étudiés en laboratoire. Les résultats sont utilisés pour interpréter les données de terrain mesurées dans la retenue de Petit Saut et dans des sols hydromorphes avoisinants, en Guyane Française (Amérique du Sud).
Dans la retenue, la décomposition des matières organiques, enoyées lors de la mise en eau, crée des conditions anoxiques, et donc une production d'espèces réduites, en accord avec les séquences thermodynamiques. Les sources de mercure dans la retenue sont les zones d'orpaillage situées en amont, ainsi que les sols, qui furent inondés lors de la mise en eaux. La disparition de l'oxygène favorise la libération du mercure par les sols inondés vers la colonne d'eau, où il se transforme chimiquement. Nos expériences de laboratoire démontrent que la production de Hg° au fond du lac est essentiellement d'origine biologique, et que la vitesse de production de Hg° est fonction de la concentration en mercure réactif. Un autre mécanisme responsable de la production de Hg° est la réduction abiotique de Hg(II) par le Fe(II) adsorbé sur des particules, ce que nous avons démontré avec des particules d'hématite et de mica.
Dans les sols, la comparaison de profils du mercure total montre de plus faibles concentrations dans les sols hydromorphes, que dans les oxisols, appartenant à la même toposéquence. Nos expériences de laboratoire démontrent que la réduction de Hg(II) en Hg° a lieu dans les sols hydromorphes en conditions anoxiques. La réduction est plus importante quand ces sols ont été amendés par du citrate de Fe(III). Tant la réduction biologique, que la réduction abiotique par le Fe(II) adsorbé sur les particules peuvent être responsables de la réduction du Hg(II) et de son départ vers l'atmosphère. La disparition du Hg(II) en conditions hydromorphes peut alors être due tant à la lixiviation des complexes organiques de l'ion Hg(II) qu'à sa volatilisation après réduction.

Mots clés : mercure, mercure élémentaire, mercure gazeux, Hg°, réduction, réservoir, sol hydromorphe.